

NON-IONIZING RADIATION, PART 2: RADIOFREQUENCY ELECTROMAGNETIC FIELDS

VOLUME 102

This publication represents the views and expert opinions of an IARC Working Group on the Evaluation of Carcinogenic Risks to Humans, which met in Lyon, 24-31 May 2011

LYON, FRANCE - 2013

IARC MONOGRAPHS
ON THE EVALUATION
OF CARCINOGENIC RISKS
TO HUMANS

1. EXPOSURE DATA

1.1 Introduction

This chapter explains the physical principles and terminology relating to sources, exposures and dosimetry for human exposures to radiofrequency electromagnetic fields (RF-EMF). It also identifies critical aspects for consideration in the interpretation of biological and epidemiological studies.

1.1.1 *Electromagnetic radiation*

Radiation is the process through which energy travels (or “propagates”) in the form of waves or particles through space or some other medium. The term “electromagnetic radiation” specifically refers to the wave-like mode of transport in which energy is carried by electric (E) and magnetic (H) fields that vary in planes perpendicular to each other and to the direction of energy propagation.

The variations in electric and magnetic field strength depend only on the source of the waves, and most man-made sources of electromagnetic radiation produce waves with field strengths that vary sinusoidally with time, as shown in Fig. 1.1. The number of cycles per second is known as the frequency (f) and is quantified in the unit hertz (Hz). The waves travel at the speed of light (c) in free space and in air, but more slowly in dielectric media, including body tissues. The wavelength (λ) is the distance between successive peaks in

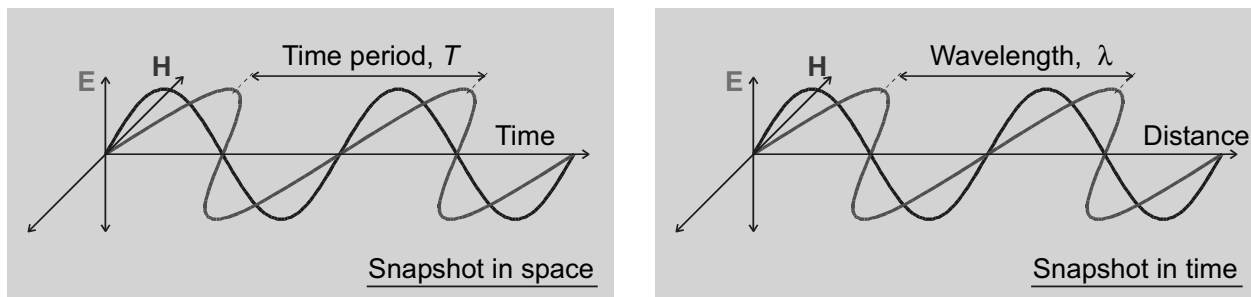
a wave (Fig. 1.1) and is related to the frequency according to $\lambda = c/f$ ([ICNIRP, 2009a](#)).

The fundamental equations of electromagnetism, Maxwell’s equations, imply that a time-varying electric field generates a time-varying magnetic field and vice versa. These varying fields are thus described as “interdependent” and together they form a propagating electromagnetic wave. The ratio of the strength of the electric-field component to that of the magnetic-field component is constant in an electromagnetic wave and is known as the characteristic impedance of the medium (η) through which the wave propagates. The characteristic impedance of free space and air is equal to 377 ohm ([ICNIRP, 2009a](#)).

It should be noted that the perfect sinusoidal case shown in Fig. 1.1, in which a wave has a sharply defined frequency, is somewhat ideal; man-made waves are usually characterized by noise-like changes in frequency over time that result in the energy they carry being spread over a range of frequencies. Waves from some sources may show purely random variation over time and no evident sinusoidal character. Some field waveforms, particularly with industrial sources, can have a distorted shape while remaining periodic, and this corresponds to the presence of harmonic components at multiples of the fundamental frequency ([ICNIRP, 2009a](#)).

The quantities and units used to characterize electromagnetic radiation are listed in [Table 1.1](#).

Fig. 1.1 A sinusoidally varying electromagnetic wave viewed in time at a point in space (a) and in space at a point in time (b)



(a)

(b)

E, electric field; H, magnetic field.
Prepared by the Working Group

1.1.2 The electromagnetic spectrum

The frequency of electromagnetic radiation determines the way in which it interacts with matter; a variety of different terms are used to refer to radiation with different physical properties. The electromagnetic spectrum, describing the range of all possible frequencies of electromagnetic radiation, is shown in Fig. 1.2.

For the purposes of this *Monograph*, radio-frequency (RF) electromagnetic radiation will be taken as extending from 30 kHz to 300 GHz, which corresponds to free-space wavelengths in the range of 10 km to 1 mm. Electromagnetic fields (EMF) in the RF range can be used readily for communication purposes as radio waves. As shown in Fig. 1.2, the International Telecommunications Union (ITU) has developed a categorization for radio waves according to their frequency decade: very low frequency (VLF); voice frequency (VF); low frequency (LF); medium frequency (MF); high frequency (HF); very high frequency (VHF); ultra-high frequency (UHF); super-high frequency (SHF); and extremely high frequency (EHF) (ITU, 2008).

Radio waves with frequencies in the range 300 MHz to 300 GHz can be referred to as microwaves, although this does not imply any sudden change in physical properties at 300 MHz. The

photon energy would be about 1 μeV (micro-electronvolt) at 300 MHz.

Above the frequencies used by radio waves are the infrared, visible ultraviolet (UV), X-ray and gamma-ray portions of the spectrum. At RF and up to around the UV region, it is conventional to refer to the radiation wavelength, rather than frequency. Photon energy is generally referred to in the X-ray and gamma-ray regions, and also to some extent in the UV range, because the particle-like properties of the EMFs become more obvious in these spectral regions.

Below the RF portion of the spectrum lie EMFs that are used for applications other than radiocommunication. The interdependence of the electric- and magnetic-field components also becomes less strong and they tend to be considered entirely separately at the frequency (50 Hz) associated with distribution of electricity (IARC, 2002).

1.1.3 Exposures to EMF

RF fields within the 30 kHz to 300 GHz region of the spectrum considered in this *Monograph* arise from a variety of sources, which are considered in Section 1.2. The strongest fields to which people are exposed arise from the intentional use of the physical properties of fields, such as

Table 1.1 Quantities and units used in the radiofrequency band

Quantity	Symbol	Unit	Symbol
Conductivity	σ	siemens per metre	S/m
Current	I	ampere	A
Current density	J	ampere per square metre	A/m ²
Electric-field strength	E	volt per metre	V/m
Frequency	f	hertz	Hz
Impedance	Z or η	ohm	Ω
Magnetic-field strength	H	ampere per metre	A/m
Permittivity	ϵ	farad per metre	F/m
Power density	S or Pd	watt per square metre	W/m ²
Propagation constant	K	per metre	m ⁻¹
Specific absorption	SA	joule per kilogram	J/kg
Specific absorption rate	SAR	watt per kilogram	W/kg
Wavelength	λ	metre	m

Adapted from [ICNIRP \(2009a\)](#)

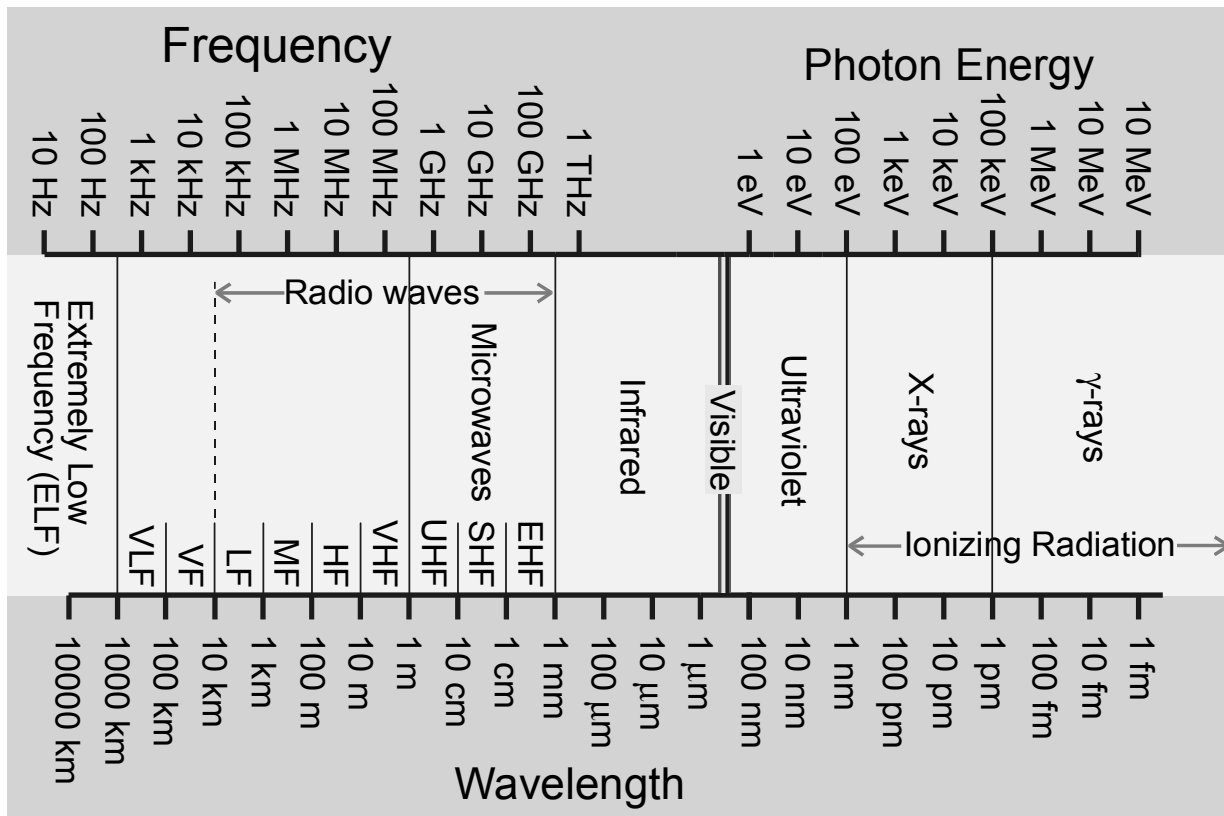
induction heating (including the industrial heating of materials and cooking hobs), remote detection of objects and devices (anti-theft devices, radar, radiofrequency identification [RFID]), telecommunications (radio, television, mobile phones, wireless networks), medical diagnostics and therapy (magnetic resonance imaging [MRI], hyperthermia), and many more. There are also unintentionally generated fields, such as those associated with the electrical ballasts used for fluorescent lighting, electronic circuits, processors and motors.

When considering human exposures it is important to recognize that, in addition to the EMFs associated with energy being radiated away from a source, there are electric and magnetic fields associated with energy stored in the vicinity of the source, and this energy is not propagating. The reactive fields associated with this stored energy are stronger than the radiated fields within the region known as the reactive near field, which extends to a distance of about a wavelength from the source. The wave impedance in the reactive near field may be higher than the impedance of free space if a source is capacitive in nature and lower if a source is inductive in nature ([AGNIR, 2003](#)).

Beyond the near field region lies the far field, where the RF fields have the characteristics of radiation, i.e. with planar wave fronts and E and H components that are perpendicular to each other and to the direction of propagation. The power density of the radiation, P_d , describes the energy flux per unit area in the plane of the fields expressed as watts per square metre (W/m²) and decreases with distance squared (the inverse square law). Power density can be determined from the field strengths (see Glossary) ([AGNIR, 2003](#)).

Sources that are large relative to the wavelength of the RF fields they produce, e.g. dish antennae, also have a region known as the radiating near field that exists in between the reactive near field and the far field. In this region the wave impedance is equal to 377 ohm, but the wave fronts do not have planar characteristics: there is an oscillatory variation in power density with distance and the angular distribution of the radiation also changes with distance. Since the radiating near field is taken to extend to a distance of $2D^2/\lambda$ (where D is the largest dimension of the antenna) from the source, it is therefore necessary to be located beyond both this distance and

Fig. 1.2 The electromagnetic spectrum



The figure shows frequency increasing from left to right expressed in hertz (Hz) and in kHz (kilo-), MHz (mega-), GHz (giga-) and THz (tera-) (denoting multipliers of 10^3 , 10^6 , 10^9 and 10^{12}). Electromagnetic fields in the radiofrequency (RF) range can be used for communication purposes as radio waves. Mobile phones operate in the low-microwave range, around 1 GHz. The terms VLF, VF, LF, MF, HF, VHF, UHF, SHF, EHF denote very low frequency, voice frequency, low frequency, medium frequency, high frequency, very high frequency, ultra-high frequency, super-high frequency, and extremely high frequency, respectively. Beyond the frequencies used by radio waves follow the infrared, visible, ultraviolet, X-ray and gamma-ray portions of the spectrum. Above radiofrequencies and up to around the ultraviolet region, it is conventional to refer to the wavelength (expressed in metres and its multipliers) of the radiation, rather than frequency. Below the radiofrequency portion of the spectrum lie electromagnetic fields that are used for applications other than radiocommunications. Photon energy is expressed in electronvolts (eV and its multipliers). Prepared by the Working Group

about a wavelength from a source to be in the far-field region ([AGNIR, 2003](#)).

The incident EMFs (external fields when the body is not present) interact or couple with the human body and induce EMFs and currents within the body tissues. A different interaction mechanism exists for the electric- and magnetic-field components, as discussed in detail in Section 1.3. In general, both quantities must be determined to fully characterize human exposure, unless the exposure is to pure radiating fields. The coupling depends on the size of the wavelength relative to

the dimensions of the human body and, therefore, dosimetric interactions are often considered in three different frequency ranges: 30 kHz to 10 MHz (body larger than the wavelength), 10 MHz to 10 GHz (body dimensions comparable to the wavelength), and 10 GHz to 300 GHz (body dimensions much larger than the wavelength).

1.2 Sources of exposure

This section describes natural and man-made sources of RF fields to which people are exposed during their everyday lives at home, work and elsewhere in the environment. Fields from natural and man-made sources differ in their spectral and time-domain characteristics and this complicates comparisons of their relative strengths. The fields produced by natural sources have a much broader frequency spectrum than those produced by man-made sources and it is necessary to define a bandwidth of interest for comparison. In a bandwidth of 1 MHz, man-made fields will typically appear to be orders of magnitude stronger than natural ones, whereas if the entire bandwidth of 300 GHz of interest to this *Monograph* is chosen, natural fields may appear to be stronger than man-made ones at typical environmental levels ([ICNIRP, 2009a](#)).

When considering sources, it is helpful to clearly delineate the concepts of emissions, exposures and dose:

Emissions from a source are characterized by the radiated power, including its spectral and time-domain distributions: the polarization and the angular distribution (pattern) of the radiation. For sources that are large relative to their distance from a location where a person is exposed, it also becomes necessary to consider the spatial distribution of the emitted radiation over the entire structure of the source to fully describe it as an emitter.

Exposure describes the EMFs from the source at a location where a person may be present in terms of the strength and direction of the electric and magnetic fields. If these vary over the volume occupied by a person (non-uniform exposure), possibly because the source is close to them, or has strongly directional characteristics, it becomes necessary to quantify the RF fields over the space occupied by the person. The exposure depends not only on the source emissions and the geometrical relationship to the

source (distance, angular direction), but also on the effect of the environment on the radiated fields. This can involve processes such as reflection, shielding, and diffraction, all of which can modify the fields substantially.

Dose is concerned with quantities of effects inside the body tissues that are induced by the exposure fields. These include the electric- or magnetic-field strength in the body tissues and the specific energy absorption rate (SAR) (see Section 1.3.2, and Glossary). The strength of the electric fields within the body tissues is generally much smaller than that of the exposure fields outside the body, and depends on the electrical parameters of the tissues ([Beiser, 1995](#)).

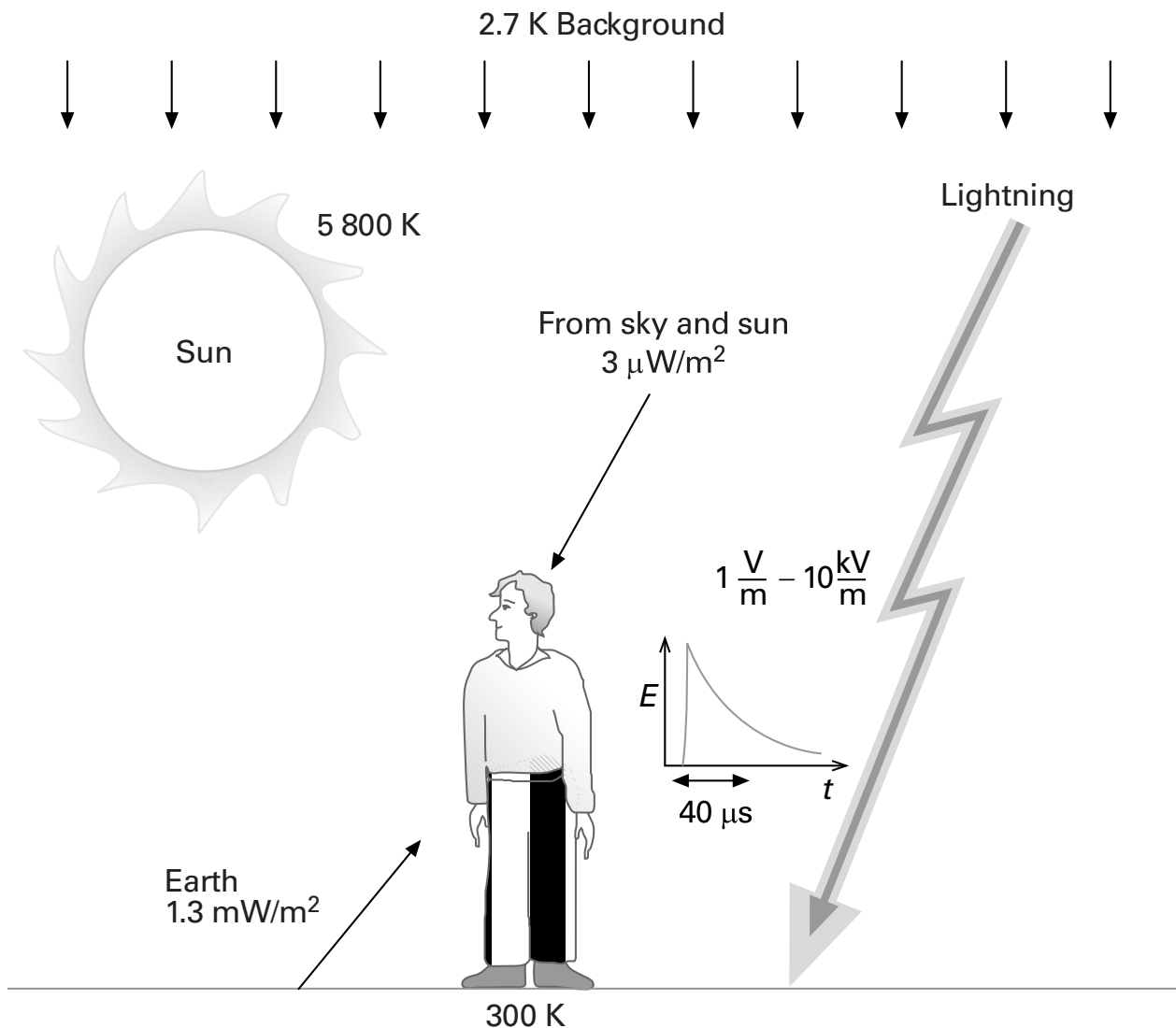
In most situations, the concept of emissions leading to exposure and then dose is helpful, but there are situations in which the presence of an exposed individual and the dose received affect the emissions from a source. This means that the intermediate concept of exposure cannot be isolated meaningfully, and dose has to be assessed directly from the source emissions either through computational modelling or via measurement of fields inside the body tissues. When the way in which a source radiates is strongly affected by the presence of an exposed person, the source and the exposed person are described as “mutually coupled”; a classic example of this is when a mobile phone is used next to the body.

1.2.1 Natural fields

The natural electromagnetic environment originates from the Earth (terrestrial sources) and from space (extraterrestrial sources) (Fig. 1.3). Compared with man-made fields, natural fields are extremely small at RFs ([ICNIRP, 2009a](#)).

The energy of natural fields tends to be spread over a very wide range of frequencies. Many natural sources emit RF radiation and optical radiation according to Planck’s law of “black-body radiation” (see Fig. 1.4; [Beiser, 1995](#)).

Fig. 1.3 Terrestrial and extraterrestrial sources of radiofrequency radiation



E, electric field strength; K, Kelvin; kV, kilovolt; m, metre; µs, microsecond; t, time; V, volt; W/m², watt per square metre. The solar radiation spectrum is similar to that of a black body with a temperature of about 5800 °K. The sun emits radiation across most of the electromagnetic spectrum, i.e. X-rays, ultraviolet radiation, visible light, infrared radiation, and radio waves. The total amount of energy received by the Earth at ground level from the sun at the zenith is approximately 1000 W/m², which is composed of approximately 53% infrared, 44% visible light, 3% ultraviolet, and a tiny fraction of radio waves (3 µW/m²). From [ICNIRP \(2009a\)](http://www.icnirp.de) <http://www.icnirp.de>

Fig. 1.4 Equations used in calculating energy and emitted power of black-body radiators

$$S(f,T) = \frac{2hf^2}{c^2} \frac{1}{\frac{hf}{e^{kT}} - 1} \quad J^* = \sigma T^4$$

(a) Planck's Law of "black body radiation"

$S(f,T)$ is the power radiated per unit area of emitting surface in the normal direction per unit solid angle per unit frequency by a black body at temperature T .

h is the Planck constant, equal to 6.626×10^{-34} Js.

c is the speed of light in a vacuum, equal to 2.998×10^8 m/s.

k is the Boltzmann constant, equal to 1.381×10^{-23} J/K.

f is the frequency of the electromagnetic radiation in hertz (Hz).

T is the temperature of the body in Kelvin (K).

(b) Stefan-Boltzmann Law

J^* , the black-body irradiance or emissive power, is directly proportional to the fourth power of the black-body thermodynamic temperature T (also called absolute temperature).

σ , the constant of proportionality, called Stefan-Boltzmann constant.

The total power emitted per unit surface area of a black-body radiator can be evaluated by integrating Planck's law over all angles in a half-space (2π steradians) and over all frequencies. This yields the Stefan-Boltzmann law (see Fig. 1.4), which describes how the power emitted by a black-body radiator increases with the fourth power of the absolute temperature ([Beiser, 1995](#)).

(a) Extraterrestrial sources

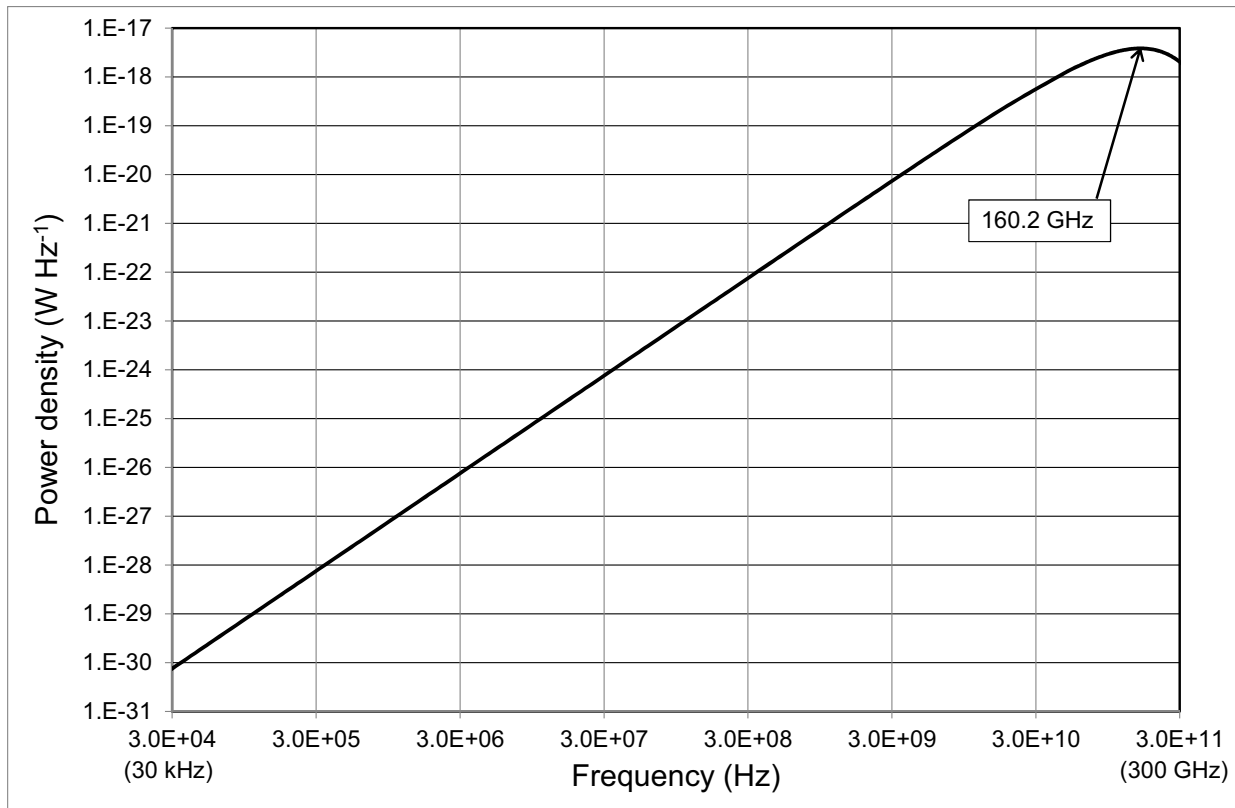
Extraterrestrial sources include electrical discharges in the Earth's atmosphere, and solar and cosmic radiation. Heat remaining from the "big bang" at the formation of the universe is evident as the cosmic microwave background (CMB), which presents as black-body radiation from all directions towards the Earth. The observed peak in the CMB spectrum is at a frequency of 160.2 GHz, which according to Planck's law (see Fig. 1.4) implies a temperature of 2.725 K ([Fixsen, 2009](#)). Fig 1.5 shows the results of evaluating Planck's law over the frequency range 30 kHz to 300 GHz. The total power density in this frequency range represents 80% of the total power density across all frequencies. Applying this factor to the results from Stefan-Boltzmann's

law at 2.725 K gives the power density at the surface of the Earth as $2.5 \mu\text{W}/\text{m}^2$.

The sun is also a black-body radiator and its spectrum shows a peak at 3.4×10^{14} Hz, a wavelength of 880 nm, commensurate with a surface temperature of 5778 K ([NASA, 2011](#)). Based on Planck's law, most of the sun's radiation is in the infrared region of the spectrum. Only a small proportion is in the frequency range 30 kHz to 300 GHz; this fraction represents about $5 \mu\text{W}/\text{m}^2$ of the total power density of $1366 \text{ W}/\text{m}^2$ incident on the Earth. This value is similar to that from the CMB, which contributes power from all directions, but the RF power from the sun is predominantly incident from the direction of the sun, and hence much reduced at night ([ICNIRP, 2009a](#)).

The atmosphere of the Earth has a marked effect on RF fields arriving from space. The ionosphere, which extends from about 60 km to 600 km above the Earth's surface, contains layers of charged particles and reflects RF fields at frequencies of up to about 30 MHz. Above a few tens of gigahertz, atmospheric water vapour and oxygen have an attenuating effect on RF fields, due to absorption. These effects mean that the RF power density incident at the Earth's surface

Fig. 1.5 Power density spectrum of the cosmic microwave background in the radiofrequency range (30 kHz to 300 GHz)



Prepared by the Working Group

from the sun and the CMB will be somewhat less than the $5 \mu\text{W}/\text{m}^2$ values given for each above. The International Commission on Non-Ionizing Radiation Protection (ICNIRP) gives the total power density arising from the sky and the sun as $3 \mu\text{W}/\text{m}^2$ at the surface of the Earth (see Fig. 1.3; [ICNIRP, 2009a](#)).

(b) Terrestrial sources

The Earth itself is a black-body radiator with a typical surface temperature of about 300 K (see Fig. 1.3). Most emissions from Earth are in the infrared part of the spectrum and only 0.0006% of the emitted power is in the RF region, which amounts to a few milliwatts per square metre from the Earth's surface. This is about a thousand times larger than the RF power density arising from the sky and the sun ([ICNIRP, 2009a](#)).

People also produce black-body radiation from their body surfaces (skin). Assuming a surface temperature of 37°C , i.e. 310 K, the power density for a person would be $2.5 \text{ mW}/\text{m}^2$ in the RF range. With a typical skin area of 1.8 m^2 , the total radiated power from a person is about 4.5 mW.

As mentioned above, the ionosphere effectively shields the Earth from extraterrestrially arising RF fields at frequencies below 30 MHz. However, lightning is an effective terrestrial source of RF fields below 30 MHz. The fields are generated impulsively as a result of the time-varying voltages and currents associated with lightning, and the waveguide formed between the surface of the Earth and the ionosphere enables the RF fields generated to propagate over large distances around the Earth.

On average, lightning strikes the Earth 40 times per second, or 10 times per square kilometre per year. Maps of annual flash rates based on observations by National Aeronautics and Space Administration (NASA) satellites can be consulted on the National Oceanic and Atmospheric Administration (NOAA) web site ([NOAA, 2011](#)). The EMFs from lightning are impulsive and vary depending on the nature of each stroke and also according to the distance at which they are measured. A typical pulse-amplitude of 4 V/m at 200 km corresponds to a peak power density of 42 mW/m², and a total pulse energy density of 2.5 mJ/m² ([ICNIRP, 2009a](#)). [Cooray \(2003\)](#) has described various mathematical models for return strokes, which are the strongest sources of RF-EMF associated with lightning. Peak electric-field strengths of up to 10 kV/m are possible within 1 km from where the lightning strikes. At distances greater than 100 km, the field strength decreases rapidly to a few volts per metre, with peak dE/dt of about 20 V/m per μ s, and then further decreases over a few tens of microseconds. [Willett et al. \(1990\)](#) measured the electric-field strength during return strokes as a function of time and conducted Fourier analysis to determine the average spectrum between 200 kHz and 30 MHz. The energy spectral density reduced according to $1/f^2$ at frequencies of up to about 10 MHz and more rapidly thereafter.

1.2.2 Man-made fields

There are numerous different sources of man-made RF fields. The more common and notable man-made sources of radiation in the RF range of 30 kHz to 300 GHz are presented in Fig. 1.6.

Sometimes such fields are an unavoidable consequence of the way systems operate, e.g. in the case of broadcasting and telecommunications, where the receiving equipment is used at locations where people are present. In other situations, the fields are associated with energy

waste from a process, e.g. in the case of systems designed to heat materials ([ICNIRP, 2009a](#)).

The typical emission characteristics of sources will be summarized here, along with exposure and dose information where available. However, it is important to recognize that fields typically vary greatly in the vicinity of sources and spot measurements reported in the literature may not be typical values. This is because assessments are often designed to identify the maximum exposures that can be reasonably foreseen, e.g. for workers near sources, and to ensure that these do not exceed exposure limits.

(a) Radio and television broadcasting

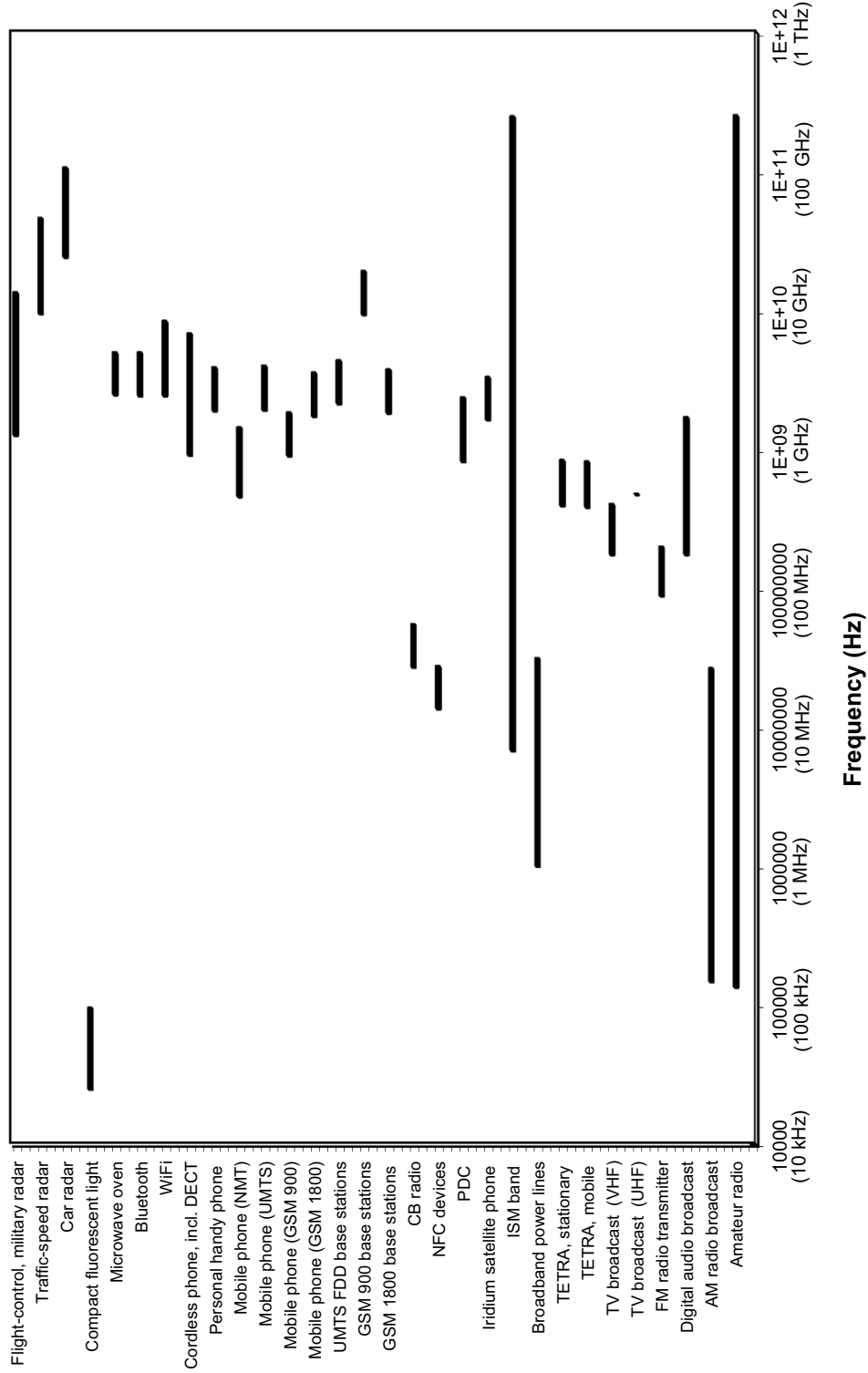
The frequency bands used for broadcasting of radio and television signals are broadly similar across countries and are shown in [Table 1.2](#).

Analogue broadcast radio has been available for many years and uses amplitude modulation (AM) in the long, medium and short-wave bands, but the sound quality is not as good as with frequency modulation (FM) in band II, which became available later and is now more popular for listening. The short-wave band continues to be important for international radio broadcasting, because signals in this frequency band can be reflected from the ionosphere to travel around the world and reach countries thousands of kilometres away ([AGNIR, 2003](#)).

Band III was the original band used for television broadcasting and continues to be used for this purpose in some countries, while others have transferred their television services to bands IV and V. Band III is also used for digital audio broadcasting (DAB), exclusively so in countries that have transferred all their television services to bands IV and V. Analogue and digital television transmissions presently share bands III, IV and V, but many countries are in the process of transferring entirely to digital broadcasting ([ICNIRP, 2009a](#)).

[AGNIR \(2003\)](#) have described broadcasting equipment in the United Kingdom in terms of

Fig. 1.6 Man-made sources of radiation in the radiofrequency range (30 kHz to 300 GHz)



AM, amplitude-modulated; CB, citizen band; DECT, digital enhanced cordless telecommunications; FDD, frequency-division duplex; FM, frequency-modulated; GSM, Global System for Mobile communications; ISM, industrial, scientific and medical; NFC, near-field communication; NMT, Nordic Mobile Telephony; PDC, personal digital cellular; TETRA, Terrestrial Trunked Radio; TV, television; UHF, ultra-high frequency; UMTS, Universal Mobile Telecommunications System; VHF, very high frequency; WiFi, standard wireless local area network (WLAN) technology.

Prepared by the Working Group

Table 1.2 Frequency bands used for broadcasting of television and radio signals

Designation	Frequency range	Usage
Long wave	145.5 – 283.5 kHz	AM radio
Medium wave	526.5 – 1606.5 kHz	AM radio
Short wave	3.9 – 26.1 MHz	International radio
UHF (Bands IV and V)	470 – 854 MHz	Analogue and digital TV
VHF (Band II)	87.5 – 108 MHz	FM radio
VHF (Band III)	174 – 223 MHz	DAB and analogue/digital TV

AM, amplitude modulation; DAB, digital audio broadcasting; FM, frequency modulation; TV, television; UHF, ultra high frequency; VHF, very high frequency

Adapted from [AGNIR \(2003\)](#)

the numbers of transmitters operating at a given power level in each frequency band ([Table 1.3](#)). The overall trends are probably similar in other countries and the main change since that time is likely to have been a growth in the number of digital transmitters for radio and television ([ICNIRP, 2009a](#)).

(i) *Long-, medium- and short-wave bands*

Antennae broadcasting in the long- and medium-wave bands tend to be constructed as tall metal towers, with cables linking the towers to each other and to the ground. Often, a single low-frequency (LF) or medium-frequency (MF) radiating structure may involve several closely located towers that are fed in such a way that a directional beam pattern is formed. Some towers are energized and insulated from the ground, while others are grounded and act as reflectors. Transmitters designed to provide local radio services, e.g. around cities, use powers in the range of 100 W to 10 kW, while a small number of transmitters that provide national services over large distances radiate up to a few hundred kilowatts ([ICNIRP, 2009a](#)).

The high-frequency (HF) band is used for international broadcasting and comprises wavelengths that are somewhat shorter than those in the long- and medium-wave bands. Curtain arrays, composed of multiple horizontal dipole antennae suspended between towers, are used to form narrow beams directed upwards towards

the required azimuth and elevation angles. The beams reflect off the ionosphere and provide services to distant countries without the need for any intermediate infrastructure. Typical curtain arrays can be up to 60 m in height and width, and might, for example, involve 16 dipoles arranged as four vertically stacked rows of four with a reflecting wire mesh screen suspended behind them. Given the transmission distances required, the powers are high, typically around 100–500 kW. The HF band has the fewest transmitters of any of the broadcast bands ([ICNIRP, 2009a](#)). [Allen et al. \(1994\)](#) reported 25 HF transmitters with powers in the range 100–500 kW and three with powers greater than 500 kW in the United Kingdom.

Broadcast sites can be quite extensive, with multiple antennae contained within an enclosed area of several square kilometres. A building containing the transmitters is generally located on the site and RF feeder cables are laid from this building to the antennae. On HF sites, switching matrices allow different transmitters to be connected to different antennae according to the broadcast schedule. The feeders may be either enclosed in coaxial arrangements or open, e.g. as twin lines having pairs of conductors around 15 cm apart suspended about 4 m above ground level.

In considering reported measurements of RF fields at MF/HF broadcast sites, it is important to note that workers may spend much of their time

Table 1.3 Approximate number of broadcast transmitters in the United Kingdom^a

Service class	Effective radiated power (kW)					
	0–0.1	> 0.1–1.0	> 1.0–10	> 10–100	> 100–500	> 500
Analogue TV	3496	589	282	122	86	19
DAB	4	126	121	–	–	–
Digital TV	134	177	192	2	–	–
MW/LW radio	14	125	38	19	12	–
VHF FM radio	632	294	232	98	72	–

^a For TV sites, each analogue channel (e.g. BBC1) or each digital multiplex counts as one transmitter.

DAB, digital audio broadcasting; FM, frequency modulation; LW, long wave; MW, medium wave; TV, television; VHF, very high frequency
Adapted from [AGNIR \(2003\)](#)

in offices, workshops or the transmitter halls. Such locations can be far from the antennae, resulting in exposure levels that are much lower than when personnel approach the antennae to carry out maintenance and installation work.

[Jokela et al. \(1994\)](#) investigated the relationship between induced RF currents flowing through the feet to ground and the RF-field strengths from MF and HF broadcast antennae. The MF antenna was a base-fed monopole, 185 m high, transmitting 600 kW at 963 MHz. At distances of 10, 20, 50, and 100 m from the antenna, the electric-field strength at 1 m height was around 420, 200, 60 and 30 V/m, respectively. At the same distances, currents in the feet were around 130, 65, 30 and 10 mA. The HF antenna was a 4 × 4 curtain array suspended between 60 m towers and radiating 500 kW at 21.55 MHz. The total field in front of the antenna at 1 m height ranged from about 32 V/m at 10 m through a maximum of 90 V/m at 30 m, a minimum of 7 V/m at 70 m and thereafter rose to around 20 V/m at distances in the range 100–160 m.

[Mantiply et al. \(1997\)](#) have summarized measurements of RF fields from MF broadcast transmitters contained in several technical reports from the mid-1980s to early 1990s from government agencies in the USA. A study based on spot measurements made at selected outdoor locations in 15 cities and linked to population statistics showed that 3% of the urban population

were exposed to electric-field strengths greater than 1 V/m, while 98% were exposed to field strengths above 70 mV/m and the median exposure was 280 mV/m. RF-field strengths were also measured near eight MF broadcast antennae, one operating at 50 kW, three at 5 kW and four at 1 kW. The measurements were made as a function of distance along three radials at most of the sites. At distances of 1–2 m, the electric-field strengths were in the range 95–720 V/m and the magnetic-field strengths were in the range 0.1–1.5 A/m, while at 100 m, electric-field strengths were 2.5–20 V/m and magnetic-field strengths were in the range 7.7–76 mA/m.

[Mantiply et al. \(1997\)](#) also reported field measurements near short-wave (HF) broadcast antennae. As mentioned earlier, these are designed to direct the beams upwards at low elevation angles. Hence, the field strengths at locations on the ground are determined by sidelobes (see Glossary) from the antennae and they vary unpredictably with distance and from one antenna to another. Measurements were made at four frequencies in the HF band and at six locations in a community around 10 km from an HF site, which was likely to have transmitted 250 kW power. Electric- and magnetic-field strengths at individual frequencies varied in the ranges 1.5–64 mV/m and 0.0055–0.16 mA/m, while the maximum field strengths just outside the site boundary were 8.6 V/m and 29 mA/m.

Field strengths measured at a distance of 100 m along a “traverse” tangential to the beam from a curtain array transmitting at 100 kW were in the ranges 4.2–9.2 V/m and 18–72 mA/m. A final set of measurements was made at a distance of 300 m from another curtain array transmitting at 100 kW, while the beam was steered through $\pm 25^\circ$ in azimuth. The field strengths were in the ranges 1.7–6.9 V/m and 14–29 mA/m.

(ii) VHF and UHF bands

The powers used for broadcasting in the VHF and UHF bands vary widely according to the area and terrain over which coverage is to be provided (Table 1.2). UHF transmissions are easily affected by terrain conditions, and shadowed areas with poor signal strength can occur, e.g. behind hills and in valleys. For this reason, in addition to a main set of high-power transmitters, large numbers of local booster transmitters are needed that receive signals from the main transmitters and rebroadcast them into shadowed areas. The main transmitters are mounted at the top of masts that are up to several hundreds of metres high and have effective radiated powers (ERPs) (see Glossary) of up to about 1 MW, while the booster transmitters have antennae that are mounted much nearer to the ground and mostly have powers of less than 100 W. VHF signals are less affected by terrain conditions and fewer booster transmitters are needed.

Typical high-power broadcast transmitter masts are shown in Fig. 1.7.

Access to the antennae on high-power VHF/UHF masts is gained by climbing a ladder inside the tower; reaching the antennae at the top involves passing in close proximity to radiating antennae at lower heights. The VHF transmissions have wavelengths of similar dimensions to the structures that form the tower itself, e.g. the lengths of the steel bars or the spaces between them, and hence tend to excite RF current flows in these items. Standing waves (see Glossary) can be present within the tower, and the measured

field strengths can be strongly affected by the presence of a person taking measurements. Thus, measurements of field strength can seem unstable and difficult to interpret. Currents flowing within the body can be measured at the wrist or ankle and these are more directly related to the specific absorption rate (SAR; dose) in the body than the fields associated with the standing waves. Hence, it can be preferable to measure body current (see Section 1.3) rather than field strength on towers with powerful VHF antennae.

Several papers discussed by [ICNIRP \(2009a\)](#) have reported measurement results in the range of tens to hundreds of volts per metre within broadcast towers, but it is not clear how representative these spot measurements are of typical worker exposures. [Cooper et al. \(2004\)](#) have used an instrument worn on the body as personal dosimeter to measure electric- and magnetic-field strengths during work activities at a transmitter site. They reported that a wide temporal variation in field strengths was typically found within any single record of exposure to electric or magnetic fields during work on a mast or tower used for high-power VHF/UHF broadcasts. Fig 1.8 shows a typical trace that was recorded for a worker during activities near the VHF antennae while climbing on a high-power VHF/UHF lattice mast. The field strength commonly ranged from below the detection threshold of about 14 V/m to a level approaching or exceeding the upper detection limit of about 77 V/m. The highest instantaneous exposures usually occurred when the subject was in the vicinity of high-power VHF antennae or when a portable VHF walkie-talkie radio was used to communicate with other workers.

Field strengths around the foot of towers/masts have also been reported and seem quite variable. [Mantiply et al. \(1997\)](#) described values in the range of 1–30 V/m for VHF television, 1–20 V/m for UHF television and 2–200 V/m for VHF FM radio sites. Certain designs of antennae have relatively strong downward-directed sidelobes,

Fig. 1.7 Typical antenna masts for power broadcasting of radio and television signals**(a)****(b)**

(a) A concrete tower, 368 m high, with a spherical structure at just above 200 m. This is accessed by lifts from ground level and contains various equipment as well as a public restaurant. The radiating antennae are above the sphere and the antennae operating at the highest frequencies are nearest to the top. Multiple dipole antennae protrude through the wall of the red/white cylinder to provide FM radio services in band II, and television and DAB services in band III. Contained within the top-most section of the tower are the band IV and V antennae for more television services.

(b) A steel-lattice tower with the television antennae in the white cylinder at the top. Antennae for VHF and DAB broadcast radio services are mounted on the outside of the tower just below the television antenna and there are multiple antennae for other communications purposes at lower heights. The transmitters are in a building near the base of the tower and the coaxial cables carrying the RF to the transmitting antennae pass up inside the tower.

Courtesy of the Health Protection Agency, United Kingdom

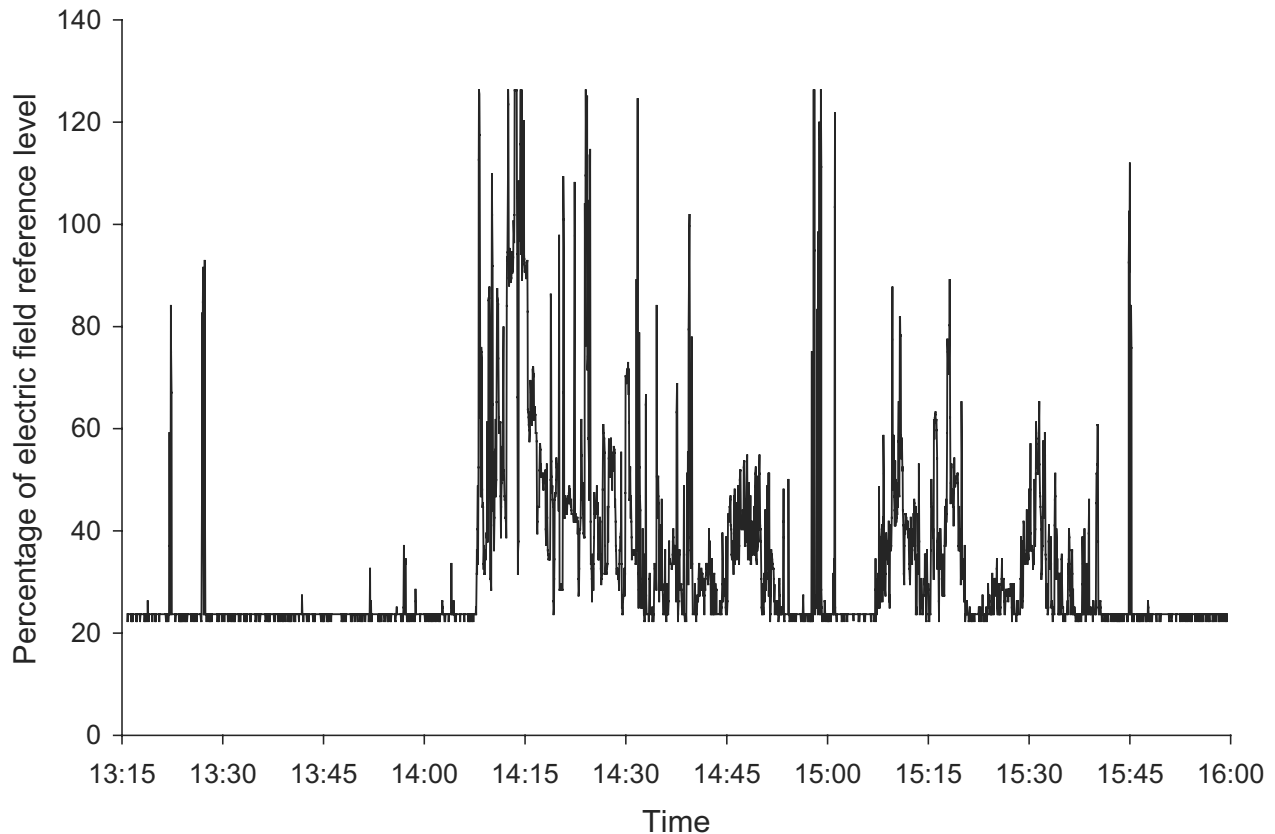
known as grating lobes, which is a possible explanation for such variability.

VHF/UHF broadcast antennae are designed to direct their beams towards the horizon, usually in all directions around the tower. Hence, field strengths at ground level and in communities near the tower are much lower than at comparable distances within the beam. When the beams do eventually reach ground level, they have spread out considerably, again implying that exposures for the general public are substantially lower than

those for workers at locations to which they have access, as summarized above ([ICNIRP, 2009a](#)).

[Mantiply et al. \(1997\)](#) report studies of population exposure in the USA conducted during the 1980s and based on spot measurements at selected outdoor locations. An estimated 50%, 32% and 20% of the population were exposed at greater than 0.1 V/m from VHF radio, VHF television and UHF television signals, respectively. VHF radio and television caused exposures to 0.5% and 0.005% of the population at greater than

Fig. 1.8 Relative electric-field strength recorded for an engineer operating on a mast supporting antennae for high-power VHF/UHF broadcast transmissions



The reference level is 61 V/m, as taken from the [ICNIRP \(1998\)](#) exposure guidelines for workers over the relevant frequency range (10–400 MHz). UHF, ultra high frequency; VHF, very high frequency. From [Cooper et al. \(2004\)](#). By permission of Oxford University Press.

2 V/m, while UHF television caused exposure to 0.01% of the population at greater than 1 V/m.

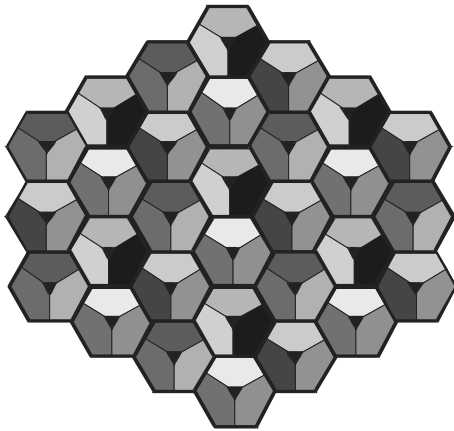
Field strengths associated with VHF/UHF radio and television broadcast signals were measured at 200 statistically distributed locations in residential areas around Munich and Nuremberg in Germany ([Schubert et al., 2007](#)). The aim of the study was to investigate whether the levels had changed as a result of the switch-over from analogue to digital broadcasting, and measurements were made before and after this change occurred at each location. The median power density was $0.3 \mu\text{W}/\text{m}^2$ (11 mV/m) for the analogue signals and $1.9 \mu\text{W}/\text{m}^2$ (27 mV/m) for the digital signals. FM radio signals had median

power densities of $0.3 \mu\text{W}/\text{m}^2$ (11 mV/m), similar to the analogue television signals, and the values ranged over approximately two orders of magnitude on either side of the medians for all types of broadcast signal. It is interesting to note that these values seem to be lower than those reported in the USA during the 1980s.

(b) Cellular (mobile-phone) networks

Unlike broadcasting, for which high-power transmitters are used to cover large areas extending 100 km or more from the transmitter, cellular networks employ large numbers of low-power transmitters, known as base stations, which are scattered throughout an area where coverage

Fig. 1.9 Example of a coverage plan for a cellular network



Each cell is hexagonal, with a base station at its centre and configured to provide signals over three sectors of 120 degrees. The shading show how coverage is provided everywhere by use of 12 frequency channels, none of which are used in the adjacent cells.

Courtesy of the Health Protection Agency, United Kingdom

is to be provided. This is because communications are two-way (duplex) in cellular networks, with each user requiring their own dedicated communication channels, both for the uplink (phone to base station) and for the downlink (base station to the phone). Each base station has limited capacity in terms of the number of calls it can serve simultaneously, so the transmitters are closer together in locations where there is a high density of users. For example, the transmitters may be about 10 km apart in sparsely populated areas, but 100 m or less apart in city centres.

An important consideration in the design of cellular networks is that operators have a limited spectrum window available and have to reuse their frequency channels to provide coverage everywhere. A typical frequency map illustrating how coverage can be provided with 12 frequency channels is shown in Fig. 1.9. Signals that use the same frequency in different cells can potentially interfere with each other, but the signal strength diminishes with increasing distance from base stations and frequencies are not reused in adjacent cells/sectors. Hence, services can be provided without interference, provided that

the radiated powers of phones and base stations are minimized during calls. This principle has important consequences for the RF exposures of people using phones and living near base stations ([ICNIRP, 2009a](#)).

Developments in mobile-phone technology are broadly categorized according to four different generations ([Table 1.4](#)). The first-generation networks (1G) were rolled-out in the mid-1980s and included Advanced Mobile Phone System (AMPS) in North America, Total Access Communication Systems (TACS) in much of Europe, Nippon Telegraph and Telephone (NTT) in Japan, and Nordic Mobile Telephony (NMT) in Scandinavia. The systems were based on analogue technology and used frequency modulation to deliver voice-communication services. These networks mostly closed down from around the year 2000, as users moved to later generations of the technology ([ICNIRP, 2009a](#)).

Second-generation networks (2G) were established in the early 1990s and continue to operate. They are based on digital technology and use voice coding to improve spectral efficiency. Many systems use time-division multiple access (TDMA) within their frequency channels and such systems include Global System for Mobile (GSM) in Europe, Personal Digital Cellular (PDC) in Japan, and both Personal Communication Systems (PCS) and D-AMPS (digital AMPS, also known as “TDMA”) in North America. Other north-American systems are known as CDMA, because they use code-division multiple access. 2G systems were extended to include some basic data services, but subsequent systems with enhanced data services were usually termed 2.5G ([ICNIRP, 2009a](#)).

The third generation of mobile phones (3G), with comprehensive data services, became available in the early 2000s. These phones have developed to become today’s “smartphones,” although it is important to recognize that they are fully backward-compatible with 2G networks and whether 2G or 3G is used at any given time

Table 1.4 Frequency bands originally used by different mobile-phone systems

Generation	Start date of commercial availability ^a	Main geographical region	System ^b	Handset band (MHz)	Base-station band (MHz)	Channel spacing (kHz)
1	1981	Nordic countries	NMT450	453.5 – 457.5	463.5 – 467.5	25
	1986		NMT900	890 – 915	935 – 960	12.5
	1985	Europe	TACS/ETACS	872 – 915	917 – 960	25
	1989	Japan	JTACS/NTACS	898 – 925	860 – 870	25/12.5
	1985	Germany	NET-C	451.3 – 455.74	461.3 – 465.74	20
	1985	USA & Canada	AMPS	824 – 849	869 – 894	30
	1985		N-AMPS	824 – 849	869 – 894	10
	1987	Japan	NTT	925 – 940	870 – 885	25
	1992	USA & Canada	TDMA800	824 – 849	869 – 894	30
	1998		TDMA1900	1850 – 1910	1930 – 1990	30
2	1992	Europe	GSM900	890 – 915	935 – 960	200
	1993		GSM1800	1710 – 1785	1805 – 1880	200
	2001	USA & Canada	GSM1900 (PCS)	1850 – 1910	1930 – 1990	200
	1993	Japan	PDC800	940 – 956	810 – 826	25
	1994		PDC1500	1429 – 1465	1477 – 1513	25
	1998	USA & Canada	CDMA800	824 – 849	869 – 894	1250
	1997		CDMA1900	1850 – 1910	1930 – 1990	1250
	3	2001	World	IMT-2000 (W-CDMA)	1920 – 1980 ^c	2110 – 2170 ^c
4		World	LTE	Many possible	Many possible	Various

^a The start dates of use will be different depending on country.

^b For abbreviations, see [Cardis et al. \(2011b\)](#) and [Singal \(2010\)](#).

^c Technical standards for a 2001 version for the 3G systems (IMT-2000). Note that standards for the 3G systems evolve quickly. Compiled by the Working Group and adapted mainly from the references mentioned in footnote b

depends on network coverage and how operators have chosen to manage call/data traffic within their network. The systems use CDMA radio-access methods ([ICNIRP, 2009a](#)).

A fourth generation (4G) of the technology is just starting to be rolled out to meet the increasing demand for data services. Some systems are known as Long-term Evolution (LTE) and use orthogonal frequency-division multiplexing (OFDM), while others are based on Worldwide Interoperability for Microwave Access (WiMax). As with 3G services, this technology will be overlaid on other services, and phones will be able to support multiple access modes (4G, 3G and 2G) ([Buddhikot et al., 2009](#)).

The frequency bands originally used by cellular networks in various parts of the world

are shown in [Table 1.4](#). It is important to note that spectrum liberalization is ongoing at present, such that operators who hold a license for a particular part of the spectrum may choose to use it to provide services with any technology they wish. For example, bands originally reserved for 2G services such as GSM are being made available for 3G/4G services in many countries as demand shifts from 2G to systems with more capacity for data services. Also, with the move to digital-television broadcasting, the spectrum in the frequency range of 698 to 854 MHz is becoming available and being reallocated to 3G/4G cellular services ([Buddhikot et al., 2009](#)).

(i) Mobile-phone handsets

The output powers and – where TDMA is used – the burst characteristics of various types of mobile phones are summarized in [Table 1.5](#). Analogue mobile phones were specified to have maximum equivalent isotropically radiated powers (EIRP) of 1 W, but the antennae were not isotropic and would have had gains of around 2 dB. This implies the radiated powers would have been around 600 mW. 2G mobile phones that use TDMA have time-averaged powers that are less than their peak powers according to their duty factors, i.e. the time they spend transmitting, as a proportion of the total. For example, GSM phones that transmit at a power level of 2 W in the 900 MHz band (GSM900) have time-averaged powers that are 12% of this, i.e. 240 mW. Maximum time-averaged output powers are generally in the range of 125–250 mW for 2G onwards.

Mobile phones are generally held with their transmitting antennae around 1–2 cm from the body, so the RF fields they produce are highly non-uniform over the body and diminish rapidly in strength with increasing distance. The fields penetrate body tissues, leading to energy absorption, which is described by the SAR. SAR values are derived by phone manufacturers under a series of prescribed tests and the maximum value recorded under any of the tests is reported in the product literature. Values in normal usage positions should be lower than the values declared by manufacturers because the positions used in the testing standards are designed to mimic near-worst-case conditions.

While [Table 1.5](#) gives maximum output powers for phones, the actual power used at any point during a call is variable up to this maximum. As mentioned above, to minimize interference in the networks, the power is dynamically reduced to the minimum necessary to carry out calls. [Vrijheid et al. \(2009a\)](#) found that the reduction was on average to around 50% of the maximum

with GSM phones, whereas [Gati et al. \(2009\)](#) reported that 3G phones only operated at a few percent of the maximum power.

Another consideration is that GSM phones employ a mode called discontinuous transmission (DTX), under which their transmission-burst pattern changes to one with a lower duty factor during the periods of a conversation when the mobile-phone user is not talking. [Wiar et al. \(2000\)](#) found that DTX reduced average power by about 30% for GSM phones.

(ii) Time trends in SAR for mobile phones

As shown in [Table 1.5](#), analogue mobile phones had higher specified maximum radiated powers than digital ones (typically 0.6 W versus 0.1–0.25 W). While these systems are no longer in use and few data on exposure are available, it is of interest to consider whether exposures from these phones would have been higher than with present-day phones. Key differences, aside from relative power levels, are that analogue phones were larger than their modern digital counterparts and that they generally had larger antennae, e.g. extractable whip antennae rather than the compact helices and patch antennae used nowadays. The increased distance between the antenna and the head would have reduced the SAR level overall, and the larger size of the antenna would have led to a more diffuse distribution of SAR in the head.

The evolution of localized SAR values over time is also interesting to consider. [Cardis et al. \(2011b\)](#) assembled a database of reported peak 1-g and 10-g SARs for phones from a range of publications and web sites. Most data covered the years 1997–2003, and no significant upward or downward trends over this time period were found for the 900 MHz or 1800 MHz bands.

In summary, the peak spatial SARs (psSAR) do not seem to have changed significantly over time as analogue phones have been replaced by digital ones. However, the more diffuse nature of the distributions produced by analogue phones

Table 1.5 Output powers and TDMA characteristics of various types of mobile phone

System	Peak power (W)		Burst duration (ms)	TDMA duty factor	Average power (W)
	EIRP	Output			
GSM900	-	2.0	0.5769	0.12	0.24
GSM1800	-	1.0	0.5769	0.12	0.12
PCS1900	-	1.0	0.5769	0.12	0.12
NMT450	1.5	0.9	-	NA	0.9
PDC	-	0.8	3.333 or 6.666	1/6 or 1/3	0.133 or 0.266
NMT900	1.0	0.6	-	NA	0.6
TACS/ETACS	1.0	0.6	-	NA	0.6
AMPS/NAMPS	1.0	0.6	-	NA	0.6
TDMA800	-	0.6	6.666	1/3	0.2
TDMA1900	-	0.6	6.666	1/3	0.2
CDMA800	-	0.25	-	NA	0.25
CDMA1900	-	0.25	-	NA	0.25
IMT-2000	-	0.25	-	NA	0.25

EIRP, equivalent isotropically radiated power; NA, not applicable; TDMA, time-division multiple access
Compiled by the Working Group

would likely have led to a greater overall SAR in the head, including the brain.

(iii) Phones not making calls

The emitted powers from phones when they are on standby and not making calls are also of interest. Systematic studies have not been published on this topic, but transmissions under these conditions are brief and infrequent, and exposure is expected to be very small when averaged over time.

Phones equipped for data services such as e-mail will transmit for longer time periods than ordinary phones because they will be checking e-mail servers and synchronizing databases held on the phone with those on remote servers. Also, uploading large files such as videos and photographs may take many minutes. The phone is unlikely to be held against the user's head while this is taking place, although it may be in the user's pocket or elsewhere on the body, which may lead to local emissions at a higher power level than during calls, e.g. if general packet radio service (GPRS) is used, involving multislot transmission with GSM.

The sending of a text message from a mobile phone involves a short period of transmission. [Gati et al. \(2009\)](#) showed that a long text message would take at most 1.5 seconds to send with GSM systems.

(iv) Hands-free kits and Bluetooth earpieces

A phone may sometimes be used with a wired hands-free kit, in which case parts of the body other than the head may be exposed to maximal localized SARs, e.g. if the phone is placed in the user's pocket during the call. While one might expect that the audio cable to the ear-piece would not efficiently guide RF fields to the ear-piece, and that the use of wired hands-free kits would lead to greatly reduced SARs in the head due to the increased distance of the phone from the head, there have been suggestions that this is not always the case.

[Porter et al. \(2005\)](#) showed that the layout of the cables of the hands-free kit was a critical factor in determining head exposures and that certain geometries could result in appreciably more power being coupled into the audio cable than others. However, in all of the combinations

tested, the maximum value for SAR 10 g was lower when a hands-free kit was used than when it was not. [Kühn *et al.* \(2009a\)](#) further developed procedures for the testing of hands-free kits under worst-case and realistic conditions of use and applied them to a set of phones and kits. The authors concluded that exposure of the entire head was lower when a hands-free kit was used than when the phone was held directly against the head, but that there might be very localized increases in exposure in the ear.

Wireless hands-free kits are available that use the Bluetooth RF communications protocol to link to a mobile-phone handset located within a few metres of the body. This protocol provides for RF transmissions in the frequency range 2.4–2.5 GHz at power levels of 1, 2.5 or 100 mW. Only the lowest of these power levels would be used with a wireless hands-free kit and these are around a hundred times lower than the maximum output powers of mobile phones. In the study on wired hands-free kits mentioned above, [Kühn *et al.* \(2009a\)](#) also tested Bluetooth wireless hands-free kits and concluded that they are responsible for a low but constant exposure.

(v) *Mobile-phone base stations*

The base stations that provide mobile-phone services to come in many different sizes and shapes, according to their individual coverage requirements.

The radiated powers and heights of mobile-phone base-station antennae are highly variable. [Cooper *et al.* \(2006\)](#) collected data on base-station antenna height and power from all cellular operators in the United Kingdom, a total of 32 837 base stations, for the year 2002. The data are presented in Fig. 1.10 and show that base-station powers typically vary from about 0.1 W to 200 W and that heights range from about 3 m to 60 m above ground level. There is a large group of base stations with heights in the range 15–25 m and powers in the range 20–100 W, and a second group with heights in the range 2–6 m

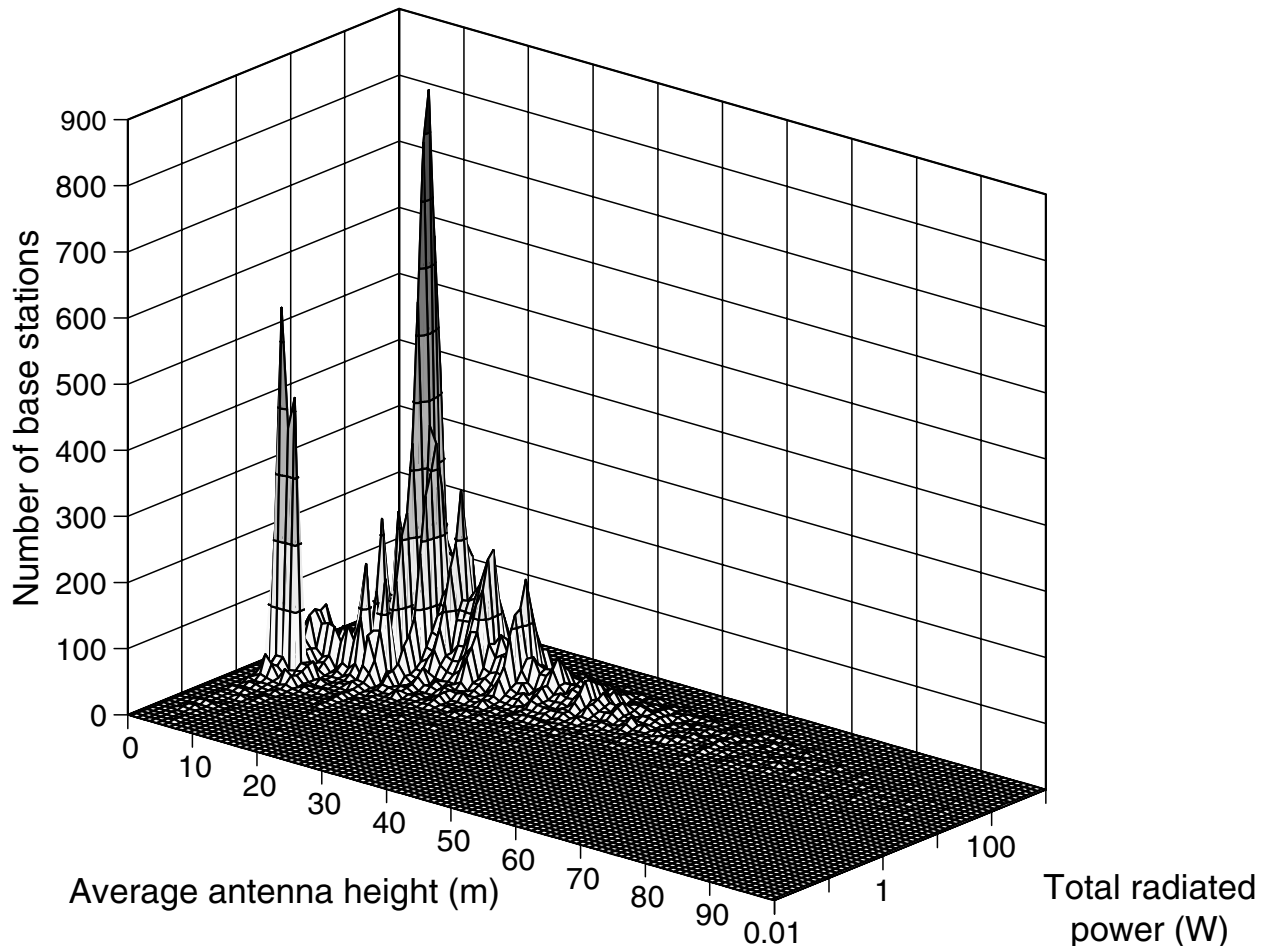
and powers of about 2 W. Cooper *et al.* concluded that the base stations in the first group are likely to serve macrocells and provide the main coverage for cellular networks, while those in the second group are likely to be microcells and provide a second layer of coverage, e.g. in densely populated areas.

Numerous spot measurements have been carried out to determine levels of exposure in the vicinity of mobile-phone base stations, often within national campaigns to address public concerns. Generally, these spot measurements take into account exposure contributions from all signals in the bands used by the base station at the time of measurement, but ignore other parts of the spectrum, such as those used by broadcast transmitters. [Mann \(2010\)](#) summarized the United Kingdom audit programme, which encompassed 3321 measurements at 541 sites comprising 339 schools, 37 hospitals and 165 other locations. Exposure quotients, describing the fraction of the ICNIRP general public reference level ([ICNIRP, 1998](#)) that is contributed collectively by the signals measured, are shown in Fig. 1.11 as a cumulative distribution.

Fig. 1.11 includes a log-normal curve fitted optimally (least squares) to the data. The curve suggests that the data are approximately log-normally distributed, although with a longer tail towards the lower values. The quotient values are 8.1×10^{-6} ($3.0 \times 10^{-8} - 2.5 \times 10^{-4}$), where the first figure is the median value and the values in parentheses indicate the range from the 5th to the 95th percentile. About 55% of the measurements were made outdoors and these were associated with higher exposure quotients than the indoor measurements. The median quotients for the outdoor and indoor measurements were 1.7×10^{-5} and 2.8×10^{-6} respectively, i.e. the outdoor median was around six times higher than the indoor median ([Mann, 2010](#)).

The exposure quotients may be converted to electric-field strengths or power densities by assuming a value for the reference level, but the

Fig. 1.10 Distribution of 32 837 base stations in the United Kingdom according to average antenna height and total radiated power



Antenna height is given as an average value since some base stations with multiple antennae have the antennae mounted at different heights. From [Cooper et al. \(2006\)](#)

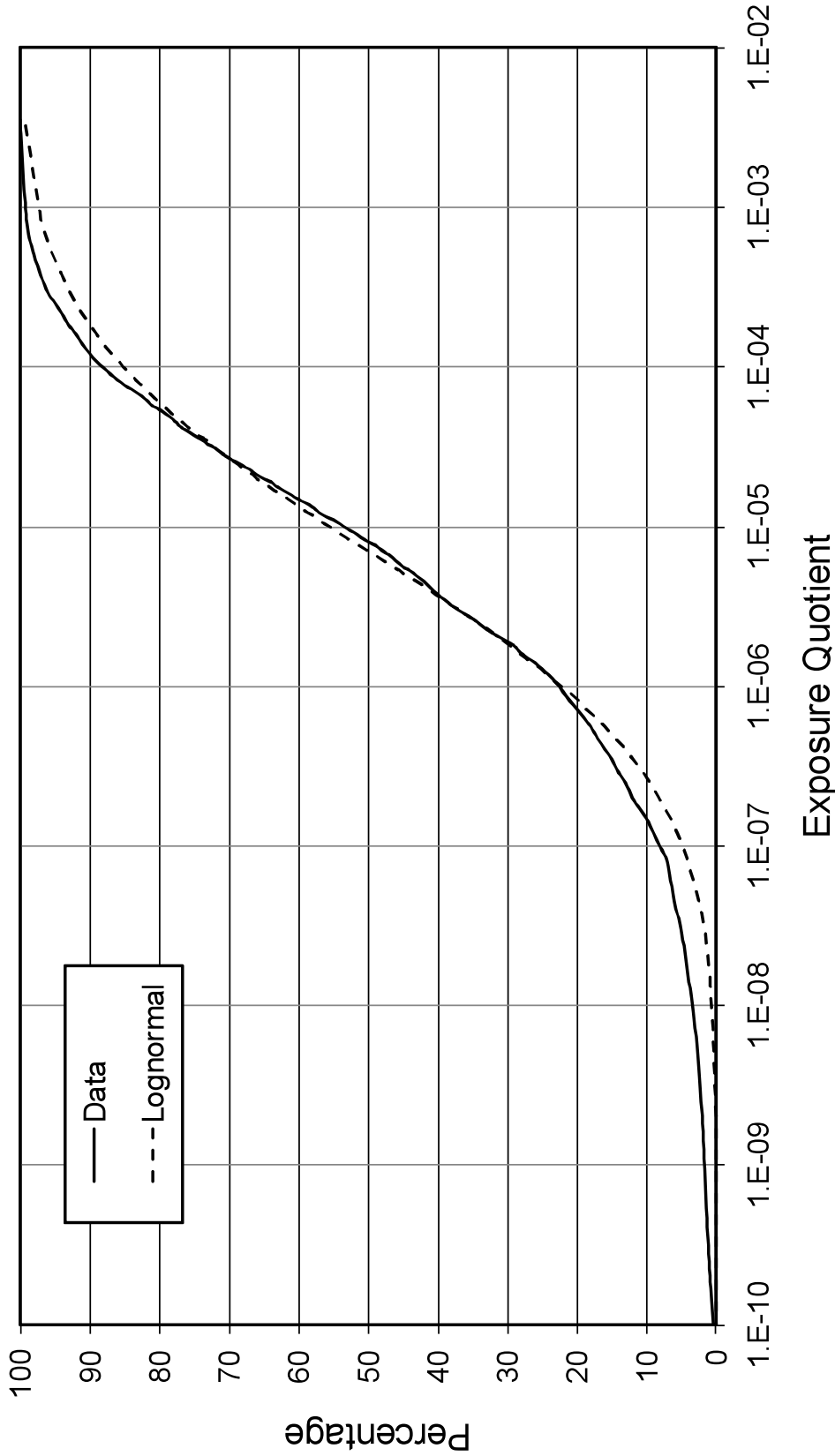
latter varies from 2 to 10 W/m² over the frequency range considered in the measurements (TETRA at 390 MHz to UMTS at 2170 MHz). The variation of the reference level is, however, very much less than the variation in the exposure quotients, so taking 4.5 W/m² as the reference level (the value at 900 MHz) still yields useful data. The power densities and electric-field strengths based on this assumed value are shown in [Table 1.6](#).

[Table 1.6](#) shows electric-field strengths that range from about ten to a few hundred millivolts per metre indoors, where people spend most of their time. However, in considering these data it

is important to recognize that the indoor sites in this study were selected according to public concern regarding a nearby base station; these field strengths may thus be higher than would be found at locations representative of exposure of the general population.

[Petersen & Testagrossa \(1992\)](#) published measurements of power densities around analogue base-station sites in the USA, transmitting in the frequency range 869–894 MHz. A basic start-up site would serve a cell with a range of up to 12–16 km and provide up to 16 signals (each serving one phone call) from a

Fig. 1.11 Cumulative distribution of exposure quotients corresponding to 3321 spot measurements made by Office of Communications at 499 sites where public concern had been expressed about nearby base stations



The exposure quotients were calculated by dividing the power density of each individually measured signal by the general public reference level at its frequency according to [ICNIRP \(1998\)](#) and then summing these individual signal quotients to obtain a total quotient of the reference level. The figure shows a log-normal curve fitted to the data. From [Mann \(2010\)](#). Copyright © 2010. Published by Elsevier Masson SAS on behalf of Académie des sciences. All rights reserved.

Table 1.6 Summary of exposure quotients measured in the United Kingdom

Category	No. of measurements	Exposure quotient ($\times 10^{-6}$)		Power density ($\mu\text{W}/\text{m}^2$)		Electric-field strength (mV/m)	
		Median	Range ^a	Median	Range ^a	Median	Range ^a
All data	3321	8.1	0.03 – 250	37	0.13 – 1100	120	7.1 – 650
Outdoor	1809	17	0.052 – 314	77	0.23 – 1400	170	9.3 – 730
Indoor	1516	2.8	0.024 – 124	13	0.11 – 560	69	6.4 – 460

^a Range from 5th to 95th percentiles

These data are from an audit of base stations up to the end of 2007. Equivalent power densities and electric-field strengths are given assuming a reference level of $4.5 \text{ W}/\text{m}^2$.

Adapted from [Mann \(2010\)](#)

single omni-directional antenna. As demand grew, sites could be expanded to split cells into three sectors with up to six antennae mounted on a triangular mast head. Again, each antenna would provide up to 16 signals, so there would be a maximum of 96 signals available, 32 of which would have been directed into each sector. Values for nominal ERP (see Glossary) were about 100 W and so the radiated power would have been of the order of 10 W per signal from omni-directional and sectored sites, with typical antenna gains in the range of 9–10 dB and 8–12 dB, respectively.

For four masts ranging from 46 to 82 m in height, measurements were made at intervals along radials from the bases of the masts out to distances of a few hundred metres. Individual signals from a given antenna were found to vary in strength at any given measurement position and the sidelobe structure of the antenna was evident in that the signal strength had an oscillatory dependence on distance. The maximum power density per signal was $< 100 \mu\text{W}/\text{m}^2$, except in proximity to metal structures near the foot of the tower. Thus, even for 96 signals transmitted simultaneously, the maximum aggregate power density possible would have been $< 10 \text{ mW}/\text{m}^2$.

[Henderson & Bangay \(2006\)](#) reported on a survey of exposures around 60 base station sites in Australia transmitting CDMA800 (29 sites), GSM900 (51 sites), GSM1800 (12 sites) and 3G UMTS (35 sites) signals. Initially, computer modelling was carried out to identify

the direction from the mast where maximum exposures were expected. Measurements were then made at distances of 50, 200 and 500 m, and further measurements were then made at the distance where maximum exposures were predicted, which varied from 14 to 480 m from the mast as a consequence of antenna height, pattern and tilt. The maximum recorded power density of $7.8 \text{ mW}/\text{m}^2$ corresponded to an exposure quotient of 0.002 (0.2%) relative to the ICNIRP public reference level (identical to the Australian standard at the frequencies concerned). The cumulative distributions also reported in this paper showed roughly similar median exposure quotients of about 0.0015 at 50 and 200 m, 0.0001 at 500 m and 0.004 at the maximum.

The study by [Cooper *et al.* \(2006\)](#) mentioned above focused on measurements around 20 GSM base stations with powers $< 5 \text{ W}$ and heights $< 10 \text{ m}$, selected randomly from all base stations in the United Kingdom. From the total of 32 837 base stations, 3008 eligible stations were identified. The antennae of the selected base stations were often fixed to the walls of buildings at a minimum height of 2.8 m. Theoretical calculations based on the radiated powers showed that the minimum height at which the reference level could be reached was 2.4 m above ground. Exposure measurements were made as a function of distance at 10 of the 20 sites and at 610 locations in total, ranging from 1 to 100 m from the antenna. The highest spot measurement at

an accessible location represented 8.6% of the reference level and the exposures more generally ranged from 0.002% to 2% of the ICNIRP public reference level. Empirical fits showed that the exposure quotients decreased in a way that was inversely proportional to the distance, for distances up to about 20 m from the antennae and thereafter diminished with the fourth power of distance. Exposures close to microcell base stations were found to be higher than close to macrocell base stations, because the antennae were at lower heights and could be approached more closely by the public.

[Kim & Park \(2010\)](#) made measurements at 50 locations between 32 and 422 m from CDMA800 and CDMA1800 base stations in the Republic of Korea. The base stations were selected to represent locations where concern had been expressed by the local population. The highest reported electric field level was 1.5 V/m, equivalent to an exposure quotient of 0.0015 (0.15%) compared with the reference level, and the median exposure quotient was below 0.0001 (0.01%).

The most recent studies have used personal-exposure meters worn for periods of up to several days by groups of volunteers. These studies are covered in Section 1.6.1, and provide information not only on exposure from base stations, but also from other environmental transmitters during typical activities.

(vi) *Terrestrial Trunked Radio (TETRA)*

TETRA is a cellular radio system designed to meet the needs of professional users and emergency services. The handsets can be used like mobile phones, but are normally used as walkie-talkies, held in front of the face and in push-to-talk (PTT) mode. Remote speaker microphones and a variety of covert add-ons are also available. When the handsets are used with accessories, the transmitting handset may be mounted on the belt, on the chest, or elsewhere on the body. Systems for use in vehicles with the transmitting antennae mounted externally are also available.

The operating principles and the detailed characteristics of the signals involved are described in a review by [AGNIR \(2001\)](#).

Several frequency bands are available between 380 and 470 MHz, as well as one set of bands near 900 MHz. Handsets can have peak emitted powers of 1 W or 3 W, while vehicle-mounted transmitters can have powers of 3 W or 10 W. Base stations have similar powers to those used for mobile-phone networks, i.e. a few tens of watts. The system uses TDMA, although the frame rate is slower than that of the TDMA systems involved with mobile phones. There are four slots per frame and 17.6 frames per second. Hence, the bursts from handsets occupy slots with a duration of 14.2 ms and the time-averaged power is a quarter of the peak powers mentioned earlier in this paragraph. The base stations transmit continuous signals [AGNIR \(2001\)](#).

The AGNIR review refers to SARs measured from 1 W and 3 W handsets held to either side of the head and in front of the face in a model of the head. With spatial averaging over 10 g, as per ICNIRP and IEEE exposure guidelines, the 1 W radio produced SARs of 0.88, 0.89 and 0.24 W/kg on the left, right and front of the face, respectively, while the 3 W radio produced SARs of 2.88, 2.33 and 0.53 W/kg, respectively, under the same conditions.

[Dimbylow *et al.* \(2003\)](#) developed a numerical model of a commercially available TETRA handset and calculated SARs in an anatomically realistic numerical model (resolution, 2 mm) of the head developed from MRI images. The handset was modelled as a metal box of dimensions 34 × 50 × 134 mm, and with either a helical (pitch, 4 mm; diameter, 8 mm) or a monopole antenna mounted on its top face, and resonant at 380 MHz. For the handset held vertically in front of the face in the position that was considered to be most representative of practical use, the averaged SARs at 10 g were 1.67 W/kg and 2.37 W/kg per watt of radiated power with the monopole and helical antennae, respectively. Various positions

were considered with the handset held to the sides of the head and the maximum SARs with the two antennae were 2.33 and 3.90 W/kg per watt. These values suggest SARs with 3 W handsets (3/4 W time-averaged) having a helical antenna could exceed the 2 W/kg restriction on exposure for the general public, if the handsets were to transmit at full power for 6 minutes while held to the side of the head.

(vii) Cordless phones

Cordless phones are used to make voice calls and are held against the head just like mobile phones. Hence, the antenna inside the phone is in close proximity to the head and its radiated fields deposit energy inside the head tissues near to the phone, in a similar way to the fields from mobile phones. With cordless phones, communications are made over shorter distances than with mobile phones and so the radiated powers used are lower, but cordless phones do not use adaptive power control, which means that, unlike mobile phones, they do not continually adapt their radiated power to the minimum necessary for satisfactory communication (ETSI, 2010).

With simple cordless installations, the phones are typically placed back on a desk or charging point after a call has finished. However, there are also more complicated installations in which multiple base stations are installed throughout a building and the phones are carried by the user as a personal phone. The radio communications are over distances of a few tens of metres and to the nearest base station, which provides the link into the main wired telephone system.

The first cordless phones used analogue technology and operated to a range of different technical standards, with continuous emitted power levels of about 10 mW during calls. Frequencies were generally in the range 30–50 MHz and therefore about 20 times lower than the frequencies used by mobile phones. Some phones used telescopic antennae of about 15–30 cm in length, while others used helical

antennae of about 5 cm in length. The lower frequencies and the greater size of the antennae used with analogue cordless phones would have resulted in a smaller proportion of the radiated power being absorbed, and also in a more diffuse pattern of absorption in the head than occurs with mobile phones (ETSI, 2010).

Modern cordless phones use digital technology, including the digital enhanced cordless telecommunications (DECT) technical standard, which operates in the frequency band 1880–1900 MHz and is the main system used in Europe. In other parts of the world, systems operating around 900, 2400 and 5800 MHz are used as well as DECT (ETSI, 2010).

DECT systems produce discontinuous emissions due to their use of TDMA. The signals from the phone and base station during calls are in the form of 100 bursts every second, each of about 0.4 ms in duration. These bursts are emitted at a peak power level of 250 mW, but the time-averaged power is 10 mW because each device only transmits for 1/24 of the time (duty factor of 4%). Handsets do not transmit unless calls are being made, but when on “standby” most base stations produce 100 beacon pulses per second, each pulse being 0.08 ms in duration. This implies a duty factor of 0.8% (ETSI, 2010).

(viii) Professional mobile radio systems

A variety of professional mobile radio systems, also called private mobile radio (PMR), have been developed over the years and these are generally licensed to professional users by spectrum-management agencies in the countries where they are used. In many countries, the emergency services (police, fire, ambulance, etc.) are converting to the use of digital cellular systems, such as TETRA, although analogue systems – which were the norm before roll-out of TETRA systems – are also used.

The PMR systems use frequencies in the VHF and UHF parts of the spectrum; VHF generally propagates further for a given radiated power

and is, therefore, preferred for longer-distance communications. On the other hand, UHF systems have smaller antennae and present as more compact terminals.

Systems exist in the form of walkie-talkies that are held in front of the face and used in push-to-talk (PTT) mode; they may be built into vehicles with external, e.g. roof-mounted, antennae or be worn on the body. The transmitting antennae can be on the handset itself, on the vehicle, or carried on the chest or waist. The radiated powers are typically in the range 1–5 W, but it is important to take into account the duty factor associated with how they are used: the PTT mode will involve only a few seconds of transmission during the time that the button is pressed down and the user is speaking.

(c) *Wireless networks*

Wireless networking has developed rapidly since about 2000 and is becoming the method of choice for connecting mobile devices such as laptop computers and mobile phones to other electronic systems and to the Internet. The networks are found in homes, schools, public places such as cafés and transport hubs, and in the workplace. The systems operate to the IEEE802.11 family of technical standards and are often known as “Wi-Fi,” after the Wi-Fi Alliance, an organization that certifies inter-operability of devices on the market.

The original version of IEEE802.11 was published in 1997 and provided for data-transfer rates of up to 2 Mbit/s through frequency channels between 2.4 and 2.5 GHz. Subsequent developments using this band were IEEE802.11b and IEEE802.11g, allowing for rates up to 11 and 54 Mbit/s, respectively. Several frequency bands between 5 and 6 GHz are exploited by IEEE802.11a and provide for 54 Mbit/s communications. The latest devices operate according to IEEE802.11n and provide up to 72 Mbit/s in a single frequency channel, but the standard allows for devices that can use multiple frequency

channels simultaneously to deliver much higher data rates ([ICNIRP, 2009a](#)).

The IEEE802.11 standard specifies maximum radiated powers, but these are above the values permitted by regulatory agencies in many parts of the world. For example, in Europe the technical standards EN300328 and EN301893 limit the EIRP to 100 mW in the 2.4-GHz band and 200 mW in the 5 GHz band, respectively. [Peyman et al. \(2011\)](#) measured the actual power radiated by a selection of Wi-Fi devices marketed among schools in the United Kingdom. The spherically integrated radiated power (IRP) ranged from 5 to 17 mW for fifteen laptops in the 2.45 GHz band and from 1 to 16 mW for eight laptops in the 5 GHz band. For practical reasons and because access points are generally wall-mounted with beams directed into the room, their powers were integrated over a hemisphere. These ranged from 3 to 28 mW for twelve access points at 2.4 GHz and from 3 to 29 mW for six access points at 5 GHz. Thus the radiated powers of laptops seem to range from a few mW up to about 30 mW. In principle, these measurements imply that the powers of access points could range from a few mW up to around 60 mW, if their patterns extend symmetrically into the unmeasured hemisphere, which seems unlikely.

The RF emissions from Wi-Fi devices are in the form of short bursts containing portions of the data being transmitted and other information, such as acknowledgements that data have been successfully received. Unlike the emissions from mobile phones using TDMA, the bursts are irregular in terms of timing and duration. Typical bursts range from about 10 μ s to about 1 ms in duration. If data are lost or corrupted during transmission, bursts are retransmitted until they are successfully received. Also, under conditions where communications are poor, e.g. due to weak signal strength, the systems can lower their data-transfer rates to have better signal-to-noise ratios and improved reliability. This increases the cumulative time that it takes to transmit a given

amount of data. Thus, high signal strengths from Wi-Fi devices (during transmission of bursts) do not necessarily translate to higher exposures, because this results in lower duty factors ([Mann, 2010](#)).

Comprehensive data are yet to be published regarding the duty factors of Wi-Fi equipment during normal use; however, [Khalid et al. \(2011\)](#) has reported initial results from the use of data-traffic capturing and packet-counting equipment in school networks. Transmitted bursts were captured to determine the proportion of time during which Wi-Fi devices transmitted while children were using laptops during their lessons. The laptops were mostly used for receiving traffic from the access points and therefore laptop-transmit times were low. Duty factors for the monitored laptops were consistently less than 1% and those of access points were less than 10%. Baseline duty factors of access points (with no data being transferred) are about 1%, due to beacon pulses of duration 1 ms that are produced at a rate of ten pulses per second ([Mann, 2010](#)).

The SAR values produced when using laptop computers equipped with Wi-Fi transmitters have been evaluated by several authors. Most devices now have built-in antennae located around and along the top edge of the screen, which are therefore at greater distances from the body than a mobile phone held against the head. The rapid reduction in field strength that occurs with increasing distance means that SARs can be expected to be much lower than from mobile phones under such scenarios. Based on a continuous radiated power of 100 mW under a range of such scenarios, [Findlay & Dimbylow \(2010\)](#) calculated a maximum 10 g averaged SAR of 5.7 mW/kg in the head.

When Wi-Fi devices are able to transmit continuously with their antennae in close proximity to the body, the SARs may be higher than in the scenario described above. For example, [Kühn et al. \(2007a\)](#) measured a SAR of 0.81 W/kg in a flat phantom with the antennae of a Wi-Fi

access point in close proximity and [Schmid et al. \(2007b\)](#) measured a SAR of 0.05 W/kg under similar conditions from a Wi-Fi equipped PCI card inserted into a laptop. The value reported by Kühn et al. is within the range of maximum localized SARs from mobile phones ([ICNIRP, 1998](#)).

Studies have also examined the general field strengths in environments where Wi-Fi networks are installed. [Foster \(2007\)](#) measured RF fields at 55 public and private sites in the USA and Europe (4 countries), which included private residences, commercial spaces, and health-care and educational institutions. In nearly all cases, the measured Wi-Fi signal levels were far lower than other RF signals in the same environment. The maximum time-averaged power density in the 2.4-GHz band measured at 1 m distance from a laptop uploading and downloading a file was 7 mW/m², which is far less than the [ICNIRP \(1998\)](#) reference level value of 10 W/m² for the general public.

[Schmid et al. \(2007a\)](#) investigated the typical exposure caused by wireless local area network (WLAN) applications in small and large indoor public areas (e.g. Internet cafés, airports). Outdoor scenarios were also considered where the exposure was measured in the vicinity of access points serving residential areas and public places. Exposure was assessed by computational methods and by on-site measurements. The highest values for indoor exposure were found close to the transmitting devices (access points or clients) where, at a distance of about 20 cm, spatial and temporal peak values of power density were found to reach about 100–200 mW/m². In general, the exposure values were several orders of magnitude below the [ICNIRP \(1998\)](#) reference levels.

(d) Industrial applications

There are several industrial applications for RF-EMF, many of which are described in review reports and papers. On the whole, the

literature is rather old and difficult to interpret since reported field values have generally been taken in the context of compliance assessments rather than epidemiological studies, so it is hard to judge what the typical exposures of workers may have been. Only a brief description of some of the sources producing the highest exposures is included here.

(i) *Industrial induction heating*

Industrial induction heating involves the use of induction furnaces equipped with large coils that produce strong magnetic fields. Conducting materials for treatment are placed inside the coils and the magnetic fields cause eddy currents, resulting in heating of the conducting materials. Typical applications include surface hardening, softening and melting metals, mixing alloys and heating gaseous conductors such as plasmas. The frequencies used span a wide range, from 50 Hz through to a few megahertz, so not all applications fall within the scope of this *Monograph*. The fields can be considerable and worker exposures are greatest for tasks that involve approaching the coils, e.g. when taking samples from within the coils of open furnaces. The coil impedances increase with frequency and electric fields can become the dominant contributor to exposure (rather than magnetic fields) at frequencies above about 100 kHz ([ICNIRP, 2009a](#)). [Allen et al. \(1994\)](#) have provided a review of measured exposures, drawing on peer-reviewed papers from several countries and measurements made in the United Kingdom.

(ii) *Dielectric heating*

RF heating and drying equipment has been used for many years and applications include pre-heating, wood-glueing and polyvinyl chloride (PVC) welding. These materials are lossy dielectrics and their conductivity at radiofrequencies means that they can become heated-up when placed in a strong electric field. Typical heaters are designed to use the industrial, scientific and

medical (ISM) bands at 13.56, 27.12 and 40.68 MHz, but reported measurements show that frequencies are variable within the range 10–80 MHz. Powers range from less than a kilowatt to tens of kilowatts for typical heat sealers, while for glue-dryers the maximum power may exceed 100 kW ([ICNIRP, 2009a](#)).

The greatest source of operator exposure comes from the use of manually actuated PVC dielectric machines, where the operator manipulates material to be welded by hand and then clamps it between a pair of electrodes between which the power is applied. Measurements and other details from studies carried out in the United Kingdom and elsewhere are described by [Allen et al. \(1994\)](#). The field strengths from dielectric heaters at the operator locations can be in excess of the [ICNIRP \(1998\)](#) reference levels, but they are non-uniform and it is necessary to evaluate the SAR in the body to determine compliance with the guidelines. [Kännälä et al. \(2008\)](#) have developed an assessment method based on measuring induced limb currents and relating these to localized and whole-body SARs (wbSARs).

(e) *Medical applications*

RF fields have several medical applications. In general, exposure for the clinician will be lower than for the patient, since the RF source will generally be located closer to the patient, but this is not always the case. RF fields can also be applied for therapeutic purposes, for moderate heating of tissue, or for much greater heating for the cutting and destruction of tissue during surgery.

(i) *Magnetic resonance imaging (MRI)*

Performing an MRI scan for diagnostic purposes involves strong RF fields. MRI uses a combination of EMFs to produce exceptionally clear images of tissue structures inside the human body, to assist with medical diagnoses. Hydrogen atoms associated with water in the

body tissues are made to resonate in a strong magnetic field such that they emit RF radiation at the resonant frequency. Therefore, variations in the water content of tissues are the basis of the contrast in the images obtained ([HPA, 2008](#)).

A permanent uniform static magnetic field, typically in the range 1–3 T, but sometimes up to 8 T or more with specialized systems, is applied over the body and causes splitting of the energy states associated with protons (hydrogen atoms). The difference between the energy states is such that protons will transfer from the lower to the upper energy state in response to an applied RF signal at the resonant frequency. Protons will also fall back to the lower energy state spontaneously, and in doing so emit RF radiation at the Larmor frequency. The Larmor frequency is given by 42.57 times the static magnetic-field strength. Thus a 1.5 T, an MRI scan involves the application and measurement of RF fields at 64 MHz ([HPA, 2008](#)).

During an MRI scan, multiple RF pulses (hundreds to thousands per second) are applied over either the whole body or the part of the body being visualized. The RF dose (SAR) received by patients inside the MRI scanners is reported by the system and can vary from < 0.1 W/kg to about 4 W/kg for more complex settings ([HPA, 2008](#)). The desire to limit temperature increases and prevent harm to the patient can be a limiting factor in how quickly scans can be performed in practice. Clinicians and any other personnel who are near to the magnet during the scans will be exposed to the RF fields, but the strength of the RF fields will diminish rapidly with increasing distance from the RF coils and the space between them inside the scanner.

(ii) *Diathermy*

Short-wave and microwave diathermy are used to gently warm muscles, tendons and joints to alleviate a variety of medical conditions. Short-wave equipment operates at frequencies of 13.56 MHz or 27.12 MHz and powers of about

400 W. Applicators for microwave diathermy operate at 2.45 GHz with powers of about 200 W and tend to take the form of a radiating antenna surrounded by reflectors that direct the emitted energy in a forward direction. While exposure of the patient is intentional, the scanner operators close to the equipment may be exposed involuntarily in areas where field strengths are high, unless they move away while the equipment is in operation ([ICNIRP, 2009a](#)).

(iii) *Surgical diathermy and ablation by radiofrequency*

RF fields and currents are widely used during surgical procedures. In surgical diathermy or electrosurgery, a small hand-held electrode acts as a cutting or coagulation instrument. The basic operating frequency is typically about 500 kHz and there are harmonics produced at frequencies up to around 20 MHz. Current densities in tissues can be as high as 10 A/cm² with source powers of up to 200 W ([IPEM, 2010](#)). Some more recent systems use a frequency of 9.2 GHz and powers of about 20 W delivered through needle-like electrodes containing coaxial lines. These systems are employed for minimally invasive surgery, e.g. focal tumour ablation and the treatment of menorrhagia by endometrial ablation ([IPEM, 2010](#)).

(f) *Domestic sources*

There are few powerful sources of RF in the home; however, among these, induction cooking hobs and microwave ovens are of note. Less powerful sources include remote-controlled toys, baby monitors, and the mobile/cordless phones and the Wi-Fi systems described earlier.

Induction cooking hobs feature coils that produce a magnetic field beneath the metal cooking pans that are placed on them. The magnetic fields produce eddy currents in the pans, which are thereby heated. The powers transferred to the pans can be several kilowatts and the frequencies involved are in the range

20–50 kHz. Magnetic fields can be in the order of the ICNIRP reference levels, but vary greatly with user position and also depend on the placement of the pan. [ICNIRP \(2009a\)](#) reviews studies that have investigated these exposures.

Microwave ovens are standard fixtures in many homes and contain microwave sources operating at a frequency of 2.45 GHz and producing powers between 500 W and 2 kW. The design of such ovens is such that leakage is kept to a minimum and a product-performance technical standard requires that microwave-power density levels fall below 50 W/m² at a distance of 5 cm. Several large surveys of leakage levels have been performed, as described in [ICNIRP \(2009a\)](#), and these indicate that approximately 99% of ovens comply with the emission limit. According to the measurements of [Bangay & Zombolas \(2003\)](#), the maximum local SAR values at the emission limit are 0.256 W/kg and the maximum 10 g averaged SAR is 0.0056 W/kg.

A new source of RF that is currently being introduced and that seems set to enter many homes is the transmitter associated with “smart” metering of electricity consumption and potentially metering for other services such as water and gas. There is no global approach to gathering information from smart meters and relaying it back to the utility companies, but it is clear that radio communications will be involved. Some systems may use mobile-phone networks for this purpose, while others may use dedicated radio infrastructures. Some systems may also involve a home area network (HAN) within which individual electrical devices in the home can relay information about usage to a central collection point, allowing residents to examine the information and make decisions about their energy consumption. Two recent investigations commissioned by the Electric Power Research Institute (available on the EPRI webpage) suggest that the power level of radio transmissions will be similar to that of mobile phones, but that the duty factors will be low (on average, such devices

will transmit for a small proportion of time only). Low duty factors, combined with the greater distances of these devices from people compared with mobile phones, imply that exposures will be low when compared with exposure guidelines.

(g) Security and safety applications, including radar and navigation

A variety of systems used for security purposes involve the application of RF, including systems for asset tracking and identification. These sources and exposures have been reviewed in [ICNIRP \(2009a\)](#).

Radar systems operate across a broad range of frequencies, mostly in the range 1–10 GHz, with some short-range applications in the range of tens of gigahertz. Emissions from these systems represent an extreme form of pulse modulation, the TDMA scheme used by some mobile phones being a less extreme example. The duty factor in a GSM TDMA signal is 1/8, whereas it is typically around 1/1000 with a radar signal. The typical duration of a pulse might be about a microsecond, while a typical pulse period might be about a millisecond, although these parameters do vary and depend on the type of radar involved. Very high power densities can be produced in the antenna beams during the pulses, and powers can still be high after duty factors are taken into account to determine the average power. To assess human exposure from radar systems it is necessary to take into account:

- The exposure metric of interest (to account for the pulsing, or simply based on the average power);
- People’s juxtaposition to the beams (are the beams going over people’s heads?);
- The duty factor associated with the pulsing;
- The duty factor associated with rotation (equal to the beam width in azimuth divided by 60 degrees; probably around 200 : 1 in the direction that a rotating beam sweeps through).

Information about radar systems can be found in the following review reports: [Allen et al. \(1994\)](#), [Cooper \(2002\)](#) and [ICNIRP \(2009a\)](#).

(i) *Air traffic control*

The most familiar application of radar is for navigation and the tracking of aircraft movements from rotating ground-based antennae, e.g. at airports. Long-range systems operate over 1–2 GHz, while moderate-range systems operate over 2–4 GHz. The antennae tend to be mounted sufficiently high that buildings cannot obstruct their view of the sky and they form narrow beams of about a degree in the horizontal plane that sweep around 360 degrees once every few seconds. Beams are broader in the vertical plane and tail off in strength towards low elevation angles to avoid reflections from objects on the ground. Aviation radar systems have quite high emitted power levels during the pulses, typically from tens of kilowatts to a few megawatts. Taking the duty factors into account leads to time-averaged emitted powers of about 100 W to a few kilowatts ([AGNIR, 2003](#)).

(ii) *Marine radar*

Marine radar systems are used to inform the crew of a ship of the presence of other vessels and thus avoid collisions. The range of these systems is shorter than that of aviation systems. It is known that targets will be at ground (sea) level, so the beam profile extends to ground level in the plane of elevation. The rotating antennae are mounted at height to allow a view of the sea that is unobstructed by the structure of the ship/vessel on which they are carried. Operating frequencies are in the ranges of 2–4 or 8–12 GHz. Mean powers are in the range 1–25 W and peak powers can be up to about 30 kW ([ICNIRP, 2009a](#)).

(iii) *Tracking radar*

Tracking radar is used in military systems to lock-on to and follow targets such as aircraft and missiles. The antennae can rotate, execute a nodding motion, point in a fixed direction, or

follow a target. Targets are not expected to assist with being tracked and may even be designed with stealth in mind and to suppress the extent to which they reflect radar pulses. Hence, tracking radar systems generally involve higher powers than navigation systems and use peak powers of up to several megawatts. Systems mostly operate between 2 and 8 GHz. Certain tracking radar systems can produce mean power densities $> 100 \text{ W/m}^2$ at distances in excess of a kilometre, even after duty-cycle correction ([ICNIRP, 2009a](#)).

(iv) *Whole-body security scanners*

Whole-body security scanners are used in places such as airports to generate images of objects carried under people's clothing without the need for physical contact. Active systems transmit either ionizing (X-rays) or non-ionizing (RF) radiation towards the body and then analyse the scattered radiation. Passive systems simply monitor the "black body" (thermal) radiation given off by the body in the RF spectrum and do not emit any radiation. Current active RF systems typically operate at about 30 GHz, although in the future systems may use frequencies of up to several hundred gigahertz. ([European Commission, 2010](#)). A note published by [AFSSET \(2010\)](#) described an assessment of an active scanner operating in the frequency range 24–30 GHz. Power densities incident on the body were reported as between 60 and 640 $\mu\text{W/m}^2$.

(v) *Other systems*

Various other radar systems include those used for monitoring weather, traffic speed, collision avoidance with vehicles and ground penetration.

1.3 Dosimetry

1.3.1 Introduction

Incident EMFs are defined as external fields in the absence of – i.e. without interaction with – the human body, animals, or tissue samples. Incident fields couple with the human body and induce EMFs and currents inside the body tissues.

Macrodosimetry is the science of quantifying the three-dimensional distribution of EMFs inside tissues and organs of biological bodies, with averaged induced fields across submillimetre tissue structures (e.g. cells). The term is also applied to measurements in media that have dielectric characteristics similar to those of biological bodies, e.g. cell cultures, tissue-simulating media, etc. The induced fields are the only exposure parameters that can interact with biological processes and, therefore, provide the primary exposure metric ([Kühn, 2009](#)).

Microdosimetry refers to the assessment of fields at subcellular resolution (e.g. across membranes, proteins, etc.). This is a relatively new research area that faces various basic problems, such as material models and transitions between classical and quantum electrodynamics. In all cases, however, macrodosimetry is the first step, since microdosimetry can only be developed from the locally averaged induced fields. This *Monograph* does not cover microdosimetry, and “dosimetry” used hereafter thus refers to macrodosimetry. Dosimetry studies of differences in dielectric properties of tissues in human and animals models published since 1984 are described in [Table 1.7](#).

The coupling mechanisms of the electric and magnetic incident-field components are different. Hence, both must be determined separately to fully characterize human exposure. Since coupling with the human body also depends on the ratio of wavelength versus body size, the RF-EMF spectrum is often divided

into at least three ranges, e.g. 30 kHz–10 MHz (below body resonance); 10 MHz to 2 GHz (body and partial body resonances); and 2 GHz to 300 GHz (surface-dominated absorption) ([ICNIRP, 2009a](#)). Furthermore, the distribution of the induced field strongly depends on various parameters, such as source (strength, frequency, polarization, direction of incidence, size, shape, etc.), distance and location of the source with respect to the body, outer anatomy, inner anatomy, body posture, and environment of the body (e.g. reflective objects).

The field variations within the body are generally large and may well exceed a factor of thousand for the locally absorbed energy. In general, field distributions change considerably between different postures and orientations of the body with respect to the field. For example, the exposure of the brain may change even though the whole-body average and the peak spatial absorption remain the same.

1.3.2 Dosimetric exposure

It has only recently become technically possible to achieve a detailed characterization of exposure to EMFs. Hence, research on dosimetry during the past 30 years has been focused on reliable determination of the exposure metric as defined in the safety guidelines, namely, the maximum average whole-body values and the maximum locally-induced field values. The most commonly used metrics are defined below.

At frequencies greater than 100 kHz, SAR is the main measure of exposure used. SAR is the absorbed electromagnetic energy per tissue mass and can be calculated directly from the electric energy loss, which is proportional to the square of the locally induced root-mean-square value (rms) of the electric field strength, the induced current density and the temperature increase (see Glossary for detailed equations). The assessment on the basis of the initial rise in temperature is only valid if the exposed body is in thermal

Table 1.7 Dosimetry studies of differences in dielectric properties of tissues

Reference	Description of the model	Main results and comments
Thurai et al. (1984)	Variation of dielectric properties of brain tissue of the mouse	Measurements were made on the cerebral cortex at frequencies of 10 MHz to 5 GHz in six groups of mice aged 3, 5, 19, 26, 33 or 58 days. Values of relative permittivity and conductivity are shown.
Thurai et al. (1985)	Dielectric properties of the developing rabbit brain	The dielectric properties of developing rabbit brain were measured at 37 °C, at frequencies between 10 MHz and 18 GHz, with time-domain and frequency-domain systems. Water dispersion in the brain becomes more complex with age.
Kuster & Balzano (1992)	Mechanism of energy absorption by biological bodies in the near field	Heterogeneous tissues and larger biological bodies of arbitrary shape are generalized for frequencies above 300 MHz. The SAR is found to be mainly proportional to the square of the incident H-field, which implies that in the close near field, the psSAR is related to the antenna current and not to the input power.
Lu et al. (1994)	Dielectric properties of human erythrocytes at radiofrequency	Dielectric properties of human erythrocytes in suspension (haematocrit, 50%) from 243 healthy persons (120 men, 123 women) were measured at 25 °C, at frequencies of 1–500 MHz, with a coaxial transmission line-reflection method (one-side measurement). A statistically significant age-dependence was found, with a critical age of about 50 yr, above which permittivity and conductivity of human erythrocytes in suspension decreased significantly.
Peyman et al. (2001)	Variation of dielectric properties of rat tissues by age, at microwave frequencies	The dielectric properties of tissues from rats of six different age-groups were measured at 37 °C in the frequency range 130 MHz to 10 GHz, with an open-ended coaxial probe. The percentage decrease in the dielectric properties of certain tissues in rats aged 30–70 days at mobile-phone frequencies was tabulated. These data contribute to rigorous dosimetry in lifetime-exposure animal experiments, and provide insight into possible differences in assessment of exposure for children and adults.
Peyman & Gabriel (2002)	Variation of dielectric properties of biological tissue, by age	Dielectric properties of the bone marrow generally decrease with age, due to changes in water content.
Jaspard et al. (2003)	Dielectric properties of blood, by haematocrit value	Two dielectric parameters appeared to be strongly dependent on the haematocrit value. The permittivity vs frequency decreases then increases when the haematocrit decreases. The conductivity increases in the whole frequency range when the haematocrit decreases.
Schmid et al. (2003)	Pre- and post-mortem dielectric properties of porcine brain tissue	Conductivity declined 15% (at 900 MHz) and 11% (at 1800 MHz) within 1 h after death. The decline in permittivity was 3–4%, and almost frequency-independent. In-vitro measurements of dielectric properties of brain tissue underestimate conductivity and permittivity of living tissue. These findings may affect generally accepted data on dielectric properties of brain tissue widely used in RF dosimetry.
Gabriel (2005)	Variation of dielectric properties of rat tissues, by age	Age-related dielectric data for 9 of 34 rat tissues were incorporated in a numerical dosimetry study on anatomically heterogeneous animals with body sizes corresponding to the ages of 10, 30, and 70 days, exposed to plane waves at spot frequencies from 27 to 2000 MHz. The variation in the dielectric properties affect the wBSAR by < 5%; the most conservative value (highest SAR) is obtained when 70-days properties are used. The dielectric properties of whole brain, skin, and skull were determined experimentally in the frequency range 300 KHz to 300 MHz.

Table 1.7 (continued)

Reference	Description of the model	Main results and comments
Lee et al. (2006)	Development of a body model for the Korean adult male	The dimensions of the human body vary by age, sex, and race. The internal structure and outer dimensions of a body exposed to an electromagnetic field are important for accurate dosimetry. Two volunteers with body dimensions representative of the average Korean adult male were recruited and scanned for phantom development by use of magnetic resonance and computed tomography. About 30 different tissues were manually classified by an anatomist on the raw images. The whole-body phantom can be used for radiation protection dosimetry.
Christ et al. (2006)	Electromagnetic near-field absorption in layered biological tissue in the frequency range 30–6000 MHz	The increase in SAR depends mainly on the thickness of the fat tissue and the frequency. For frequencies between 236 MHz and 5.8GHz, the peak spatial average SAR can increase by a factor between 1.6 and 3.5 compared with homogeneous tissue-simulating liquid. In the near-field zone, reactive E-field components give rise to increased peak spatial averaged SAR, due to high absorption in the skin
Peyman & Gabriel (2007)	Development and characterization of tissue-equivalent liquids	Dielectric properties of two tissue-equivalent liquids were measured in the frequency range 30–3000 MHz. A sucrose-based solution had a permittivity of 61.3 ± 1.0 and a conductivity of 0.63 ± 0.02 S/m at 30 MHz. An aqueous diacetone solution had a permittivity of 54.2 ± 1.2 and a conductivity of 0.75 ± 0.01 S/m at 30 MHz. At 150 and 300 MHz, the two liquids met the specified target to within 5% and 10%, respectively.
Peyman et al. (2007)	Dielectric properties of porcine cerebrospinal tissues <i>in vivo</i> , <i>in vitro</i> , and by systematic variation of age	Dielectric properties of pig cerebrospinal tissue were measured <i>in vivo</i> and <i>in vitro</i> , in the frequency range of 50 MHz to 20 GHz. The study <i>in vivo</i> included tissues from pigs of different ages, weighing about 10, 50 and 250 kg. Dielectric properties of white matter and spinal chord, but not grey matter, showed significant variation with age.
Lee et al. (2009)	Development of a body model for a Korean child aged 7 yr	A whole-body voxel model of a 7-yr-old male volunteer was developed from 384 axial MRIs. The model was adjusted to the physical average of Korean boys aged 7 yr. The body weight of the adjusted model, calculated with the mass-tissue densities, is within 6% of the 50th percentile weight.
Peyman et al. (2009)	Dielectric properties of tissues and SAR in children exposed to walkie-talkie devices	Dielectric properties of porcine tissues <i>in vitro</i> – measured from 50 MHz to 20 GHz – show significant reduction with age. Both permittivity and conductivity decreased in 10 out of 15 tissues measured, mainly due to reduction in the water content of tissues in the ageing animal. The results were then used to calculate the SAR values in children aged 3–7 yr exposed to RF induced by walkie-talkie devices. No significant differences between the SAR values for the children of either age or for adults were observed.

MRI, magnetic resonance imaging; RF, radiofrequency; SAR, specific absorption rate; wk, week or weeks; yr, year or years

equilibrium or in a steady thermal state at the beginning of the exposure.

The SARs usually reported are values averaged over time, either over the periodicity of the signal or over any period of 6 minutes. Two metrics are most often determined:

- The whole-body-averaged SAR (wbSAR) is the total electromagnetic power absorbed by a body divided by its mass.
- The maximum peak spatial SAR (psSAR) averaged over any cube inside the body with a tissue mass of 1 g (psSAR-1 g) or 10 g (psSAR-10 g). Specific evaluation rules have been defined in which the cube is grown around the observation point, whereas special rules apply in case of air interfaces (see [ANSI/IEEE, 2002a](#)). This value is usually reported independently of the exposed tissue.

In recent years, the focus has shifted towards more tissue-specific measures of exposure that can be correlated with biological effects ([Kuster et al., 2006](#); [Boutry et al., 2008](#)). Examples are:

- Instant, time-averaged or cumulative organ- and tissue-specific SAR;
- Distributions and histograms of the spatially averaged SAR (sSAR) values over a mass of 1 g or 10 g of tissue in the shape of a cube (sSAR-1 g or sSAR-10 g) or 10 g of contiguous tissue (sSAR-10 g c) (see also [Ebert, 2009](#)).

At frequencies below 10 MHz, the following quantities are used:

- Current density averaged over any 1 cm² of tissue from the central nervous system (CNS) perpendicular to the current direction ([ICNIRP, 1998](#));
- Electric field integrated over any line segment of 5 mm in length oriented in any direction within the tissue ([IEEE, 2005](#));
- Electric field averaged in any 2 × 2 × 2 mm³ volume ([ICNIRP, 2010](#)).

1.3.3 Coupling of incident fields with the body

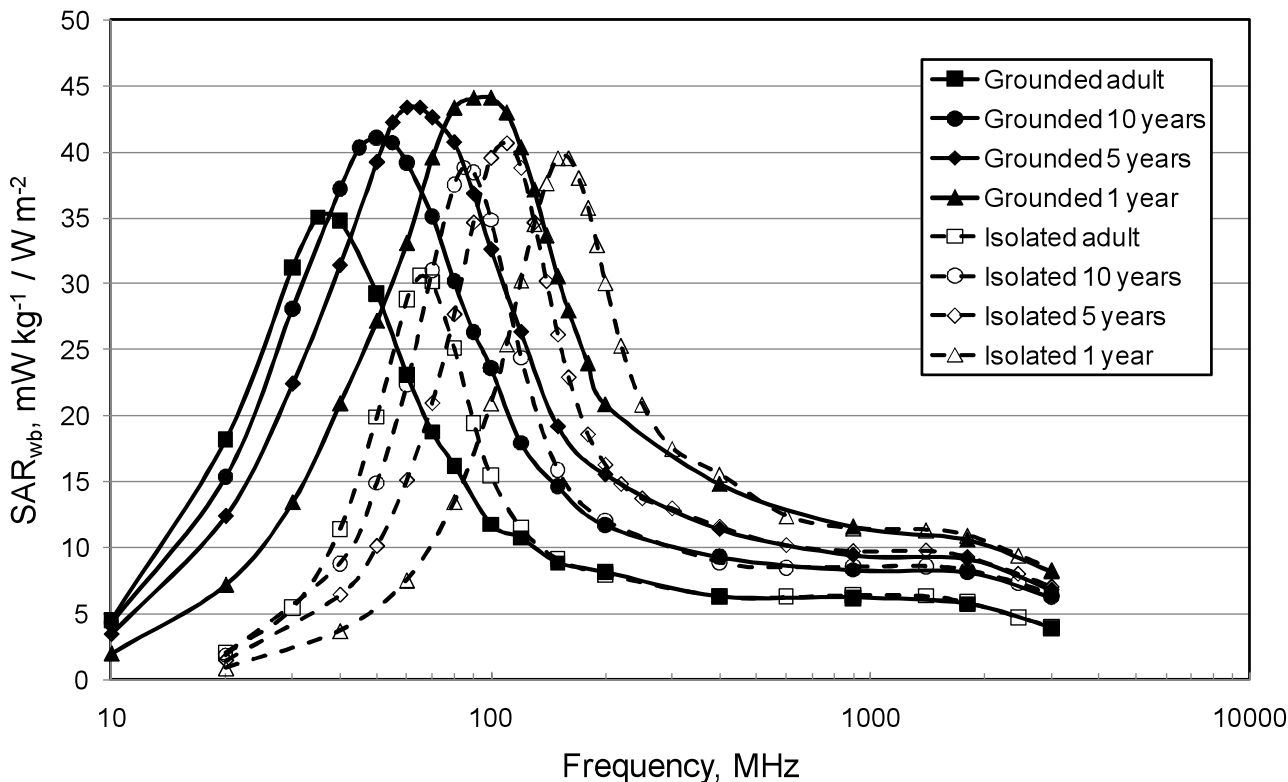
(a) Body-mounted devices

For transmitters operating at frequencies greater than 300 MHz, the absorption in proximate human tissue is approximately proportional to the square of the incident magnetic field (H_{inc}) at the skin surface of the person exposed ([Kuster & Balzano, 1992](#)). H_{inc} is approximately given by the square of the equivalent RF current in the device (I_{RF}) divided by its distance from the human body (d).

The equations presented by these authors explain many aspects of human exposure to radiation from mobile phones discussed in this *Monograph*, namely:

- Mobile phones close to the body ($d < 0.01$ m) are the dominant source of exposure, particularly of the brain, when the phone is held at the ear, compared with exposure from the more powerful base stations at larger distances ($d > 10$ m).
- Exposure from a mobile phone operated by a bystander ($d < 1$ m) may still exceed the exposure from a base station at moderate distance.
- The absorption of energy by different tissues is strongly dependent on the design of the phone, and may vary more than 20-fold according to, e.g. the location of the antenna, and the current distribution with respect to the tissue ([Kuster et al., 2004](#)).
- The level of local exposure is also relatively strongly dependent on the position of the phone at the head, and may vary by a factor of more than 10 ([Wuart et al., 2007](#); [Gosselin et al., 2011](#)).
- The exposure of children is higher than that of adults by a factor of approximately two due to the different shape of children's heads, which brings the phone geometrically closer to the brain in children

Fig. 1.12 Variation in the whole-body specific absorption rate (SAR) produced per unit power density as a function of frequency in the adult male phantom NORMAN, and child phantoms of three different ages, standing on a conductive floor (grounded) and insulated



From Mann (2010). Copyright © 2010. Published by Elsevier Masson SAS on behalf of Académie des sciences. All rights reserved.

than in adults (see Section 1.6.1 (ii); [Wiart et al., 2008](#)).

- Hand-free kits reduce the psSAR in head tissue by a factor of 100 and more ([Porter et al., 2005](#); [Kühn et al., 2009b](#); also see Section 1.2.2).
- Bluetooth headsets operate at 1 mW and the maximum psSAR is a factor of about 100 lower than that for a mobile phone operating at the ear ([Kühn et al., 2007a](#)).
- WLAN transmitters in a laptop computer also result in lower exposures to the brain than a mobile phone operated at the ear.
- Exposures from DECT base-station antennae located in the same room as the person are similar to those from mobile-phone base stations in the neighbourhood ([Kühn et al., 2007a](#)).

(b) Whole-body and partial-body resonances

The human body can be described as an elongated poor conductor. Therefore, it couples energy best if the electric field is polarized along the long body axis and when the electrical length of the body is resonant, i.e. approximately half a wavelength ($\lambda/2$) for an ungrounded body and one quarter wavelength ($\lambda/4$) for a person standing on a grounded floor. This was first investigated with ellipsoids and recently refined with newly available human models (e.g. [Dimbylow, 2007a](#); [Conil et al., 2008](#); [Kühn et al., 2009b](#)). The typical variation in wbSAR as a function of frequency is shown in Fig. 1.12. The same effects have been investigated for partial-body resonances ([Kühn et al., 2009b](#)). The results of these modelling studies explain the main characteristics

Table 1.8 Depth of penetration of muscle and fat by radiofrequency fields at typical telecommunication frequencies

Frequency (MHz)	Muscle			Fat		
	Relative permittivity	Conductivity (S/m)	Penetration depth (mm)	Relative permittivity	Conductivity (S/m)	Penetration depth ^a (mm)
400	57.13	0.80	52	5.58	0.041	310
900	55.03	0.94	42	5.46	0.051	244
1800	53.55	1.34	29	5.35	0.078	158
2450	52.73	1.74	22	5.28	0.105	116
5200	49.28	4.27	8.8	5.01	0.255	47

^a Penetration depths have been calculated based on the equation given in the Glossary.

MHz, megahertz; mm, millimetre; S/m, siemens per metre

Compiled by the Working Group from *Tissue Properties Database: Dielectric Properties* by IT'IS Foundation: <http://www.itis.ethz.ch/itis-for-health/tissue-properties/database/dielectric-properties/>

of far-field exposures of between 10 MHz and 2 GHz, i.e. a strong dependence on body size and posture, and on polarization.

(c) *Below whole-body and partial-body resonances*

At exposures below the body-resonance frequency, i.e. < 10 MHz, the body can be described as a short poor conductor. The dominant exposures of concern are from near-field sources that generally have strong field gradients. Under these conditions, the energy is capacitively coupled in the case of a dominant electric-field source (dielectric heaters, diathermy applicators, etc.) or inductively coupled in the case of a dominant magnetic-field source (e.g. inductive cooking hobs, anti-theft systems, wireless power transfer systems, MRI, etc.). Strong induced currents are also caused by touching metallic objects such as fences or towers exposed to fields from transmitting antennae (contact currents).

(d) *Above whole-body and partial-body resonances*

At exposures above the body-resonance frequency, i.e. > 2 GHz, the body can be described as a dielectric object that is large with respect to the wavelength and the penetration depth (see [Table 1.8](#)). Therefore, the absorption

is approximately proportional to the exposed surface area of the body ([Gosselin et al., 2011](#)). In this case, the wbSAR is proportional to the largest ratio of body surface and weight ([Kühn, 2009](#)), whereas the RF energy is predominantly absorbed at the body surface.

1.3.4 Dependence on local anatomy

(a) *General*

Local exposure is altered by local anatomy due to inhomogeneity of the body tissues. In particular, local enhancements or hot spots can be expected as a result of impedance matching on layered structures, e.g. skin–fat–muscle layers ([Christ et al., 2006](#)), and due to narrowing cross-sections of highly conductive tissues. An example of the latter is high exposure in the ankles when the body is grounded and the electric-field frequency is in the range of or below body resonance; the ankle consists mostly of low-conductive cartilage and the integrated current is largest close to the feet of the grounded person ([Dimbylow, 2005](#)).

(b) *Mobile phones*

During the last decade, the dosimetric analysis of exposure to radiation from mobile phones has focused on reliable compliance testing of the phones with respect to the limits defined

for psSAR-1 g and psSAR-10 g. The absorption values for different mobile phones are determined in homogeneous head phantoms, i.e. the specific anthropometric mannequin (SAM) in touch and tilted positions. The SAR values for different phone positions have been compared in various anatomical models of the head of adults and children. Reviews of these studies concluded that the psSAR assessed with the SAM is a conservative measure of exposure of both adults and children ([Christ & Kuster, 2005](#); [Martens, 2005](#); [Wiart *et al.*, 2005](#)) and that variations in psSAR among different models can be attributed to individual anatomical differences, but not to age-dependent changes in head size ([Kainz *et al.*, 2005](#)).

The effects of age-dependent changes in tissue conductivity have been studied by several authors in various rodent species ([Thurai *et al.*, 1984, 1985](#); [Peyman *et al.*, 2001](#); [Gabriel, 2005](#); [Schmid & Überbacher, 2005](#)).

[Christ *et al.* \(2010a\)](#) investigated the effect of the anatomical differences on specific tissue exposures in humans. These studies concluded that:

- Exposure of regions inside the brain of young children (e.g. hippocampus, hypothalamus, etc.) can be higher by 1.6–3-fold than that in adults.
- Exposure of the bone marrow in the skull of children can exceed that in adults by a factor of about 10, which is due to the high electric conductivity of this tissue at a young age.
- Exposure of the eyes of children is higher than that of adults. Regarding thermal effects, however, this does not present a problem as exposure to the eyes from mobile phones is very low, i.e. < 10% of the psSAR.
- Because of their different locations relative to the ear, brain regions close to the surface of the skull can exhibit large differences in exposure between adults and children. The cerebellum of children can

show a psSAR that is > 2.5-fold that of the local exposure of the cortex of adults. It should be noted that these differences are strongly dependent on the current distribution in the phone, i.e. on the phone design.

- Tissues or anatomical regions that are located at a comparable distance from the phone in adults and children, e.g. the pineal glands, do not show age-dependent variations in exposure.

1.3.5 Estimation of local tissue temperature based on psSAR

In general, the relationship between tissue temperature and psSAR depends strongly upon blood perfusion of the tissue, which varies across the body. In addition, local hot spots (points of elevated temperature) are influenced by thermal conductivity.

The correlation between psSAR and the increase in temperature for exposures to dipoles and mobile phones operated close to the head has been studied ([Hirata *et al.*, 2003](#); [Fujimoto *et al.*, 2006](#); [Hirata *et al.*, 2006a, b, 2008](#)). The results of these studies show that the correlation for a given frequency and exposure type is often good, but that the scaling factor strongly depends on the frequency, the spatial averaging scheme and mass, the tissue perfusion, and geometrical aspects such as anatomical surface curvature. The correlation between local averaged SAR and temperature elevation is weak when multiple tissues are involved. In the brain, the relationship between psSAR and peak temperature is found to be poor, and the tissue distribution and the exact exposure situation have a strong impact on brain heating, with thermo-physiological tissue properties particularly affecting the temperature increase in the head for a given psSAR ([Samaras *et al.*, 2007](#); [McIntosh & Anderson, 2010](#)).

The temperature increase for multiple anatomical models was estimated over a wide

range of frequencies (0.01–5.6 GHz) for plane waves with different polarization and incident angles. The peak temperature increase for a given psSAR was strongly dependent on anatomy and frequency, with variations of one order of magnitude for the cases investigated ([Bakker et al., 2010](#)).

A comparative analysis of seven publications on the increase in brain temperature during mobile-phone use found a high variation (66% at 1800 MHz) in the peak increase in brain temperature relative to the peak averaged SAR in the head ([Samaras et al., 2007](#)). These results confirm the finding that the peak temperature increase in the brain should therefore be correlated with peak averaged SAR in the brain and not with the peak averaged SAR in the whole head. Generally, this peak temperature increase in the brain is strongly influenced by absorption in the neighbouring tissues, thus tissue distribution in that anatomical region is important (e.g. the impact of the cerebrospinal fluid) ([Hirata et al., 2003](#)).

1.3.6 Dosimetry methods

To demonstrate compliance with safety guidelines, wbSAR and psSAR values are estimated conservatively. In most cases, psSAR values are not correlated with a specific tissue or with typical exposures and, therefore, they can only be used for epidemiological studies when additional assessments and considerations are taken into account.

It is practically impossible to measure EMFs non-invasively or *in vivo*; thus, measurements can only be obtained post mortem. The limitations associated with post-mortem evaluations include: (1) accessibility to certain tissues only; (2) field distortions caused by the invasively introduced probe and dielectric changes due to decreased tissue temperature and blood content; and (3) large uncertainties associated with obtaining accurate measurements near and

across tissue boundaries. Only the integrated, total absorbed power can be determined relatively easily by means of the calorimetric method (see Section 1.4.4).

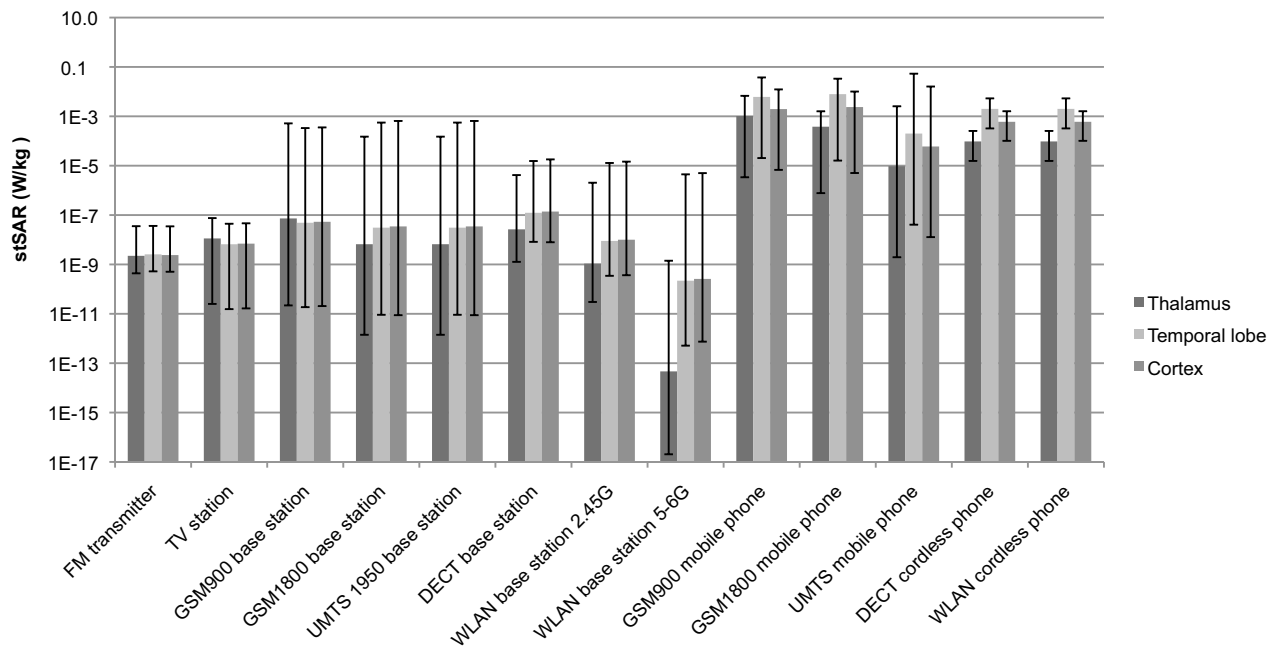
Progress in computational electromagnetics and the exponential growth of computational power and computer memory have facilitated the determination of field distributions in full anatomical models of human bodies with resolutions much smaller than 1 mm³. The dissipative properties and the low quality-factor of complex anatomical structures pose no special problem for numerical analyses such as the finite-difference time-domain (FDTD) method. A grid resolution of less than 0.2 mm in a specific region of the body and of 0.5–1 mm for uniform resolution is the standard for today's FDTD computations. Finite-element methods (FEM) are also increasingly used, especially for evaluation of exposures below 10 MHz. Approaches such as the combination of the method of moment (MoM) with FDTD, are also regularly applied ([Meyer et al., 2003](#)).

Numerical techniques have also become more powerful with the availability of human models that will soon represent the full range of anatomical variation within the human population. Reviews of these models are available ([Dimbylow et al., 2009](#); [Christ et al., 2010b](#); [Wu et al., 2011](#)). In some of these models, body posture can be varied. These models are applied to assess typical exposures, to determine interaction mechanisms, and to derive simplified phantoms for compliance testing.

(a) *Methods to demonstrate compliance with guidelines*

For compliance testing of commercial mobile telecommunication devices that operate very close to the human body, experimental dosimetry is often superior to numerical approaches. The measurement instruments and methods are described in Section 1.4. The sources usually consist of highly resonant components assembled

Fig. 1.13 Estimated tissue-averaged specific absorption rate (stSAR) of the thalamus, temporal lobe and cortex of the brain, induced by various transmission sources



Produced by the Working Group from [Kühn et al. \(2010\)](#)

with other electronic and metallic structures. It is difficult to use simulations to predict with certainty if and how secondary resonant structures may be excited, especially in view of the effect of the reflected field of biological bodies on the performance of the device. Small spatial differences can easily result in deviations of more than a factor of two from the actual value. Only when the structure is electromagnetically well defined can a good agreement between simulation and measurement be achieved, i.e. with deviations of less than 20% ([Chavannes et al., 2003](#)). It should be noted that detailed information about field distributions inside anatomical bodies is often irrelevant because it cannot be generalized and because differences in anatomy and posture can result in significantly different SAR distributions. However, for safety reasons, the upper boundary (typically the 95th percentile) of the exposure for the entire population is relevant, rather than individual exposure levels. Hence, worst-case phantoms, derived by means

of the numerical methods mentioned above, are often applied to assess the upper exposure limits for specific exposure conditions, e.g. during the use of mobile-phone handsets.

(b) Methods to estimate typical exposures

Estimation of typical exposures for specific tissues requires the numerical evaluation of the user's anatomy and usage pattern for the average output power, including its variations. Procedures to make such estimations for different brain regions exposed to mobile-phone radiation have recently been developed ([Gosselin et al., 2011](#)). Similar procedures can be applied for other sources. Quantitative estimates are given in Fig. 1.13, which illustrates the estimated tissue-averaged SARs for the thalamus, temporal lobe and cortex when induced by various transmission sources. The typical minimal and maximal values are also given. The basis for these values is shown in [Table 1.9](#). The largest exposure is

Table 1.9 Estimated minimum, maximum and average exposures in the brain from various sources of radiofrequency radiation

Source	Frequency (MHz)	Exposure			
		Average	Minimum	Maximum	Unit
FM transmitter	100	0.02	0.01	0.07	V/m
TV station	700	0.02	0.001	0.05	V/m
GSM900 base station	950	0.05	0.001	4	V/m
GSM1800 base station	1850	0.05	0.001	6	V/m
DECT base station	1890	0.1	0.03	1	V/m
UMTS 1950 base station	2140	0.05	0.001	6	V/m
WLAN base station	2450	0.03	0.007	1	V/m
WLAN base station	5200/5800	0.01	0.001	1	V/m
GSM900 mobile phone	900	50	0.2	250	mW
GSM1800 mobile phone	1750	40	0.1	125	mW
DECT cordless phone	1890	10	3	20	mW
UMTS mobile phone	1950	1	0.0003	200	mW
WLAN cordless phone	2450	10	3	20	mW

Note: Far-field exposures are estimated in terms of incident-field values and exposures from handsets are calculated from time-averaged output power.

Compiled and calculated by the Working Group from [Kühn et al. \(2010\)](#)

caused by the GSM mobile telephone, followed by exposures from DECT and WLAN cordless handsets. The new wideband code-division multiple access (WCDMA) systems result in much lower exposure values. It should be noted that the maximum exposure level is very similar for all mobile handsets. The averaged induced fields in the brain resulting from exposure to electromagnetic radiation from base stations of any technology are more than four orders of magnitude lower than those from a handset.

1.3.7 Exposure set-ups for laboratory studies

Properly designed laboratory exposure set-ups with sensitive monitoring systems are critical for producing reliable and reproducible results on the potential health effects of RF radiation. The selection of an exposure set-up is intimately linked to the design and objectives of the study, and includes factors such as the efficiency of the coupling of the incident field with the biological system, the number of animals or cell-culture samples needed per exposure level

for statistical analyses, the daily exposure times, and the overall duration of the study. Examples of exposure systems used for this type of study include:

- *Far-field/anechoic chamber*: a room designed to minimize reflections of either sound or electromagnetic waves. To prevent the latter, the inner walls of the chamber are covered with pyramid-shaped RF radiation-absorbent material ([Chou & Guy, 1982](#)). Animals or tissue-culture dishes are exposed to RF radiation via an antenna (e.g. horn antenna).
- *Near-field systems*: antennae are used to obtain partial body exposures. In the Carousel system, the animals in restraining tubes are oriented radially around a central antenna at a fixed distance between the nose of the animal and the antenna ([Adey et al., 1999](#)). Loop antennae have been used to predominantly expose a particular part of the brain ([Lévêque et al., 2004](#)).

- *Transverse electromagnetic (TEM) cell*: an RF-shielded box in which tissue cultures are positioned with a defined orientation relative to the direction of wave propagation and the electric field. A rectangular coaxial transmission line tapered at both ends provides a uniform incident plane wave when RF energy is coupled to the line ([Crawford, 1974](#)). Studies with cell cultures and animal models have been conducted in various modified TEM cells ([Nikoloski et al., 2005](#)).
- *Waveguide*: a structure that guides and confines electromagnetic waves to propagation in one dimension within a round or rectangular metallic tube. Waveguides have the advantage that only the fundamental mode can propagate within a certain frequency band, correlated with its dimensions. Therefore, resonant systems can be easily used. The power losses of the propagating wave must be carefully evaluated if larger objects are exposed. Standing waves must be appropriately used in case of resonant waveguides or waveguides terminated by a short circuit. Waveguides are widely used for *in-vitro* systems (e.g. [Schuderer et al., 2004b](#)). Non-resonant waveguides have also been used to expose rodents (e.g. [Guy et al., 1979](#)) and a cascade of 17 sectorial resonant waveguides excited by one quad-loop antenna have been employed to expose one rat per waveguide ([Kainz et al., 2006](#)).
- *Radial transmission line (RTL)*: a structure that confines the wave to propagate in two dimensions with two parallel metal plates excited between their centres by an antenna. In the case of a non-resonant application, the wave is terminated at the perimeter of the lateral plates with absorbers ([Hansen et al., 1999](#); [Moros et al., 1999](#)). The system has been used for studies *in vivo* or *in vitro* by placing the

cell cultures or animals at a fixed distance from the antenna. RTL has also been used as a resonant structure in which the wave is terminated with metallic rods instead of absorbers. This configuration has also been called a “Ferris wheel,” whereby the animals in restraining tubes are positioned at a fixed distance to the reflecting rods ([Balzano et al., 2000](#)). Several improvements have been suggested and implemented ([Ebert, 2009](#)).

- *Reverberation chamber*: a shielded room with minimal absorption of electromagnetic energy. To create statistically homogeneous fields inside the chamber when exposure is averaged over time, rotating metallic reflectors (stirrers) constantly create changing boundary conditions. Animals are unrestrained during exposure ([Jung et al., 2008](#)).

Regardless of the type of exposure system, for a correct interpretation of the findings and replication of the experiments in other laboratories, it is important that all pertinent electromagnetic-field exposure characteristics (particularly dosimetry) and biological parameters be fully addressed in the experimental design, and properly described in the study reports ([Valberg, 1995](#); [Kuster & Schönborn, 2000](#); [Kuster et al., 2006](#); [Belyaev, 2010](#)). These factors are briefly discussed in the next two sections.

1.3.8 Exposure characterization in laboratory studies

The experimental conditions during studies on the effects of exposure to EMF should be described in detail as listed below:

- Signal characteristics should include: carrier frequency, modulation scheme, power level and stability;
- Zone of exposure (near field or far field);

- Polarization (e.g. linear or circular polarization) of the induced EMF with respect to the biological system;
- Performance of the setup: determination of induced electric- and magnetic-field strengths and SAR levels and distribution (numerical dosimetry) in the cell culture, or per organ site in animal experiments; this part should also include an uncertainty analysis;
- Field distribution: should be homogeneous ($SD < 30\%$ in cell cultures) and variations in the exposure levels of individual tissues of the exposed animals should be characterized, including details on animal age, movement, posture, weight, etc.;
- The increase in temperature caused by the RF field must be well characterized and reported;
- Control of acoustic noise/vibration level and exposure to ambient RF fields and static fields;
- Monitoring: should include verification of incident field strengths and homogeneity, induced fields, and any changes in the performance of elements of the exposure system over the duration of the experiment, including the long-term reliability of monitoring equipment;
- Experimental design requirements: duration of exposure (hours per day and total number of days), continuous or intermittent (on/off cycles), time of day;
- Inclusion of a sham-exposure group.

1.3.9 Biological factors in studies in experimental animals

The biological factors that may affect the study results are briefly described below:

(a) *Studies in vivo*

- Identification and justification of the selected animal model (species, strain, sex, age at start and end of study, genotype and phenotype, exposure to other agents);
- Animal husbandry: diet (ingredients, nutrient composition and contaminant levels), drinking-water source and treatment, availability or restriction of feed and water during exposures, absence of specific pathogens, caging (cage material, number of animals per cage, bedding material), prevention of exposure to electric currents from water supply, absence/presence of animal restraining devices;
- Environmental controls: temperature, relative humidity, lighting (on/off cycle, intensity), airflow, noise, and background fields;
- Characterization of animal weight, positioning/orientation, movement in the exposure system, and proximity of other animals and cage boundaries during exposure periods.

(b) *Studies in vitro*

- Composition of the incubation media, including antioxidant levels, free-radical scavengers, presence of magnetic particles;
- Source and/or derivation of the cell system and its characteristics: cell type, species, strain, sex, age, genotype and phenotype;
- Quality of the cell-culture system and its functional condition: cell viability, growth phase and cell-cycling rate, metabolic status, and cell density (which may affect cell–cell interactions);
- Size, shape, and position of the cell-culture vessel;
- Environmental controls, including temperature, oxygen/carbon dioxide levels, air flow.

Table 1.10 Summary of studies on models of partial body exposure

Reference	Description of the model	Main results and comments
Gandhi <i>et al.</i> (1999)	EM absorption in the head and neck region	A FDTD method and a new phantom model of the human body at millimetre resolution were used to study EM energy coupled to the head from mobile phones at 835 and 1900 MHz. Homogeneous models are shown to grossly overestimate both the peak 1-voxel and 1-g SARs. It is possible to use truncated one-half or one-third models of the human head with negligible errors in the calculated SAR distributions.
Hombach <i>et al.</i> (1996)	EM energy absorption upon modelling of the human head at 900 MHz	Dependence on anatomy and modelling in the human head were investigated for EM energy absorption at 900 MHz from RF sources operating very close to the head. Different head phantoms based on MRI scans of three adults were used with voxel sizes down to 1 mm ³ . The phantoms differ greatly in terms of shape, size, and internal anatomy. The results demonstrate that size and shape are of minor importance. The volume-averaged pSAR obtained with the homogeneous phantoms only slightly overestimates that of the worst-case exposure in the inhomogeneous phantoms.
Schönborn <i>et al.</i> (1998)	Energy absorption in the head of adults and children	The levels of EM energy absorbed at 835 MHz and 1900 MHz in the heads of mobile-phone users were compared for adults and children. No significant differences between adults and children were found in the absorption of EM radiation in the near field of sources. The same conclusion holds when children are approximated as scaled adults.
Bit-Babik <i>et al.</i> (2005)	Estimation of SAR in the head of adults and children	The peak local average SAR over 1 g and 10 g of tissue and the EM energy penetration depths are about the same in all of the head models under the same exposure conditions.
Wang & Fujiwara (2003)	Evaluation of EM absorption in head models of adults and children	Based on statistical data on external shape of the head in Japanese children, two models were developed to assess SAR values in the head of a child exposed to RF radiation. Compared with the local peak SAR in the model of the adult head, there was a considerable increase in the child's head when the output power of the monopole-type antenna was fixed, but no significant difference when the effective current of the dipole-type antenna was fixed.
Anderson (2003)	Peak SAR levels in head models of children and adults	Multipole analysis of a three-layered (scalp/cranium/brain) spherical head model exposed to a nearby 0.4-lambda dipole at 900 MHz was used to assess differences in SAR in the brain of adults and children. Compared with an average adult, the peak SAR-10 g in the brain of children with a mean age of 4, 8, 12 or 16 yr is increased by a factor of 1.31, 1.23, 1.15 and 1.07, respectively. The maximum rise in brain temperature is about 0.14 °C for an average child aged 4 yr, i.e. well within safe levels and normal physiological parameters.
Martínez-Búrdalo <i>et al.</i> (2004)	Peak SAR levels in head models of adults and children	The FDTD method was used to assess differences in SAR in the brain of adults and children, at 900 and 1800 MHz. Peak SAR-1 g and peak SAR-10 g all decrease with decreasing head size, but the percentage of energy absorbed in the brain increases.
Fernández <i>et al.</i> (2005)	EM absorption in head models of adults and children	The peak SAR in the head model for a child aged 10 yr was 27% higher than that in the phantom of an adult head, when dielectric properties of a child's tissue were applied, based on fitted parameters. For the peak SAR-10 g, an increase of 32.5% was observed.
Keshvari & Lang (2005)	RF energy absorption in the ear and eye of children and adults	The FDTD computational method was used to calculate a set of SARs in the ear and eye region for anatomically correct head models for adults and children. A half-wave dipole was used as an exposure source at 900, 1800 and 2450 MHz. The head models were greatly different in terms of size, external shape and internal anatomy. The SAR difference between adults and children is more likely to be caused by general differences in the head anatomy and geometry of the individuals rather than by age.
Christ & Kuster (2005)	RF energy absorption in the head of adults and children	The conclusions of this review do not support the assumption that energy exposure to children is increased due to smaller size of the head compared with adults, but points at dielectric tissue parameters and the thickness of the pinna (the external part of the ear) as factors that determine RF energy absorption.

Table 1.10 (continued)

Reference	Description of the model	Main results and comments
Hadjem <i>et al.</i> (2005a)	SAR induced in models of the head of children and adults	The FDTD computational method was used to calculate SARs for two child-size head models and two adult-size head models, with a dual-band mobile phone. No important difference was observed in the peak SAR-10 g between the two adult models, or between the two child models.
Hadjem <i>et al.</i> (2005b)	Ear morphology and SAR induced in a child's head	Using the FDTD method, SARs induced in the heads of children aged 12 yr were calculated for different ear dimensions, at 900 and 1800 MHz. Exposure to the brain was dependent on the morphology of the ear.
Wiart <i>et al.</i> (2005)	Modelling of RF exposure in a child's head	Parameters that influence the SAR in children's heads, such as the evolution of head shape and the growth of, e.g. skull thickness, were analysed. The SAR-1 g in specific tissue was assessed in different models of a child's head based on MRI and on non-uniformly down-scaled adult heads. A handset with a patch antenna operating at 900 MHz was used as the exposure source.
Kainz <i>et al.</i> (2005)	Dosimetric comparison of SAM to anatomical models of the head	The SAM was used to estimate exposure in anatomically correct head models for head-only tissue. Frequency, phone position and head size influence the calculated SAR-10 g, which in the pinna can be up to 2.1 times greater than the psSAR.
de Salles <i>et al.</i> (2006)	Absorption of RF radiation in the head of adults and children	The SAR produced by mobile phones in the head of adults and children was simulated with an FDTD-derived algorithm, with EM parameters fitted to realistic models of the head of a child and an adult. Microstrip or patch antennae and quarter-wavelength monopole antennae were used at 1850 and 850 MHz. Under similar conditions, the SAR-1 g calculated for children is higher than that for adults. In the model of a child aged 10 yr, SAR values > 60% of those for adults are obtained.
Joó <i>et al.</i> (2006)	Metal-framed spectacles and implants and SAR in models of the heads of adults and children	The SAR from mobile telephones in the head of adults and children wearing metal-rim spectacles and having metallic implants was calculated by the FDTD method, and compared with the ANSI/IEEE standards and with the EU standard limits for radiation at 900/1800/2100 MHz. A maximum of the SAR in the child's head was found, which in children with metallic implants could be as much as 100% higher than in the adult head. In the case of exposure at 2100 MHz with vertical position of the phone for adults and at 900 MHz for children with metallic implants, the ANSI/IEEE limits were exceeded.
Fujimoto <i>et al.</i> (2006)	Temperature increase and peak SAR in head models for children and adults	The correlation between peak SAR and rise in temperature was studied in head models of adults and children exposed to radiation from a dipole antenna. The maximum rise in temperature can be estimated linearly in terms of peak SAR-1 g or peak SAR-10 g of tissue. No clear difference was observed between adults and children in terms of the slopes correlating the maximum rise in temperature with the peak SAR. The effect of electrical and thermal constants of the tissue on this correlation was marginal.
Beard <i>et al.</i> (2006)	SAR comparison between SAM phantom and human head models	The SAM was used to calculate the SAR of the pinna, separately from that of the head. In this case, the SAR found in the head was higher than that found with anatomically correct head models. The peak SAR-1 g or SAR-10 g was statistically significantly higher in the larger (adult) head than in the smaller (child) head for all conditions of frequency and position.
Lee <i>et al.</i> (2007)	Changes of SAR in head models by age	Four head models, representing different ages, were used to calculate SARs from exposure to three bar-type phones, according to positioning against the ear. Input resistance of the phone antennae in the cheek position increased when head size grew with age, but for the tilt position this value showed a slight decrease. For a fixed input power, the head models by age showed a 15% change in peak SAR-1 g and peak SAR-10 g. For a fixed radiated power, the peak SARs diminished in the smaller head model and were higher in the larger model, compared with those for the fixed input power. A simultaneous change (up to 20–30%) in the conductivity and permittivity of head tissue had no effect on energy absorption.

Table 1.10 (continued)

Reference	Description of the model	Main results and comments
Wiaart <i>et al.</i> (2007, 2008)	RF exposure assessment in children head	RF exposure in the head tissues of children was analysed with phantom models and with a dipole and a generic handset at 900, 1800, 2100 and 2400 MHz. The SAR-10 g in the head was studied in heterogeneous head models (seven for children, six for adults). The maximum SAR-10 g estimated in the head models of adults and children were small compared with the SDs. However, the maximum SAR-1 g in peripheral brain tissues of the child models (age, 5–8 yr) is about twice that in adult models, which is not seen with head models for children older than 8 yr. The differences can be explained by the lower thicknesses of pinna, skin and skull of the models for the younger child.
Christ <i>et al.</i> (2007)	The exposure of the human body to fields from wireless body-mounted or hand-held devices	A generic body model and simulations of anatomical models were used to evaluate the worst-case tissue composition with respect to the absorption of EM energy from wireless body-mounted or hand-held devices. Standing-wave effects and enhanced coupling of reactive near-field components can lead to an increased SAR compared with homogeneous tissue. With respect to compliance testing, the increased SAR may require the introduction of a multiplication factor for the psSAR measured in the liquid-filled phantom to obtain a conservative exposure assessment. The observed tissue heating at the body surface under adiabatic conditions can be significant, whereas the rise in temperature in the inner organs is negligible.
Christ <i>et al.</i> (2010b)	RF absorption in the heads of adult and juvenile mobile-phone users	The external ear (pinna) is the spacer between the top of a phone and the head tissue. Variations of this distance as a function of age, the mechanical force on the pinna, and how it affects the psSAR were investigated among adults and children (age, 6–8 yr) while applying a defined force on the ear. The average distances were 10.5 ± 2.0 (SD) mm for children (age, 6–8 yr) and 9.5 ± 2.0 (SD) mm for adults. The pinnae of three anatomical high-resolution head models (one adult, two child) were transformed accordingly. Numerical exposure analysis showed that the reduced distance due to compression of the pinna can increase the maximum psSAR by approximately 2 dB for adults and children, if the exposure maximum is associated with the upper part of the phone.
Lee & Yun (2011)	Comparison of SARs for the SAM phantom and head models for children	SARs in three head models for children (Korean aged 7 yr; European aged 5 or 9 yr) were compared with those of the SAM phantom for exposure at 835 and 1900 MHz. Compression of the pinnae, different positions of the earpiece against the ear entrance canal, different skin and fat properties, and different internal fat and muscle morphologies in the tissue near the phone, were analysed. A phone with a monopole antenna was used for the calculation at each frequency. Results show that a compressed pinna did change the SAR values at 835 MHz, but at 1900 MHz there was an average 25–29% increase in SAR-10 g for pinna-excluded and pinna-included tissue. The peak SAR-10 g was very sensitive to subcutaneous fat and muscle structure when touched by the mobile phone; a muscle-dominant internal head structure led to a higher peak SAR-10 g. The SAM phantom does not seem to provide a conservative estimation of exposure of children's heads at 1900 MHz.

ANSI, American National Standards Institute; EM, electromagnetic; EU, European Union; FDTD, finite-difference time-domain; IEEE, Institute of Electrical and Electronic Engineers; MRI, magnetic resonance imaging; psSAR, peak spatial SAR; RF, radiofrequency; SAM, specific anthropomorphic mannequin; SAR, specific absorption rate; SD, standard deviation; yr, year or years

Table 1.11 Summary of studies on models of whole-body exposure

Reference	Description of the model	Main results and comments
Dimbylow (1997)	Calculation of whole-body-averaged SAR in a voxel model	FDTD calculations were made of the whole-body-averaged SAR in an anatomically realistic voxel model of the human body, which consists of approximately 9 million voxels segmented into 37 tissue types. SAR values are presented for an adult phantom and for scaled models of children aged 10, 5 or 1 yr, grounded and isolated in air from 1 MHz to 1 GHz for plane-wave exposure. External electric-field values corresponding to a whole-body-averaged SAR of 0.4 W/kg are also presented.
Tinniswood et al. (1998)	Calculation of power deposition in the head and the neck for plane-wave exposures	When the human head becomes a resonant structure at certain frequencies, the power absorbed by the head and neck becomes significantly larger than would normally be expected from its shadow cross-section. Resonant frequencies were 207 MHz and 193 MHz for the isolated and grounded conditions, with absorption cross-sections that are respectively 3.27 and 2.62 times the shadow cross-section.
Hurt et al. (2000)	Effects of variation in permittivity on SAR calculations	The authors studied the effect of variation in permittivity values on SAR calculations. Whole-sphere averaged and localized SAR values along the diameter of a 4-cm sphere were calculated for exposures of 1 MHz to 1 GHz. When the sphere is small compared with the wavelength, the whole-sphere averaged SAR is inversely proportional to the permittivity of the material composing the sphere, but the localized SAR values vary greatly depending on the location within the sphere.
Dimbylow (2002)	Calculation of SAR up to 3 GHz	FDTD calculations of whole-body-averaged SAR values were made for frequencies from 100 MHz to 3 GHz at 2-mm resolution without any rescaling to larger cell sizes. The small voxel size allows SAR to be calculated at higher frequencies. In addition, the calculations were extended down to 10 MHz, covering whole-body resonance regions at 4-mm resolution. SAR values were also calculated for scaled versions representing children aged 10, 5 or 1 yr for both grounded and isolated conditions.
Bernardi et al. (2003)	SAR and rise in temperature in the far field of RF sources at 10–900 MHz	The EMF inside an anatomical heterogeneous model of the human body exposed at 10–900 MHz was computed with the FDTD method; the corresponding increase in temperature was also evaluated. The thermal model took account of the thermoregulatory system of the human body. Compared with the whole-body averaged SAR, the SAR-10 g shows an increase of 25-fold in the trunk and 50-fold in the limbs, whereas the peak SAR-1 g shows an increase of 30–60-fold in the trunk, and up to 135-fold in the ankles.
Findlay & Dimbylow (2005)	Effects of posture on SAR	A change in posture can significantly affect the way in which the human body absorbs RF EM radiation. The FDTD method was used to calculate the whole-body-averaged SAR at frequencies from 10 MHz to 300 MHz at a resolution of 4 mm. Raising an arm above the head increased the SAR value at resonance by up to 35% compared with the standard, arms-by-the-side position.
Wang et al. (2006)	Whole-body averaged SAR in adult and child models	Due to the difficulty of measuring SAR in an actual human body exposed to RF-EMF, the incident electric field or power density is often used as a reference. In verifying the validity of the reference level, it is essential to have accurate modelling for humans. A detailed error analysis in the whole-body-averaged SAR calculation was done with the FDTD method in conjunction with the perfectly matched layer (PML) absorbing boundaries. To clarify whole-body-averaged SAR values, a Japanese adult model and a scaled child model were used. The whole-body-averaged SAR under the reference level exceeded the basic safety limit by nearly 30% for the child model, both in the resonance frequency and in the band 2 GHz.
Dimbylow (2007a)	SAR values in voxel models of mother and fetus	An FDTD calculation was conducted of SAR values (20 MHz to 3 GHz) in hybrid voxel-mathematical models of the pregnant female. Models of the developing fetus at 8, 13, 26 and 38 wk of gestation were converted into voxels and combined with the adult female model, at a resolution of 2 mm. Whole-body-averaged SAR in the mother, the average SAR over the fetus, over the fetal brain, and in 10 g of the fetus were calculated.

Table 1.11 (continued)

Reference	Description of the model	Main results and comments
Dimbylow & Bolch (2007b)	Whole-body-averaged SAR in voxel phantoms for a child	Five paediatric phantoms (representing boys aged 9 months, 11 yr and 14 yr, and girls aged 4 and 8 yr) were adapted to calculate the whole-body-averaged SARs in children for plane-wave exposure from 50 MHz to 4 GHz. A comparison was made with previous linearly scaled versions, at a resolution of 2 mm. Further FDTD calculations were performed at resolutions of 1 and 0.7 mm above 900 MHz, to elucidate the effects of variation in grid resolution.
Hirata <i>et al.</i> (2003)	Temperature increase in head and brain	The temperature increase (ΔT) in a human head exposed to EM waves (900 MHz to 2.45 GHz) from a dipole antenna was investigated. The maximum ΔT in the head and brain was compared with values from the literature of 10 °C and 3.5 °C for microwave-induced physiological damage. The SAR in the head model was initially calculated by the FDTD method. The ΔT distribution in the head is largely dependent on the frequency of the EM waves, and the maximum ΔT values in the head and brain are significantly affected by the frequency and polarization of the waves. The maximum ΔT in the head (excluding auricles) and brain are determined through linear extrapolation of the peak average SAR in these regions. The peak SAR-1 g should be approximately 65 W/kg to achieve a maximum ΔT of 10 °C in the head, excluding auricles.
Vermeeren <i>et al.</i> (2008)	Statistical method to calculate absorption of RF energy	Quantifying the absorption of EM radiation in a human body in a realistic, multipath exposure environment requires a statistical approach, because it needs to be determined for several thousands of possible exposures. To avoid having to make this large number of time-consuming calculations with the FDTD method, a fast numerical method was developed to determine the whole-body absorption in a spheroid human-body model in a realistic exposure environment. This method uses field distributions of a limited set of incident plane waves to rapidly calculate whole-body absorption for any single or multiple plane-wave exposure. This fast method has now been extended to realistic heterogeneous human-body models.
Nagaoka <i>et al.</i> (2007)	SAR of a whole-body phantom for pregnant women	A new model for the fetus, including inherent tissues of pregnant women, was constructed on the basis of abdominal MRI data for a woman at week 26 of pregnancy. A whole-body pregnant-woman model was developed by combining the fetus model with a nonpregnant-woman model, developed previously. The model consists of about 7 million cubical voxels (size, 2 mm) and is segmented into 56 tissues and organs. The basic SAR characteristics are presented of the pregnant-woman model exposed to vertically and horizontally polarized EM waves from 10 MHz to 2 GHz.
Nagaoka <i>et al.</i> (2008)	SAR for a phantom model of Japanese children	An existing voxel model of a Japanese adult in combination with 3D deformation was used to develop three voxel models that match the average body proportions of Japanese children at age 3, 5 and 7 yr. The models consist of cubic voxels (size, 2 mm) and are segmented into 51 tissues and organs. Whole-body-averaged SARs and tissue-averaged SARs were calculated for the child models, for exposures to plane waves from 30 MHz to 3 GHz.
Togashi <i>et al.</i> (2008)	SAR for the fetus in a pregnant-woman model	Dosimetry of EM radiation is described in a pregnant woman in the proximity of a mobile-phone terminal by use of the numerical model of a woman in the seventh month of pregnancy. The model is based on the high-resolution whole-body voxel model of a Japanese adult woman. It is composed of 56 organs, which include the intrinsic organs of a pregnant woman.

Table 1.11 (continued)

Reference	Description of the model	Main results and comments
Conil <i>et al.</i> (2008)	SAR for different adult and child models using the FDTD method	Six adult anthropomorphic voxel models were collected and used to build models for children aged 5, 8 and 12 yr, with a morphing method that respects anatomical parameters. FDTD calculations of SARs were performed for frequencies from 20 MHz to 2.4 GHz for isolated models exposed to plane waves. A whole-body-averaged SAR, average SARs on specific tissues such as skin, muscles, fat or bones, and the average SAR on specific parts of the body such as head, legs, arms or torso, were calculated. The SD of the whole-body-averaged SAR of adult models can reach 40%. For adults, compliance with reference levels ensures compliance with basic restrictions. For children, the whole-body-averaged SAR exceeds the fundamental safety limits by up to 40%.
Kühn <i>et al.</i> (2009b)	Assessment of induced EMFs in various human models	The absorption characteristics are given for various anatomies ranging from a child aged 6 yr to a large adult male, by numerical modelling, with exposure to plane waves incident from all six major sides of the humans with two orthogonal polarizations each. Worst-case scattered-field exposure scenarios were constructed to test the implemented procedures of current in situ compliance measurement standards. The results suggest that the reference levels of current EM safety guidelines for demonstrating compliance, as well as some of the current measurement standards, are not consistent with the basic restrictions and need to be revised.
Neubauer <i>et al.</i> (2009)	SAR and EMF intensity for heterogeneous exposure	The relation between the incident EMF strength, the wBSAR, and the local SAR, was investigated for heterogeneous exposure scenarios at mobile communication frequencies. For whole-body exposure at 946 MHz, 12% of all heterogeneous cases examined represent worse exposure conditions than plane-wave exposure. This percentage increases to 15% at 1840 MHz, and to 22% at 2140 MHz. The results indicate the need to extend investigations to numerical simulations with additional human phantoms representing parts of the human population having different anatomy and morphology compared with the phantom used here. This also applies to phantoms of children.
Hirata <i>et al.</i> (2009)	Whole-body-averaged SAR in children	The whole-body-averaged SAR was calculated in an infant model with the FDTD method, and the effect of polarization of incident EM waves on this SAR was investigated. The whole-body-averaged SAR for plane-wave exposure with a vertically aligned electric field is smaller than that with a horizontally aligned electric field for frequencies above 2 GHz. The main reason for this difference is probably the component of the surface area perpendicular to the electric field of the incident wave.
Nagaoka & Watanabe (2009)	Estimation of SAR in different models for children	To estimate individual variability in SAR for children of different age and with different physical features, a large set of 3D body-shape data from actual children aged 3 yr was used to develop several homogeneous models of these children. The variability in SAR of these models of whole-body exposure to RF-EMF in the VHF band was calculated by the FDTD method.
Findlay <i>et al.</i> (2009)	SAR for voxel models for children in different postures	SAR calculations were performed on two voxel models (NORMAN, FTRI) for a child aged 7 yr in different postures (standing with arms down, standing with arms up, sitting) for plane-wave exposure under isolated and grounded conditions between 10 MHz and 3 GHz. There was little difference at each resonant frequency between the whole-body-averaged SARs calculated for the two models for each of the postures studied. However, compared with the arms-down posture, raising the arms increased the SAR by up to 25%.

Table 1.11 (continued)

Reference	Description of the model	Main results and comments
Kühn <i>et al.</i> (2009b)	SAR induced in the human head from mobile phones used with hands-free kits	To determine the extent to which the use of wired and wireless hands-free kits can reduce human exposure, the SARs from these kits were determined experimentally while connected to mobile phones (GSM900/1800, UMTS1950) under maximized current coupling onto the cable and various wire-routing configurations. The maximum psSAR in the head when using wired hands-free kits was more than five times lower than current recommended limits. The SAR in the head depends on the output power of the mobile phone, the coupling between the antenna and cable, external attenuation and potential cable-specific attenuation. In general, a wired hands-free kit considerably reduces the exposure of the entire head region compared with mobile phones operated at the head.
Gosselin <i>et al.</i> (2009)	Human exposure in the close vicinity of mobile-phone base-station antennae	Human exposure in close vicinity of mobile-phone base-station antennae was assessed by means of FDTD simulations. The peak spatial average SAR and the whole-body-averaged SAR were calculated for three different anatomical models (55–101 kg) at distances between 0.5 and 4 m from various antenna types, at frequencies of 450–2140 MHz. The whole-body absorption generally determines the maximum permissible output power for collinear array antennae. In particular for short antennae, the peak spatial average SAR can be more restrictive than the whole-body absorption because they may only expose a fraction of the body.
Vermeeren <i>et al.</i> (2010)	SARs in a phantom for a human male exposed to representative base-station antennae	The variation in whole-body and peak spatially averaged SARs was determined for the heterogeneous “virtual family” male model placed at 30 cm, 1 m, 3 m and 10 m in front of different base-station antennae in a reflective environment. SAR values were also compared with those in the free-space situation. The six base-station antennae operated at 300 MHz, 450 MHz, 900 MHz, 2.1 GHz, 3.5 GHz and 5.0 GHz, respectively. The ratio of the SAR in a reflective environment and the SAR in the free-space environment ranged from –8.7 dB up to 8.0 dB.
Uusitupa <i>et al.</i> (2010)	SAR variation for 15 voxel models including different postures	A study on SARs covering 720 simulations and 15 voxel models (body weight range, 18–105 kg) was performed by applying the parallel FDTD method. The models were irradiated with plane waves (300 MHz to 5 GHz) with various incoming directions and polarizations. For an adult, the effect of incoming direction on wbSAR is larger in the GHz range than at around 300–450 MHz, and the effect is stronger with vertical polarization. For a child (height, ~1.2 m), the effect of incoming direction is similar as for an adult, except at 300 MHz for horizontal polarization. Body posture has little effect on wbSAR in the GHz range, but at around 300–450 MHz, a rise of 2 dB in wbSAR may occur when posture is changed from the standing position. Between 2 and 5 GHz for adults, wbSAR is higher for horizontal than for vertical polarization. In the GHz range, horizontal polarization gives higher wbSAR, especially for irradiation from the lateral direction. A homogenized model underestimates wbSAR, especially at approximately 2 GHz.
Kawai <i>et al.</i> (2010)	Computational dosimetry of SAR in models of embryos of different age	SAR dosimetry is presented in models of pregnant (4 and 8 wk) Japanese women, with a cubic (4 wk) or spheroidal (8 wk) embryo, exposed to plane waves at frequencies of 10 MHz to 1.5 GHz. The averaged SARs were calculated in the embryos exposed to vertically and horizontally polarized plane waves. The maximum average SAR in the exposed embryos is < 0.08 W/kg when the incident power density is at the recommended environmental level for the general public.

3D, three-dimensional; ANSI, American National Standards Institute; EMF, electromagnetic field; EU, European Union; FDTD, finite-difference time-domain; IEEE, Institute of Electrical and Electronic Engineers; mo, month or months; MRI, magnetic resonance imaging; psSAR, peak spatial SAR; PML, perfectly matched layer; RF, radiofrequency; SAM, specific anthropomorphic mannequin; SAR, specific absorption rate; sSAR, spatially averaged SAR; SD, standard deviation; VHF, very high frequency; wbSAR, whole-body SAR; wk, week or weeks; yr, year or years

For a summary of studies with models for partial- or whole-body exposure, see [Tables 1.10](#) and [1.11](#).

1.4 Measurement techniques

1.4.1 Introduction

Assessment of the incident exposure is simple for plane-wave or far-field conditions. Unfortunately, when high exposures are involved, far-field conditions rarely occur, due to the proximity of the source. In addition, the reflecting environments result in fading, producing fields that are highly variable spatially and temporally.

In general, far-field conditions are approximately met locally by changing the amplitude in space at distances larger than the extension of the reactive near-field zone ([CENELEC, 2008](#)):

Thus, for distances meeting the requirements of the equation, only the maximum of the field components must be determined to demonstrate compliance. For any distance smaller than the requirements of the equation, the maximum of both components must be spatially scanned to reliably predict that the maximal induced fields are below a certain limit. Fine volume scanning of transmitting antennae in the very near field yields greater uncertainty, neglects reflection back to the source antenna due to the presence of a lossy body, and is more time-consuming than dosimetric measurements in homogeneous phantoms. Since such near-field assessments are more conservative, they are rarely conducted in the context of exposure assessments.

In summary, reference levels are easy to assess if the plane-wave or far-field conditions are approximately met (see Section 1.3.2) and the resulting SAR and induced current densities are below the corresponding basic restrictions under all circumstances. The reference limits for occupational/controlled and for the general public/uncontrolled exposure are given in [NCRP \(1986\)](#), [ANSI/IEEE \(1991, 2002b\)](#) and [ICNIRP](#)

([1998](#)). However, sometimes only the incident electric field (E-field) or the E-field-based equivalent power density is also reported for cases in which the above equation is not satisfied and therefore may not well represent true exposure. It should also be noted that the maximum value that is often reported is suitable for reporting compliance with guidelines, but may greatly overestimate typical exposures at that location.

1.4.2 Near-field and dosimetric probes

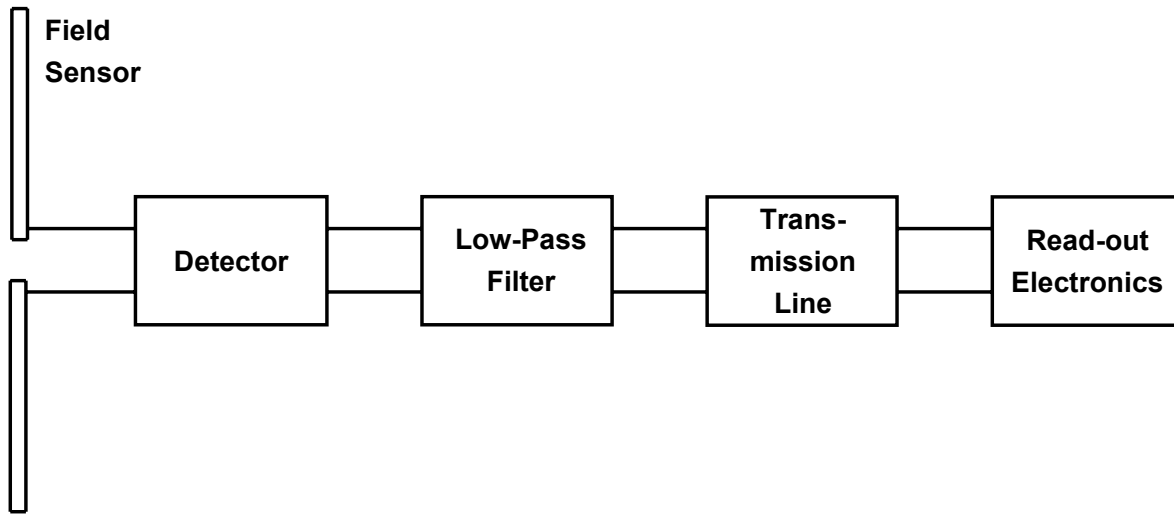
The first instruments were developed in the early 1970s and they covered the 10 MHz to 10 GHz region of the spectrum. One involved the use of two pairs of thin-film thermo-coupling vacuum-evaporated electrothermic elements that functioned as both antenna and detector ([Aslan, 1970](#)). In another instance, two small diode-loaded dipoles were employed as sensor elements ([Rudge, 1970](#)). In 1975, the first prototype of an isotropic, miniature field probe was introduced ([Bassen et al., 1975](#)). Fibre-optic field probes were proposed as early as the 1970s ([Bassen et al., 1977](#)). Comprehensive overviews of field probes have been published ([Bassen & Smith, 1983](#); [Poković, 1999](#)).

(a) Broadband E-field probes

Diode-based field probes are most commonly used for dosimetric assessments. These instruments consist of field sensors, a detector, transmission lines and readout electronics (Fig. 1.14). The probe is constituted of three mutually orthogonal diode-loaded dipoles with an isotropic receiving pattern. Different orthogonal sensor configurations are available.

An RF detector Schottky-type diode is placed at the centre of the dipole sensor. If the detector diode operates in the square-root law region, the detected voltage is proportional to the RF power. The data-acquisition electronics are connected to the detector diodes by high-resistance transmission lines to minimize incident-field perturbation

Fig. 1.14 Simplified schematic of a broadband-field probe



Republished with permission of Taylor and Francis Group LLC Books, from [Kühn & Kuster \(2007\)](#); permission conveyed through Copyright Clearance Center, Inc.

and spurious pick-up effects. A detailed investigation of transmissionline design can be found in [Smith \(1981\)](#).

Magnetic-field (H-field) probes are also available; the basic theory on which such probes are designed can be found in [Whiteside & King \(1964\)](#). H-field probes and E-field probes have similar features except that H-field probes employ a small loop element instead of a dipole sensor. Loop-based sensors present the disadvantage of a strong frequency dependence and induction of currents by both H- and E-fields. Different methods for flattening the frequency response of loop probes have been suggested ([Kanda, 1993](#); [Poković, 1999](#)). Lossy covers have been proposed to further suppress the E-field sensitivity of the loop ([Poković, 1999](#)).

A general problem of diode-based probes is their inherent nonlinearity over their dynamic range. Methods to overcome these limitations are presented in [Kühn et al. \(2007b\)](#).

Unlike diode-based sensors, thermocouple probes are true square-law detectors. Such sensors are particularly useful in free-space field surveys ([Narda STS, 2005](#)). These sensors are, however,

impractical for dosimetric and near-field measurements because of their size, generally lower sensitivity and dynamic range.

Thermistors are also small true square-law detectors. They can have a higher resolution than thermocouples, but need more frequent calibration.

The performance of these probes depends strongly on the following parameters:

- Frequency, modulation, and field strength;
- Polarization, direction of propagation, and field gradients;
- Material boundaries near the probe sensors;
- Sources of interference (noise, static and low-frequency fields, vibration, temperature, etc.).

The influence of these parameters must be characterized by individual calibration under well-defined conditions for each probe. A detailed summary of different calibration methods for field probes and a characterization of the most crucial parameters contributing to the measurement of uncertainty are given in [Poković \(1999\)](#). The influence of these parameters must

be included in the resulting uncertainty assessment, since the conditions of actual use of the probes may differ considerably from the conditions under which they are calibrated.

Modern free-space and dosimetric field probes operate in the frequency band from 10 MHz up to 6 GHz. They have an isotropy error smaller than ± 0.5 dB and sensitivities in the range 5–10 $\mu\text{W/g}$. These probes have very small sensor tips (2.5 mm) to allow high spatial resolution and measurements very close to material boundaries. A probe with reduced size (tip diameter, 1.0 mm) has been described for accurate dosimetric measurements at frequencies exceeding 10 GHz ([Poković et al., 2000a](#)). Probes for determining both the electrical- and magnetic-field pseudo-vector information are presented in [Poković et al. \(2000b\)](#).

(b) *Electro-optical sensors*

Modern, electro-optical sensors allow the measurement of the full RF-frequency domain and phase as well as intermediate-frequency time-domain signal information while maintaining a superior electrical isolation through the use of optical fibres for signal transmission.

In general, two sensor concepts are used today: (1) passive optical sensors ([Togo et al., 2007](#)); and (2) active optical sensors [Kramer et al. \(2006\)](#). Modern passive electro-optical sensors typically modulate the information on laser light passing through electro-optically active crystals embedded in a fibre-optic system. Common crystal materials include cadmium telluride (CdTe) and lithium niobate (LiNbO₃), which change their refractive indices depending on the E-field applied across the crystal, or cadmium manganese telluride (CdMnTe), which is sensitive to the magnetic fields applied across the crystal ([Poković, 1999](#)). The sensitivities of modern active optical sensors can be as low as 100 $\mu\text{V/m}$ per Hz^2 , or greater than 0.3 V/m when measuring a signal of width of 5 MHz ([Kramer et al., 2006](#)).

1.4.3 *Measurement antennae*

Different types of broadband-matched antennae are usually applied for the frequency-selective exposure assessment of incident fields. These broadband antennae are matched to 50 ohm to be compatible with standard RF receivers. They have applications in far-field measurement of radiation, e.g. from cellular base stations and broadcast services.

Common broadband RF-measurement antennae such as horn or log-periodic antennae have a certain directivity. This reduces the applicability of these antennae for complex propagation scenarios, particularly at locations where the incident field is not dominated by a direct line-of-sight propagation path, but by multipath propagation ([Kühn, 2009](#)).

Tuned dipole antennae have an isotropic pattern (no directivity) in azimuth, but lack broadband characteristics.

Conical dipole antennae have an isotropic pattern in azimuth and generally good broadband characteristics ([Seibersdorf Research, 2011](#)), which substantially reduces the number of measurements needed.

1.4.4 *Temperature instrumentation*

(a) *Temperature probes*

Local SAR values can also be assessed by temperature measurements (see Section 1.3); however, thermal-diffusion effects must be practically absent. This is only possible if the system is in thermal equilibrium at the beginning of the exposure, or if heat-diffusion processes are known for the assessment period. Heat losses due to radiation and convection during the measurement interval must be negligible, or known and corrected for. If these heat-diffusion processes are unknown, the response time of the thermal measurement equipment must be sufficiently short to avoid underestimation of the exposure ([Schuderer et al., 2004a](#)).

Two types of temperature probes exist: thermistor-based and those based on optical effects. The requirements for temperature probes for SAR assessments are:

- Small size: the probe must be small to resolve high temperature gradients, without disturbing the temperature distribution or the RF field;
- Non-conductive materials: only electrically non-conductive materials prevent heating of the probe by induced currents because they are transparent to EMFs;
- Low noise level: small differences in temperature must be detected accurately, especially for dynamic temperature measurements, e.g. of SAR, and thus the noise level should be much less than 10 mK;
- Short response time: this is essential for SAR measurements as the temperature rise (dT/dt) is proportional to the SAR only in the absence of heat diffusion. A probe suitable for SAR measurements must have reaction times much faster than 100 ms ([Schuderer et al., 2004a](#)).

A novel design for temperature probes for dosimetric assessments, introduced by [Schuderer et al. \(2004a\)](#), provides a spatial resolution of 0.02 mm^2 , a noise level of the temperature of 4 mK, and a sensitivity of 0.5 mK/s with a response time of $< 14 \text{ ms}$.

Temperature probes based on thermo-optical effects are applied in high-voltage transformers, industrial microwave ovens and in treatment for hyperthermia. One exploited effect is the decay rate of a phosphorescent layer at the tip of a fibre-optic cable ([Wickersheim & Sun, 1987](#)). These commercially available probes have a noise level of 0.1 K, with reaction times of 250 ms. Another optical effect is the interferometric property of a cavity filled with materials that have highly temperature-dependent refractive indices. These probes reach sensitivities of 2–3 mK/s ([Burkhardt et al., 1996](#)).

(b) Infrared photography

The measurement of temperature by black-body-equivalent radiation (infrared photography) is an alternative to invasive measurements using temperature probes. The resolution of infrared thermographs can be very high and the sensitivity of affordable infrared detection systems has improved substantially over the past 30 years. This was also one of the first methods used to measure SAR ([Guy, 1971](#)), as the surface radiation can be recorded quickly with infrared cameras without perturbing the incident field. Infrared cameras were used to measure the temperature increase on a human head exposed to GSM mobile phones ([Taurisano & Vander Vorst, 2000](#)). The technique has several disadvantages:

- Limited sensitivity compared with temperature or dosimetric probes;
- Can be used only for measurements of surface temperature;
- The thermal radiation characteristics of the materials must be determined accurately;
- The background radiation must be homogeneous;
- Evaporation and convection can cause substantial errors and must be controlled;
- Different viewing angles of the camera can yield different results, since surfaces are not isotropic infrared radiators.

(c) Microcapsulated thermo-chromic liquid crystals

A novel idea to assess three-dimensional temperature distributions optically and in quasi real-time was proposed by [Baba et al. \(2005\)](#). Microcapsulated thermochromic liquid crystals (MTLC) were suspended uniformly in a gel with the dielectric properties of human muscle tissue. The temperature of the gel is determined by measuring the light scattered from a laser beam

that scans through the liquid. The technique has limited dynamic range and sensitivity.

(d) *Calorimeters*

Calorimetry encompasses methods for measuring heat produced by biological, chemical or physical endothermic or exothermic processes. Calorimetric methods are suitable for determining average *wbSAR*, but they cannot provide information about *SAR* distribution.

Calorimetry can be subdivided into two types:

- Direct calorimetry: the heat is measured directly by use of calorimeters;
- Indirect calorimetry: the quantity of heat is determined by measuring the amount of oxygen consumption and relating it to the oxaloric equivalent of the reaction.

Basically, calorimetric dosimetry analyses the heating and cooling processes of a sample exposed to RF radiation. Typical direct calorimeters used in microwave dosimetry are the Dewar flask and the twin-well calorimeter ([Gajsek et al., 2003](#)).

1.4.5 *Measuring SAR and the near field*

Dosimetric evaluation inside test phantoms such as SAM requires the measurement of *SAR* at several hundreds of points distributed over a complex three-dimensional phantom. The process is divided into: (1) searching for the location of the maximum absorption on a two-dimensional grid; and (2) determining the *psSAR* value on a fine three-dimensional grid. These points must be determined with high accuracy, especially at high frequencies, to achieve low measurement uncertainty despite high attenuation and large variations in spatial-field intensity. Automated systems for dosimetric assessment have been developed to perform these compliance tests. A typical system for dosimetric assessment is a computer-controlled six-axis robotic positioner. It is used to move the dosimetric E-field probe

within a scanning grid, which can be adaptive, e.g. it follows the surface that is being detected during the scanning job and positions the probe axis orthogonal to that surface. The measurement results, i.e. field and *SAR* distributions, as well as 1 g and 10 g spatial average peak *SAR*, are automatically evaluated and visualized. The expanded standard uncertainty ($k = 2$) is less than 20%. It should be noted that this approach provides reliable conservative estimates of the maximum peak spatial *SAR* that might occur in the user population, but offers little information about the exposure of specific tissues or individual exposure ([Kühn, 2009](#)).

In summary, compliance evaluation of body-mounted transceivers provides reliable conservative estimates of maximum *psSAR*-1 g and *psSAR*-10 g anywhere in the body, but these estimates are generally poorly correlated with the maximum exposure of specific tissues (e.g. brain tissue) or typical exposure levels during daily usage of the device (system- and network-dependent). In other words, the information has only limited value for epidemiological studies.

1.4.6 *Incident-field measurements in the far field*

Evaluation of the exposure in the far field of a transmitter is usually conducted for fixed installations such as radio and television broadcast antennae, radar sites, or cellular base stations. Exposure assessments are carried out in areas that are generally accessible or for which access is restricted to qualified working personnel only. Compliance is tested with respect to the reference levels by assuming free-space field impedance for the RF energy, i.e. by E-field evaluation. Only one measurement point is required under real far-field conditions. However, actual environments usually involve nearby reflectors and scatterers, i.e. a scanning procedure is required to find the maximum incident fields ([Kühn, 2009](#)).

Since the transmitters under evaluation do not always operate at maximum power – the transmitted power of base stations being dependent on traffic intensity – broadband instantaneous measurements are often insufficient to determine the highest level of exposure. In such cases, information on the maximum exposure with respect to the measured values must be available and soundly applied to establish exposure in the worst-case scenario. [Table 1.12](#) lists the parameters necessary for extrapolation of exposure in the worst case and to reduce the uncertainty of the actual measurement campaign. It is easier to determine the measurement methods when additional parameters are known. General sources of error are:

- Field perturbation by measurement personnel, e.g. scattering and absorption of EMFs due to the body of the measurement engineer;
- Application of an inappropriate measurement antenna, e.g. disregard for antenna directivity and polarization;
- Application of ineffectively decoupled cables, acting as secondary antennae;
- Application of incorrect measurement settings of the RF receiver for the type of signal to be measured;
- Incorrect selection of the measurement location, e.g. measurement points that are not appropriate for yielding the maximum EMF exposure or measurement points close to bodies that influence the calibration of the measurement antennae ([Kühn, 2009](#)).

Different methods for assessing EMF exposure in the far field have been proposed. One approach is the antenna-sweeping method. This method requires the engineer to slowly move the measurement antenna with varying polarizations and directions through the volume of interest ([Sektion NIS, 2002](#)). Another method is based on the examination of several well defined points in the area of interest. In this case, the antenna is

mounted on a tripod and the different directions and polarizations are examined at the considered points ([ANFR, 2004](#)). The first method is conservative, but sensitive to the position of the operator with respect to the antenna. With the second method, measurements can be performed with the engineer located further away, but the number of measurements in the volume is small. A combination of both methods is presented by [Coray et al. \(2002\)](#), who suggest that the region is first scanned for the field maximum in the area of interest and that an isotropic and frequency-selective measurement is then performed at the location of the maximum.

Often, far-field techniques are employed in the near field of transmitters, e.g. on transmitter towers. Some standards allow a spatial averaging of E-field evaluations ([ANSI/IEEE, 1991](#)), the rationale of which is based on the wbSAR limit. However, this constitutes a relaxation of the safety criteria as it does not consider H-field coupling as the dominant mechanism in the near field nor the limits of psSAR. On the basis of current knowledge, such relaxations do not exclude the possibility of exceeding the basic restrictions or underestimating the local exposure ([Kühn, 2009](#)).

The advantages and limitations of different measurement equipment for assessing the exposure of unknown transmitters are discussed below.

1.4.7 Broadband measurements

Broadband-measurement probes are single-axis or three-axis sensors (dipole or loop) constructed in a similar way to the near-field sensors. No information on the spectral characteristics of the field is provided by these probes. Therefore, if a broadband meter is used for compliance testing, the measured field value must be no higher than the lowest permissible limit defined for the frequency range of the meter. Broadband survey meters are also

Table 1.12 Important parameters of radiofrequency transmitter sites assessed in the far field

Site parameter	Explanation
Location	The location of the transmitter with respect to the measurement point
Line of sight/nonline of sight	Determines if a prevalent propagation path may be expected
Type of site	Single or multiple antenna site
Antenna directivity	Antenna beam characteristics
Antenna radiation direction	The direction of maximum radiation
Antenna power at measurement	The antenna input power at the time the measurement takes place
Maximum antenna input power	Maximum permissible antenna input power
Frequency	Frequencies at which the site transmits
Communication system	Communication system that is used, i.e. which signal modulation characteristics are to be expected
Other sources of radiation	The field at the measurement points when the assessed transmitter is switched off

Adapted from [Kühn \(2009\)](#)

relatively inexpensive and easy to use, and are thus often used for field-survey measurements ([Kühn, 2009](#)).

Fig. 1.15 displays the components of typical broadband field-survey meters. Fig 1.16 shows the frequency response of two broadband probes.

Some broadband probes are designed to match the frequency dependence of the human exposure limits. In all cases, it is advised that the out-of-band response of these instruments is carefully characterized to avoid spurious readings. If a specific transmitter is the dominant source, compliance testing is substantially simplified ([CENELEC, 2005](#)).

The main sources of uncertainty regarding broadband survey meters are: calibration, linearity, frequency response, isotropy, time-domain response, and temperature response; so the accuracy of broadband evaluations is significantly limited, but generally conservative ([Kühn, 2009](#)).

(a) Frequency-selective measurements

Frequency-selective measurement techniques can overcome the difficulties of the unknown spectrum of the field. However, the execution of the measurement is more complicated and requires specialized engineers.

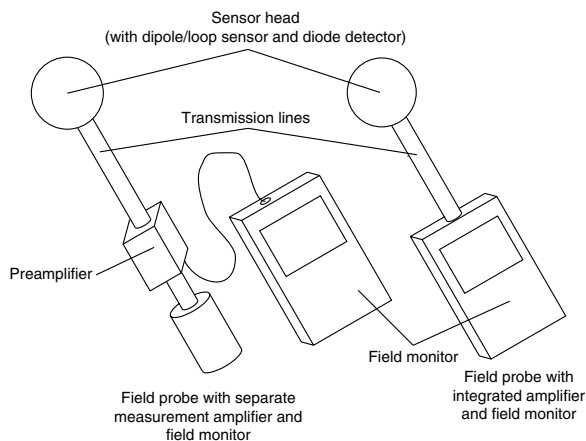
Measurements in the frequency domain are performed with an antenna connected to a spectrum analyser.

Most spectrum analysers provide video filters for additional smoothing of the spectral signal. Optimal parameter settings for the analyser for GSM and UMTS based on a simulation approach have been presented ([Olivier & Martens, 2005, 2006](#)). The application of spectrum analysers is a complex topic. Procedures dealing with frequency-selective measurements should always describe the parameter settings of the spectrum analyser to produce correct, reproducible and comparable results. Nevertheless, the engineer should test the actual applicability of these settings for the particular measurement equipment ([Kühn, 2009](#)).

The main sources of uncertainty regarding frequency-selective measurements are:

- Calibration of the spectrum analyser, cable, and measurement antenna;
- Linearity of the spectrum analyser, cable, and measurement antenna;
- Frequency response of the spectrum analyser, cable, and measurement antenna;
- Demodulation method of the spectrum analyser (detector type);

Fig. 1.15 Schematic of the most common broadband radiofrequency field-survey meters



Republished with permission of Taylor and Francis Group LLC Books, from [Kühn & Kuster \(2007\)](#); permission conveyed through Copyright Clearance Center, Inc.

- Temperature response of the spectrum analyser, cable, and measurement antenna; and
- Mismatch between measurement equipment.

Although frequency-selective measurement methods overcome most of the problems affecting use of broadband-survey meters, they are not always sufficient to correctly evaluate exposure from different transmitters operating at the same frequency. In this case, measurement receivers should be applied ([Kühn, 2009](#)), as presented below.

(b) Code-selective measurements

Code-selective measurements are specifically necessary when the exposure from a transmitter involves code-division multiple access (CDMA), e.g. when a Universal Mobile Telecommunications System (UMTS) is to be assessed. All UMTS base stations usually transmit in the same frequency band. With a frequency-selective receiver, it is not possible to discriminate between exposures from different base stations, because a single frequency band is used and the channels are multiplexed in the code domain. Code-selective

receivers decode the signal received from a base station, i.e. the receiver is able to discriminate between the received field strength from its base station and other noise-like sources. The receiver measures only the field received from its transmitting base station if the particular descrambling code is used for decoding. Basically, the same sources of uncertainty must be considered for code- and frequency-selective measurements. In general, if measurement receivers are applied, the overestimation of the measured field values is expected to be smaller than for frequency-selective and broadband measurements ([Kühn, 2009](#)).

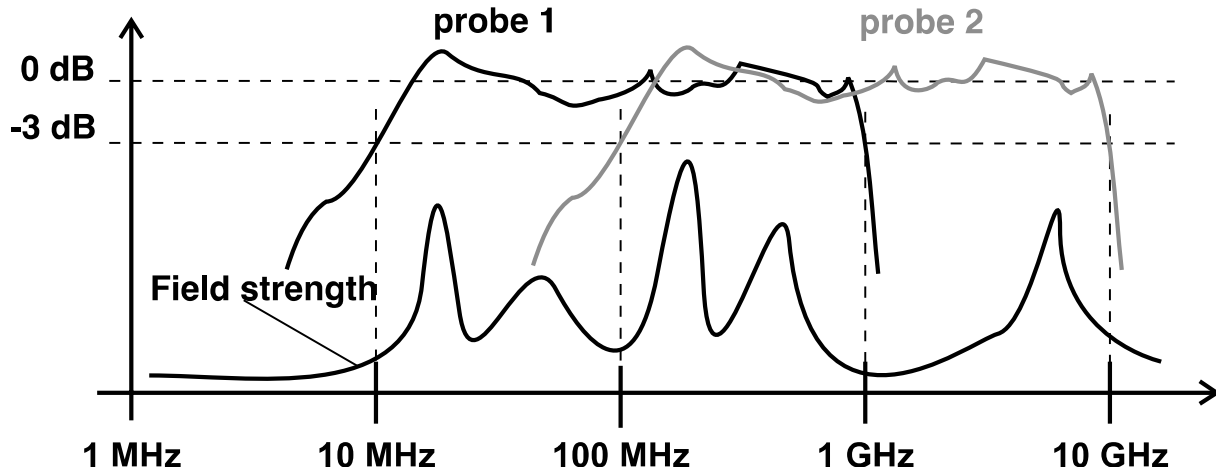
1.4.8 Calibration

Measurement with known uncertainty can only be performed if the measurement equipment is appropriately calibrated. In general, calibration of the measurement equipment is demanding (sensitivity as a function of frequency and modulation, linearity for different modulations, deviation from isotropy, etc.). High-quality calibration documentation is essential to determine the accuracy of the measurements or their uncertainty, respectively.

1.4.9 Uncertainty assessment

Exposure assessments are prone to many uncertainties that must be carefully determined. This is the most difficult aspect of any measurement protocol, because it usually covers many more parameters than only the uncertainties associated with the measurement equipment. For example, in the case of demonstration of compliance with respect to basic restrictions, it includes estimation of the coverage factor for the exposed populations. In the case of uniform incident field, it is necessary to determine the uncertainty of the field measured during the period of measurement with respect to the maximum exposure at this site. In case of non-uniform fields, it needs to

Fig. 1.16 Frequency response of two broadband radiofrequency field-survey meters



The fields in the frequency ranges are summed. If the outputs from probes 1 and 2 are added, then the fields in the overlapping frequency range are counted twice. The field values measured with probe 1 must comply with the lowest limit in the frequency band 10 MHz to 1 GHz, while the readout of probe 2 must comply with the lowest limit between 100 MHz and 10 GHz. The overlapping frequency range is surveyed twice if the exposure values are superimposed to cover the entire frequency range. Republished with permission of Taylor and Francis Group LLC Books, from [Kühn & Kuster \(2007\)](#); permission conveyed through Copyright Clearance Center, Inc.

be demonstrated that the ratio of measured fields to reference levels is conservative with respect to the induced fields.

[The Working Group noted that it should be good measurement practice for the results of any measurement campaign to be presented only when accompanied by an extensive uncertainty assessment.]

1.4.10 Specific measurement problems

(a) Demonstration of compliance with dosimetric safety limits

The objective of compliance demonstration is to determine the exposure conservatively for the range of intended usage of the device or equipment with respect to the entire user group. In general, there is a strong dependence on position, distance, anatomy and posture. This dependence can only be determined by numerical simulations. Given an acceptable uncertainty, several hundred permutations of the most important parameters must be performed. In other words, the parameter space is large and the assessment

must be done with sufficient care and followed by an extensive discussion on the parameters investigated and the resulting uncertainties.

(b) Assessing personal exposure

In its most recent update of *Research Agenda for Radiofrequency Fields*, the World Health Organization (WHO) has recommended improvement of exposure assessment in epidemiological studies as a high-priority research need: “Quantify personal exposures from a range of radiofrequency sources and identify the determinants of exposure in the general population” ([WHO, 2010a](#)).

Associated problems with personal exposure assessment are:

- Compliance tests versus real-life exposure;
- Assessment of incident versus induced fields;
- Appropriate dosimetric quantities;
- Combination of exposure from multiple sources operating at different distances and frequencies;

- Strong temporal, geographical and usage dependence of the exposure, especially in relation to the exposure period relevant to the epidemiological data;
- Technology dependence of exposure and rapid technological changes; and
- Selection and, even more importantly, exclusion of potential exposure proxies.

As mentioned before, the worst-case levels of exposure determined during compliance testing of, e.g. mobile phones or base stations are in many cases not representative of actual real-life and everyday exposure. The protocols for compliance testing are generally optimized to provide a conservative estimate of maximum exposure. However, exposure assessment in epidemiological research aims at categorizing actual personal exposure. Results from compliance testing can, however, be useful to validate propagation models ([Bürge et al., 2008](#)), or to compare potential proxies that can be independently assessed, such as those based on mobile-phone design ([Kühn, 2009](#)).

Assessment and dosimetry of EMF exposure in epidemiological and human studies have been and often still are performed in terms of quantities that are only representative for demonstration of compliance with safety guidelines, e.g. incident-field quantification, or induced wbSAR and psSAR. The dosimetric meaning of the aforementioned quantities is questionable for current studies, which all aim at detecting potential effects for exposures well below established safety levels. In addition, the end-points investigated are typically effects on specific tissues, organs or functional regions of the brain and the quantification of the classical dose evaluations often does not allow a clear distinction between body regions or an accumulation of the dose from various sources. Quantification of exposure in terms of incident fields is especially problematic, since incident fields are often not directly related to induced fields. A common mistake is to combine exposure in terms of incident fields at different

frequencies by applying the root-sum-square (see Glossary) over the individual frequency contributions. Currently, novel dosimetric models are being developed to relate incident to induced EMF ([Djafarzadeh et al., 2009](#)) or to relate SAR-compliance test data measured in homogeneous media to SAR in specific anatomical regions of the human brain ([Gosselin et al., 2011](#)). By expressing exposure directly in terms of induced EMF or SAR in specific regions, the combination of multiple sources also becomes straightforward. Also, it allows a direct assessment of different source contributions according to geographical location or usage.

Variations due to geographical location in the far-field of transmitters should only be addressed with validated propagation models (e.g. [Andersen et al., 2007](#); [Frei et al., 2009a](#)), and not with, e.g. simplistic distance metrics. For near-field exposure, e.g. from mobile phones, the orientation of the source with respect to the body is relatively well defined; however, due to the output power control of modern mobile devices, there can be large variation in exposure depending on geographical location (more than twofold) and, even more importantly, the communication system (a factor of 100 or more). The assessment of these variations is typically addressed in terms of measurements in situ ([Wiart et al., 2000](#); [Kühn, 2009](#); [Kelsh et al., 2010](#)).

(c) *Measurement of the very close near field below 10 MHz*

The assessment of human exposure at frequencies between 30 MHz and 6 GHz is well established. International standards and national guidelines provide detailed assessment methods that are well specified with relatively low uncertainty. The measurement of incident fields at frequencies below 10 MHz is also well established. However, there is comparatively little research on the measurement of induced fields at frequencies below 10 MHz. The problems

associated with induced-field measurement at frequencies below 10 MHz include:

- Strong spatial non-uniformity of the fields, requiring high resolution of measurements;
- Strong temporal variation in the fields, especially from signals with transients, requiring equipment to have a large operating bandwidth;
- Field values measured very close to the source greatly overestimate the induced values, i.e. compliance often needs to be demonstrated by assessment of the induced fields;
- High variation in the permittivity and conductivity of tissues, making human modelling (e.g. development of phantoms) difficult;
- Practical limitations in the use of time-domain numerical electromagnetic solvers at low frequencies, resulting in slow convergence; and
- Limitations in the applicability of certain frequency-domain numerical electromagnetic solvers (e.g. electro-quasistatic solvers) due to assumptions and approximations.

(d) Measurement of signals with complex modulations

Today, most broadband field probes, as well as personal exposure meters, are calibrated with narrow-band (single-frequency) continuous wave signals. However, the measured signals differ greatly from continuous wave signals in terms of variation in time-domain amplitude and signal bandwidth. Variation in the time-domain amplitude of modern communication signals (peak-to-average power ratio [PAPR] of up to 14) places great demands on the linearity of the detectors in broadband probes and exposure meters, and in spectrum analysers. These requirements are often not fulfilled for the detectors and filters in traditional field probes

and exposure meters, such that these respond differently when comparing continuous wave and waveforms applying modern modulation schemes. For compliance testing, field probes can be calibrated with the actual test signals. For measurements in situ, e.g. with exposure meters, such a calibration is not straightforward since the real-life communication-signal characteristics might not always remain constant during measurement. Care should be taken also when using narrow-band receivers, i.e. spectrum analysers, when measuring complex-modulation waveforms. Also, these receivers require modulation-specific measurement settings, e.g. filter, detector, resolution bandwidth, sweep time etc. to perform field measurements with reasonably small uncertainties ([Joseph et al., 2002, 2008](#); [Olivier & Martens, 2005, 2006](#)).

1.5 Interaction of RF-EMF with biological systems

Although numerous experimental studies have been published on the non-thermal biological effects of RF-EMF, multiple computational analyses based on biophysical and thermodynamic considerations have concluded that it is theoretically implausible for physiological effects (except for reactions mediated by free radical pairs) to be induced at exposure intensities that do not cause an increase in tissue temperature ([Foster, 2000](#); [Adair, 2002, 2003](#); [Sheppard et al., 2008](#)).

RF electromagnetic radiation is classed as non-ionizing radiation as it comprises photons that do not have sufficient energy to break chemical bonds or ionize biological molecules ([Stuchly, 1979](#)). The energy of a photon of an electromagnetic wave is given by $E = hf$, where h is Planck's constant (6.626×10^{-34} J•s or 4.136×10^{-15} eV•s) and f is frequency, thus the energy of a photon in the RF spectrum varies from approximately 4.1×10^{-6} eV (6.6×10^{-25} J) at 1 GHz to 1.2×10^{-3} eV

(2.0×10^{-22} J) at 300 GHz. This is thus far less than the minimum amount of energy needed to ionize organic materials or metals, which is approximately 5–10 eV.

When a biological body (animal or human) or tissue is exposed to an RF-EMF, the RF energy is scattered and attenuated as it penetrates body tissues. Energy absorption is largely a function of the radiation frequency and the composition of the exposed tissue. Because of the high dielectric constant of water, the water content of the tissue determines to a large extent the penetration of a frequency-specified electromagnetic wave. The rate of energy absorbed by or deposited per unit mass per unit time is the specific absorption rate (SAR); this value is proportional to the root-mean-square (rms) of the induced electrical field strength $[E]^2$ and to the electrical conductivity (σ) of the tissue per tissue density (ρ):

$$\text{SAR} = [E]^2 \cdot \sigma / \rho$$

The SAR expressed in units of watts per kilogram (or mW/g) can also be estimated from measurements of the rise in temperature caused by RF-energy absorption in tissue:

$$\text{SAR} = C_p \cdot \delta T / \delta t$$

where C_p is the specific heat of the tissue or medium, $\delta T / \delta t$ is the initial rise in temperature over time. Values for the dielectric constant and conductivity vary substantially over the RF range (30 MHz to 300 GHz).

To cause a biological response, the EMF must penetrate the exposed biological system and induce internal EMFs. RF-energy absorption depends on incident field parameters (frequency, intensity, polarization), zone of exposure (near field or far field), characteristics of the exposed object (size, geometry, dielectric permittivity and electric conductivity), and absorption or scattering effects of objects near the exposed body ([Stuchly, 1979](#)).

Based on the relationship between wavelength (λ) and frequency

$$c = f \cdot \lambda$$

where c is the speed of light (3×10^8 m/s), it is obvious that the wavelength of RF radiation varies substantially between 30 kHz (10 km) and 300 GHz (0.1 cm). At the frequencies used for mobile phones (approximately 1–2 GHz), the corresponding wavelengths are 30 and 15 cm. Considering that near-field exposures occur at distances from a radiating antenna within approximately one wavelength of the radiated EMF and that far-field exposures occur at distances that exceed one wavelength of the radiated EMF, it is clear that reactive near-field and far-field exposures may occur, depending on the frequency of the incident field and the distance of the exposed person from the radiating antenna. Both near-field and far-field exposures can occur with the use of wireless telecommunication devices. In the near-field region, the electric and magnetic fields are decoupled and not uniform, wave impedance varies from point to point, power is transferred back and forth between the antenna and the surrounding object, and the energy distribution is a function of both the incident angle and distance from the antenna ([Lin, 2007](#)). Because the electric and magnetic fields are decoupled in the near field, the induced field can be obtained by combining the independent strengths of the electric and magnetic fields, i.e. the electric and the magnetically induced electric fields inside the body ([Lin, 2007](#)).

1.5.1 Thermal effects

The most recognized effect of RF radiation in biological systems is tissue heating. The absorption of RF-EMF energy by biological systems generates an oscillating current that is transferred into molecular motion of charged particles and water molecules, which are strongly dipolar and

are the major component of biological tissues. Polar molecules move to align themselves with the EMF to minimize the potential energy of the dipoles. Absorption and resonant oscillations in polar subgroups of macromolecules (e.g. proteins, DNA) are largely damped by collisions with surrounding water molecules. Damping or friction slows the motion of the oscillator. These collisions disperse the energy of the RF signal into random molecular motion. Tissue heating occurs because the rotational motion of molecular dipoles is hindered by the viscosity of water and interactions with other molecules, i.e. the rotational energy is transferred to the surrounding aqueous environment as heat. The magnitude of motion that results from the interaction of polar substances with electric fields is dependent on the strength and frequency of the field. In addition, the actual increase in temperature is dependent on the ability of the organism to thermoregulate. At high frequencies where the orientation of dipoles cannot keep up with the oscillations of the field, the system behaves like a non-polar substance (Stuchly, 1979).

As electrical fields penetrate complex biological tissues, the electric field is reduced as a result of dielectric constituents becoming polarized in response to the field. Standards for RF exposure of workers and the general population are based on protection against adverse effects that might occur due to increases in tissue or body temperature of 1 °C (wbSAR, ~4 W/kg) or less (after applying safety factors). Because RF-energy penetration and induced effects are dependent on the frequency of incident-field parameters and the composition of exposed tissues, quantifying SARs in small averaging regions is more relevant for evaluations of human health effects. Estimates of SARs in the head of individuals exposed to RF radiation during use of mobile phones that operate at a power output of 0.25 W indicate that the emitted energy would cause a rise in brain temperature of approximately 0.1 °C (Van Leeuwen *et al.*, 1999; Wainwright, 2000);

therefore, it has been suggested it is unlikely that effects in the brain would be caused by increases in temperature (Repacholi, 2001). However, it is possible that temperature-sensitive molecular and physiological effects occur already with an increase of the temperature of ≤ 0.1 °C, while temperature changes approaching 1 °C are likely to affect several biological processes (Foster & Glaser, 2007).

Rates of temperature increase may be important in affecting a physiological change. Indeed, microwave-induced heating has been attributed to a rapid rate of heating 1–10 °C/s, which leads to acoustic waves due to expansion of tissue water. This auditory effect associated with brief pulses (1–10 μ s) at frequencies of 1–10 GHz and peak power-densities of $\sim 10^4$ W/m² (10³ mW/cm²) occurs with only small increases in temperature in the head (Foster & Glaser, 2007). Low levels of exposure to RF radiation may result in small temperature changes that cause conformational changes in temperature-sensitive proteins and induce the expression of heat-shock proteins; studies on the effects of low intensity RF-EMF exposures on temperature changes and expression of heat-shock proteins are described in Section 4 of this *Monograph*.

1.5.2 Physiological effects

Non-thermal effects (or effects associated with a negligible increase in temperature) are defined as biological changes that occur with body temperature changes that are < 1 °C, below measurable heating, or in the range of thermal noise. Several arguments have been presented against the plausibility of a non-thermal mechanism by which RF radiation could affect physiological changes; these include: (a) damping effects of the water surrounding biological structures are too strong to allow resonances to exist at radiofrequencies (Adair, 2002); (b) the relaxation time – the time for a molecule to return from an excited state to equilibrium – for excitations produced

by RF fields (e.g. vibrations in molecules), is similar to the relaxation time for thermal noise, and shorter than the lifetime of the absorption and transfer of energy into resonant modes of oscillating elements in biological systems ([Adair, 2003](#)); and (c) the perturbation of the biological structure induced by the applied field must be greater than the effects of random thermal motion and the effects of other dissipative forces, such as viscous damping by the surrounding medium ([Foster, 2000](#)). Random thermal motion of charged components in biological systems (i.e. thermal noise) creates random fluctuating EMFs. [Adair \(2003\)](#) has concluded that it is unlikely that RF radiation with a power density of less than 10 mW/cm^2 (100 W/m^2) could have a significant effect on biological processes by non-thermal mechanisms.

[Sheppard et al. \(2008\)](#) have evaluated several potential mechanisms of interaction of RF radiation with biological systems and concluded that, other than heating and possible effects on reactions mediated by free radical pairs, RF field strengths in excess of system noise (collisions among various molecular oscillators generated largely by thermal agitation) could not alter physiological activities without also causing detectable tissue heating. Some mechanistic considerations addressed by these authors include:

- *Endogenous electric fields* involved in physiological processes (e.g. embryonic development, wound healing, and neuronal activity) have strengths in the range 1–200 V/m. While neuronal circuit oscillations were affected *in vitro* by extremely low-frequency electric fields, no mechanisms for inducing changes in cell-membrane potential at frequencies above ~10 MHz have been demonstrated. Furthermore, the net field effect on such a biological system would be the sum of the endogenous and applied fields. Thus, to alter a biological response such as ion

transport through a membrane channel, the amplitude of the external signal would need to be of the same order of magnitude as the endogenous field ([Adair, 2003](#); [Sheppard et al., 2008](#)).

- *Specialized sensory systems* may be capable of detecting weak EMFs by integrating signals from numerous sensors over space and time. While specific sensory systems have been shown to exist for low-frequency, infrared and visible radiation, there is no evidence for the existence of RF-sensitive receptors in biological systems ([Sheppard et al., 2008](#)). However, some sensory systems may respond to very small increases in temperature ($< 0.1 \text{ }^\circ\text{C}$).
- *Effects of weak RF fields that do not cause heating* would be likely to require frequency-dependent resonant absorption or multiple-photon absorption to induce an amplified signal strong enough to overcome intrinsic molecular noise ([Sheppard et al., 2008](#)). This is because the photon energy of RF radiation is much smaller than thermal energy at body temperature ($k \cdot T$, where k is the Boltzmann constant, $1.38 \times 10^{-23} \text{ J/K}$ ($8.62 \times 10^{-5} \text{ eV/K}$), and T is the absolute temperature), i.e. $27 \times 10^{-3} \text{ eV}$ per oscillating mode at body temperature. However, biological systems appear to absorb RF signals like a broadband receiver rather than eliciting line spectra characteristic of resonant vibrational motion ([Prohofsky, 2004](#); [Sheppard et al., 2008](#)). In addition, RF electric field strengths of up to 200 V/m cannot transfer sufficient energy to organelles or biological molecules to alter biological activities or affect thermal noise (kT) fluctuations, such as the opening of voltage-gated ion channels, spatial arrangements of membrane-associated ions, collision rates of charged ligands with proteins, or enzyme reaction kinetics ([Adair, 2002, 2003](#);

[Sheppard et al., 2008](#)). [Adair \(2002\)](#) suggested that, while coupling of RF-EMF to biological systems may exhibit resonance behaviour, damping of the vibrational motion by interactions with the aqueous environment prevents the absorption of sufficient energy to induce a biological effect. To significantly affect a biological system, the response from the RF signal must be comparable to the effect of thermal noise ([Adair, 2003](#)).

- *RF-EMF may be directed to specific sites* of a biological structure, leading to local areas of enhanced field strength. However, the smallest focal spot of concentrated energy would have a radius of the order of a wavelength, which is much larger than most cells (e.g. at 300 GHz, $\lambda = 1000 \mu\text{m}$). Thus, on a cellular basis, RF-energy absorption is very small. [Fröhlich \(1968\)](#) has suggested that incident RF energy may be captured by a large group of oscillating dipoles and integrated into a single mode of coherent vibrational energy. For this to occur and produce a coherent response, [Sheppard et al. \(2008\)](#) suggested that the energy stored in the coupled oscillators would need to be comparable to thermal energy and protected from damping by water or other molecules. In addition, energy and thermal diffusion prevent the formation of significant temperature differences at the cellular and subcellular levels.
- *In order for RF electric fields to induce small changes in protein structure* that would affect binding of substrates or ligands to enzymes or receptor proteins, extremely high field strengths would be required ($\sim 10^9 \text{ V/m}$) ([Sheppard et al., 2008](#)).

Since living systems are not in thermal equilibrium, mechanistic theories on interactions between RF-EMF and biological tissues must consider the non-equilibrium and nonlinearity

of these systems. [Binhi & Rubin \(2007\)](#) suggest that biochemical effects may be induced by weak EMFs in targeted systems that are in non-equilibrium states in which the time to transition from an intermediate metastable state to a final active or inactive state may be less than the thermalization time of the induced field.

[Prohofsky \(2004\)](#) has suggested that protein conformation might be affected by RF radiation if amplitudes of specific vibrational modes were altered. However, only intermolecular vibrational modes of proteins and the surrounding tissue are possible at RF frequencies, because high-frequency intramolecular resonant vibrational modes exist above several hundred GHz. Further, this author concluded that the biological effects of RF radiation in macromolecules (proteins and DNA) can only be due to temperature changes, because the absorbed energy associated with intermolecular vibrations is rapidly thermalized; the relaxation time for coupling RF waves to surrounding water (i.e. damping) is faster than the speed with which it can be transferred to intramolecular resonant modes. A non-thermal effect might exist if there were a very strong energy coupling between the intermolecular and intramolecular modes. Exceptions to the above-mentioned considerations are proteins such as myoglobin or haemoglobin, in which the haem group can oscillate in the protein pocket at lower frequencies (184 GHz is the lowest mode in myoglobin) ([Prohofsky, 2004](#)).

Any theories on the potential effects on biological systems of RF energy at low field strengths must account for the facts that biological systems do not exist at equilibrium, that the dynamic nature of these systems is controlled by enzyme-mediated reactions, and that primary effects may be amplified by nonlinear biological processes ([Georgiou, 2010](#)). The reproducibility of reported effects may be influenced by exposure characteristics (including SAR or power density, duration of exposure, carrier frequency, type of modulation, polarization, continuous versus

intermittent exposures, pulsed-field variables, and background electromagnetic environment), biological parameters (including cell type, growth phase, cell density, sex, and age) and environmental conditions (including culture medium, aeration, and antioxidant levels) ([Belyaev, 2010](#)).

A biophysical theory on how low-intensity RF-EMF exposures might affect physiological functions involves the alteration of ligand binding to hydrophobic sites in receptor proteins ([Chiabrera et al., 2000](#)). Collisions of the ligand ion in the hydrophobic region of the receptor protein result in loss of its vibrational energy. In order for RF exposures to affect the binding probability of an ion ligand with a membrane protein receptor, basal metabolic energy would have to amplify the effect of the RF field by maintaining the cell in thermodynamic non-equilibrium. Otherwise, the low-intensity exposure would be negligible compared with thermal noise. Other elements of this model that were used to evaluate the effects of low-intensity RF exposures on ligand binding are the extremely fast (“instantaneous”) rearrangement of atoms in the hydrophobic core of protein by the ligand ion, the fact that the endogenous field at the protein boundaries is large enough to exclude water molecules from the hydrophobic core, and that the ion-collision frequency near the hydrophobic binding site is much less than it is in water. The authors of this study noted that thermal noise must be taken into account when evaluating potential biological effects of RF exposures ([Chiabrera et al., 2000](#)).

Demodulation of pulsed RF signals (e.g. GSM pulsed at 217 Hz) might produce low-frequency electric fields ([Challis, 2005](#)). To confirm a biological effect from a low-frequency, amplitude-modulated RF signal, a nonlinear response in the biological sample would be expected ([Balzano & Sheppard, 2003](#)). Except for the case of an incident flux of RF energy at extremely high field-strength pulses that causes mechanical vibrations, most oscillators in a biological system respond linearly to the incident low-energy

photons in the RF spectrum; the dispersion of RF energy into random molecular motion energy occurs without generating harmonics of the incident signal in the energy spectrum of re-radiated photons by the exposed material. However, the authors of this study considered the possibility that demodulation of high-frequency incident RF signals might produce nonlinear interactions with biochemically induced transient oscillators in living tissues (e.g. uncoupled electrons of free radicals) by extracting low-energy signals. If this occurred, then the spectrum of RF-emission energy emitted from the exposed tissue would be altered, producing a second harmonic that would show up as a spectral line at twice the frequency of the incident signal ([Balzano & Sheppard, 2003](#)). Sensitive, frequency-selective instruments are available to detect the presence of frequency-doubling signals produced by nonlinear interactions between amplitude-modulated RF signals and molecular oscillators vibrating in unison in living cells ([Balzano, 2003](#)). Exposure of several different types of cell and tissue to continuous wave fields (input powers of 0.1 or 1 mW) in a double-resonant cavity at the resonant frequency of the loaded cavity for each sample (~880–890 MHz) did not emit second harmonic signals at twice the frequency of the incident signal ([Kowalczyk et al., 2010](#)). SAR values were approximately 11 mW/g for cells and 2.5 mW/g for tissues exposed to 1 mW RF fields. Although these results were inconsistent with the hypothesis that living cells can act as effective radio receivers and demodulate RF energy, a second harmonic response may be elicited by much more intense continuous waves (which would be likely to cause rapid heating) or very short-pulsed RF signals ([Kowalczyk et al., 2010](#)). [Sheppard et al. \(2008\)](#) concluded that it is unlikely that modulated RF fields significantly affect physiological activities of membranes, because non-thermal stimulation of cell membranes has not been observed above approximately 10 MHz and the voltage across a cell membrane from an

amplitude-modulated RF electric field of 100 V/m is much lower than the low-frequency voltage noise associated with membrane voltage fluctuations. Much higher incident field strengths, at levels that would cause significant tissue heating, would be needed to create electric fields comparable with endogenous fields.

Lipid-protein complexes appear to be more sensitive to perturbations from RF radiation at membrane phase-transition temperatures ([Liburdy & Penn, 1984](#); [Allis & Sinha-Robinson, 1987](#)). [Blackman et al. \(1989\)](#) suggested that the chick brain surface is also poised at a phase transition at physiological temperatures, and the long-range order that occurs in such a state would minimize the thermal noise limitations calculated for single-phase systems on signal detection of weak RF radiation. Consistent with this hypothesis, [Blackman et al. \(1991\)](#) observed that RF radiation-induced calcium-ion efflux-changes occurred only within the narrow temperature range of 36–37 °C.

The aggregation of dielectric objects by attractive forces between them is referred to as the pearl-chain effect ([Challis, 2005](#)). RF fields of about 125 V/m and at frequencies of up to about 100 MHz can produce oscillating fields in cells that enhance their attraction. At higher frequencies the induced dipoles might not have sufficient time to reverse direction and, therefore, stronger fields would be needed to produce the same attractive energy.

Electroporation is a process by which short pulses (~100 μs) of strong electric fields (e.g. 10–100 kV/m) are applied to cell membranes to induce transient pores that allow uptake of drugs, DNA, or other membrane-impermeable substances ([Foster, 2000](#); [Sheppard et al., 2008](#)). These changes occur without causing significant tissue heating or thermal damage.

1.5.3 Magnetic-field effects

Low-frequency magnetic fields might produce biological effects if they induce ferromagnetic resonance in tissues that contain high concentrations of iron particles (magnetite) ([Challis, 2005](#)).

Free radicals, which are highly reactive molecules or ions with unpaired electrons, are formed when radical pairs dissociate. By altering the recombination of short-lived radical pairs with antiparallel spins, low-intensity magnetic fields may increase the concentration of free radicals ([Challis, 2005](#); [Georgiou, 2010](#)). The expected increase in radical concentration is 30% or less ([Timmel et al., 1998](#)). The extent to which this increase can produce oxidative stress-induced tissue damage (e.g. membrane-lipid peroxidation or DNA damage) is not known. Furthermore, radicals are also a part of normal cellular physiology, being involved in intracellular signal transduction ([Finkel, 2003](#)). Therefore, even small effects on radical concentration could potentially affect multiple biological functions. By prolonging the lifetime of free radicals, RF fields can increase the probability of free-radical-induced biological damage. To affect DNA recombination and thus the repair of damage caused by radicals, external magnetic fields must act over the times that the radical pairs dissociate ($> 10^{-9}$ s); hence, [Adair \(2003\)](#) concludes that the effect of RF fields on free-radical concentrations would likely be limited to about 10 MHz or less. Resonance phenomena occur below 10 MHz, and may result in biological effects from low-level RF fields at about 1 MHz ([Henbest et al., 2004](#); [Ritz et al., 2009](#)).

[Georgiou \(2010\)](#) cited several studies that provide evidence for the induction of oxidative stress via the free-radical pair mechanism in biological systems exposed to RF radiation; some of the reported effects include increased production of reactive oxygen species, enhancement of oxidative stress-related metabolic processes, an increase in DNA single-strand breaks, increased

lipid peroxidation, and alterations in the activities of enzymes associated with antioxidative defence. Furthermore, many of the changes observed in RF-exposed cells were prevented by (pre)treatment with antioxidants.

1.5.4 Conclusion

In conclusion, tissue heating is the best-established mechanism for RF radiation-induced effects in biological systems. However, there are also numerous reports of specific biological effects from modulated RF-EMF, particularly low-frequency modulated fields (see Section 4). Mechanistic studies will be needed to determine how effects that are reproducible might be occurring, e.g. via the induction of reactive oxygen species, induction of ferromagnetic resonance, demodulation of pulsed RF signals, or alteration of ligand binding to hydrophobic sites in receptor proteins. Although it has been argued that RF radiation cannot induce physiological effects at exposure intensities that do not cause an increase in tissue temperature, it is likely that not all mechanisms of interaction between weak RF-EMF (with the various signal modulations used in wireless communications) and biological structures have been discovered or fully characterized. Biological systems are complex and factors such as metabolic activity, growth phase, cell density, and antioxidant level might alter the potential effects of RF radiation. Alternative mechanisms will need to be considered and explored to explain consistently observed RF-dependent changes in controlled studies of biological exposure (see Section 4 for examples of reported biological effects). While the debate continues on whether or not non-thermal biological effects occur as a result of exposures to low-intensity RF radiation, it may be difficult to specify observed effects as non-thermal because of the high sensitivities of certain physiological responses to small increases in temperature.

1.6 Exposure to RF radiation

Exposure of workers and the general community to RF radiation can occur from many different sources and in a wide variety of circumstances. These exposures can be grouped into three major categories: personal, occupational and environmental.

1.6.1 Personal exposure

The general community can come into contact with several potentially important sources of RF radiation as part of their personal life, involving some degree of choice, including use of a mobile phone, other communication technologies, or household devices (see Section 1.2).

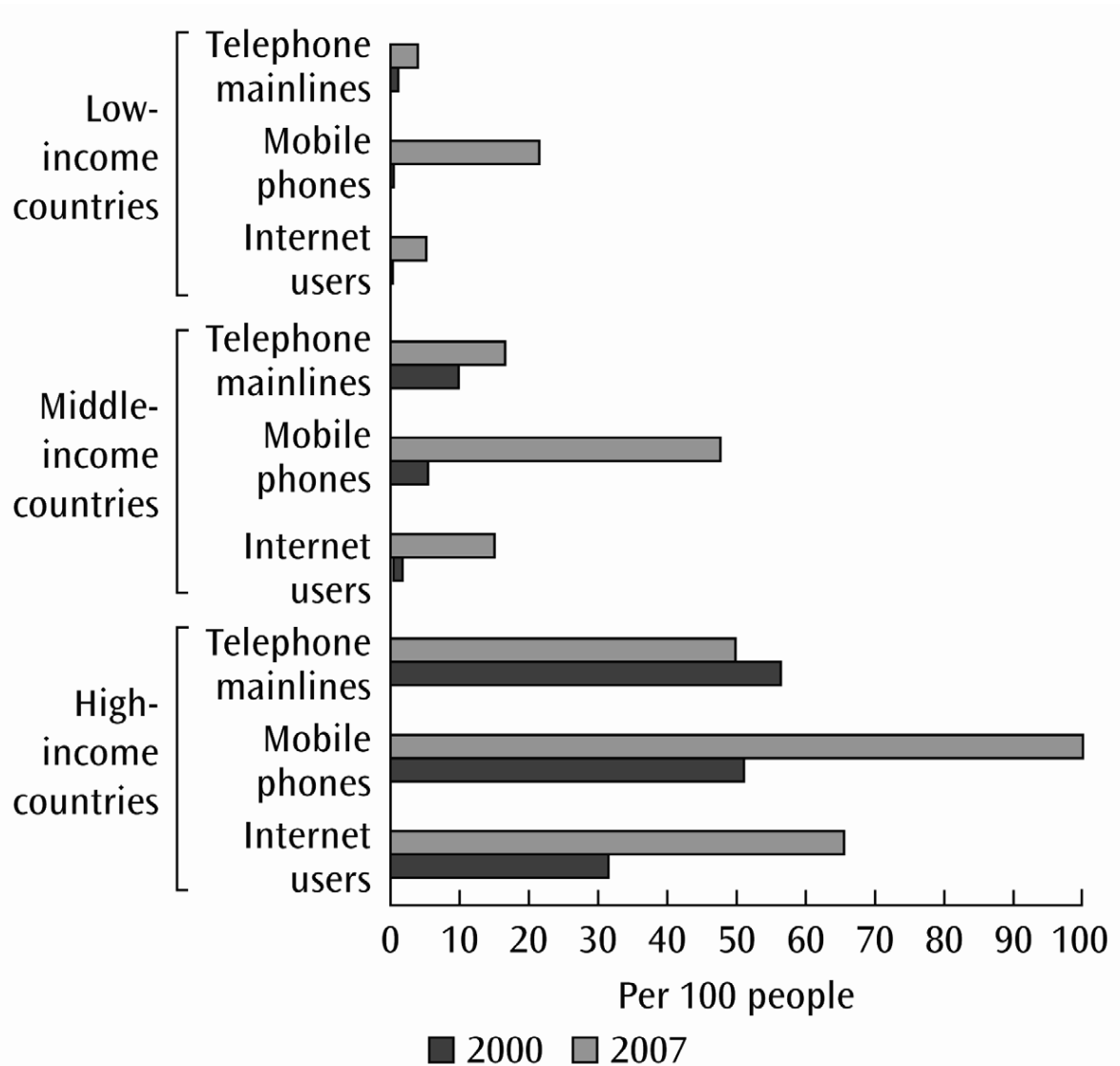
(a) Mobile phones

(i) Increase in mobile-phone subscriptions

Analogue mobile phones were first introduced around 1980 and GSM phones in the mid-1990s. Over the past two decades, the number of people owning a mobile phone has increased rapidly around the world. For example, the number of mobile-phone subscribers in the USA has risen from 0.34 million in 1985 to 109 million in 2000, and 263 million in 2008 ([InfoPlease, 2011](#)). WHO has estimated that at the end of 2009 there were 4.6 billion mobile-phone subscriptions globally ([WHO, 2010b](#)). Fig 1.17 illustrates the rapid rise in mobile-phone subscriptions compared with other types of phone and Internet usage over the past decade, although it should be noted that the number of subscriptions does not equate to number of users, as some people have more than one subscription and a single subscription can be used by more than one person.

This rapid increase in mobile-phone use is not just restricted to the industrialized countries. Fig 1.17 shows the increase in mobile-phone subscriptions from 2000 to 2007 in high-, middle- and low-income countries ([World Bank, 2009](#)). While industrialized countries continue to

Fig. 1.17 Mobile-phone subscriptions per 100 people in high-, middle-, and low-income countries, 2000 and 2007



© World Bank
From [World Bank; International Monetary Fund \(2009\)](#)

have the highest number of subscriptions per 100 people, the percentage increase over this time has been much greater in low- and middle-income countries. In low-income countries, subscription rates in 2000 were negligible, but in 2007 they were 25% of the rate in high-income countries, while in middle-income countries the rise was from about 10 to 50 subscriptions per 100 people, to reach about 50% of the rate in high-income countries in 2007.

There have also been considerable changes in the types of mobile phone used over the past 10 years, which has important implications for RF exposure of the user (see Section 1.2). Earlier mobile phones used analogue technology, which emitted waves of 450–900 MHz. Digital phones, with RF frequencies of up to 2200 MHz, were introduced in the mid-1990s and by the year 2000 had almost completely replaced analogue phones. The largest growth in recent years has been for smartphones, which allow the user access to a wide range of non-voice data applications (taking photographs, Internet access, playing games, music, and recording videos). In the USA, 18% of phones in 2010 were smartphones, up from 13% in 2008 ([Nielsen, 2010](#)).

(ii) Mobile-phone use among children

Within the increasing subscription figures, there have been questions raised about increasing use of mobile phones by children. As was seen in Section 1.3, published dosimetry studies using phantom heads have found that RF absorption can be higher in children than in adults, due to anatomical and physiological differences. A recent study used a modified version of the Interphone questionnaire in 317 children in secondary school (median age, 13 years) in one state of Australia, and found that 80% used a mobile phone ([Redmayne et al., 2010](#)). Data on national use of mobile phones in 2009, collected by the Australian Bureau of Statistics (ABS), has shown that 31% of Australian children had a mobile phone, with the highest ownership being

in the age group 12–14 years (76%) ([ABS, 2009](#)). Similar rates of mobile-phone use by children were found in three major cities in Hungary in 2005, where 76% of children in secondary school owned a mobile phone, 24% used a mobile phone daily to make calls, and an additional 33% used mobile phones to make calls at least several times per week ([Mezei et al., 2007](#)).

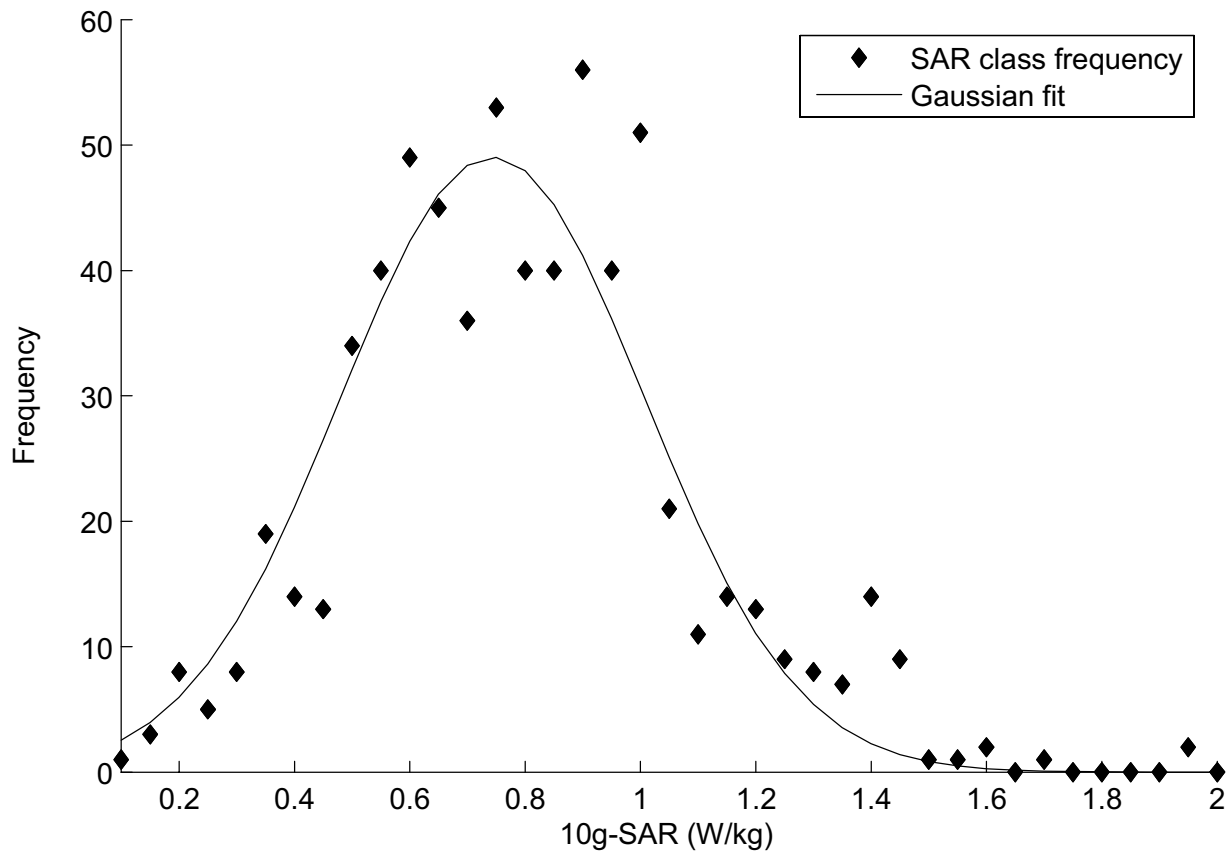
While the increase in mobile-phone subscriptions over the past 15 years is well documented, less is known about changes in call frequency and duration over that time. One study in Finland found that the median duration of calls per month was 186 minutes in 2007, increasing to 221 minutes in 2009, while the average monthly number of calls increased slightly from 52 to 57 calls ([Heinävaara et al., 2011](#)). The daily local RF exposure of the general public has increased by several orders of magnitude with the introduction and proliferation of mobile handsets. This has triggered concern among health agencies and the public, since the tissue with the highest exposure is the brain. Figs 1.18 and 1.19 display the frequency of worst-case SAR from mobile phones, measured according to [IEEE \(2003\)](#) and [CENELEC \(2001\)](#) guidelines.

Fig. 1.18 represents the typical SAR values for Europe (mean psSAR-10 g, 0.74) and Fig. 1.19 for North America (mean psSAR-1 g, 0.96). The different averaging masses are due to different legal regulations in Europe and the USA. These values are a considerable percentage of the limit values (see Section 1.7). A recent statistical analysis of the SAR database of the Federal Communications Commission (FCC) found that the SAR values of newer phones are typically lower than those of older phones, despite the greatly reduced size (see Section 1.3).

(iii) Exposure metrics for epidemiological studies

To develop suitable exposure metrics for use in epidemiological studies on RF exposure from mobile phones and health effects such as cancer, there is a need to access technical data such as

Fig. 1.18 Statistical distribution of maximum psSAR-10 g measured for 668 mobile phones, according to standard EN50361 ([CENELEC, 2001](#))



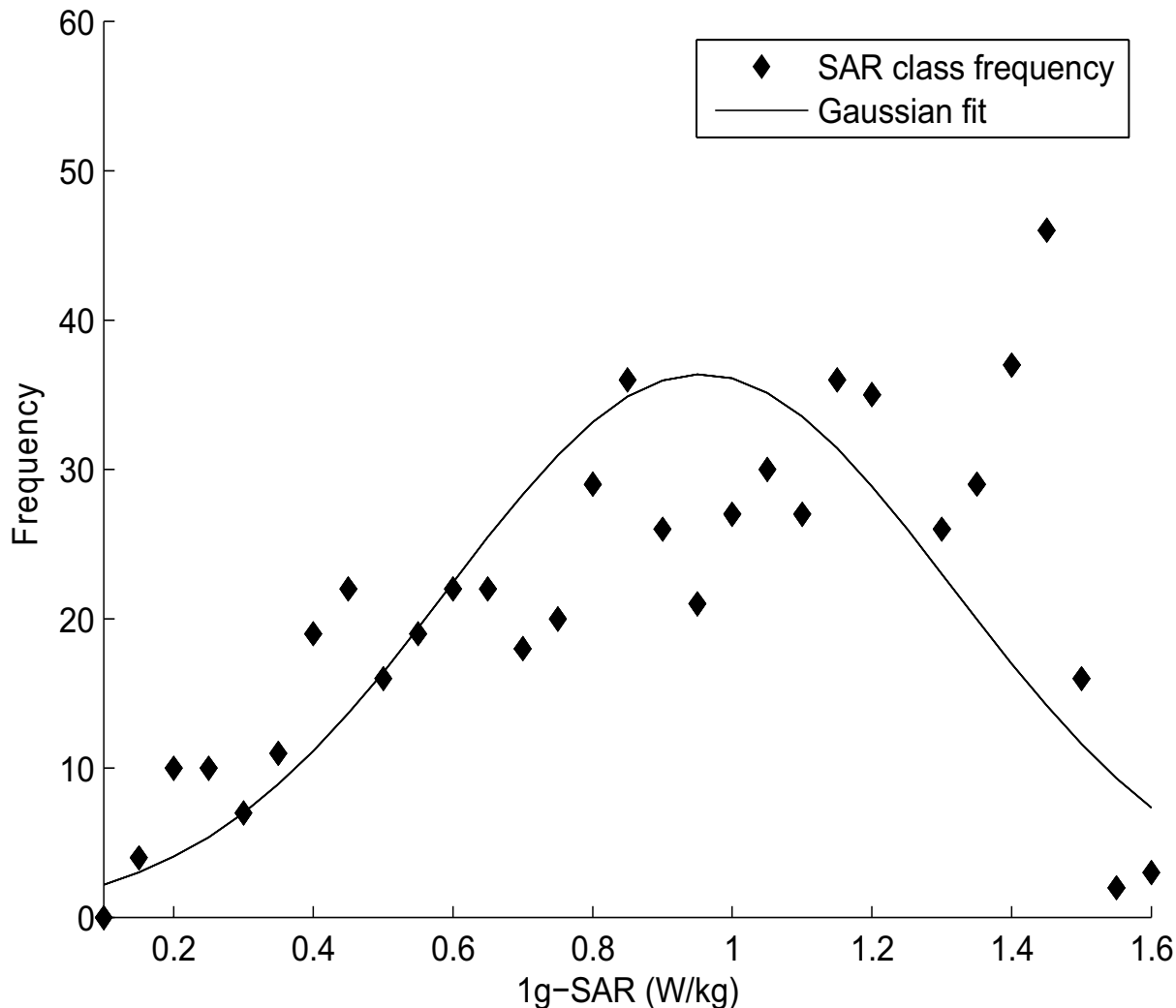
Data from German Federal Office for Radiation Protection, in [Kühn & Kuster \(2007\)](#)

the generation of phone, frequency, modulation and network-related factors that might influence the output power of the phone, as well as reliable information about the pattern of mobile-phone use from each subject. This includes such variables as reported number of calls, duration of calls and laterality, i.e. the side of the head on which the phone is most often placed by the subject when talking on the phone.

As exposure data related to mobile-phone use are usually collected from the subjects themselves, several studies have been conducted to test the validity of this type of self-reported information. Several methods are available to validate self-report, including telephone-company records, software-modified phones

and hardware-modified phones ([Inyang *et al.*, 2008](#)). A study of 59 children in the seventh year of school (age 11–12 years) in Australia used GSM-type software-modified phones to record exposure details (e.g. number and duration of calls) to validate questionnaire data on mobile-phone use. This study found a modest correlation of 0.3 for recall of number of calls, but almost no correlation (0.1) for duration ([Inyang *et al.*, 2009](#)). There was little difference with the main findings for different demographic groups, although for some subgroups, numbers were small. This study was carried out over one week and a possible explanation of the poor correlations is that the change in phone type imposed by the study protocol (from 3G to GSM) may have

Fig. 1.19 Statistical distribution of maximum psSAR-1 g measured for 687 mobile phones, according to standard IEEE-1528 ([CENELEC, 2001](#))



Data from Federal Communications Commission, in [Kühn & Kuster \(2007\)](#)

resulted in a change in phone-use behaviour for many of the children.

Another potential problem is differential recall of mobile-phone use in case-control studies. In the CEFALO case-control study of brain tumours in adolescents, a validation study was undertaken to estimate the effect of both random and systematic errors in 59 cases (26% of all cases who owned a mobile phone) and 91 controls (22% of all controls who owned a mobile phone) for whom phone-use data were available

from the mobile-phone provider ([Aydin *et al.*, 2011](#)). The study found that cases overestimated their number of calls by 9% on average, and controls overestimated by 34% on average. Cases also overestimated the duration of their calls by 52% on average, while controls overestimated by a much greater 163%, suggesting that duration-of-call data from self-reports are less reliable and may be more prone to recall bias than self-reports of number of calls in studies of cancer in children.

Such differential reporting between cases and controls was not such a problem in two validation studies undertaken as part of the Interphone case-control study of brain tumours in adults. A 6-month volunteer study used the Interphone questionnaire and either phone records or software-modified phones in 11 countries and found that, although there was considerable random error, there was fair to moderate agreement for both number and duration of calls, with weighted kappas ranging from 0.20 to 0.60 ([Vrijheid et al., 2006](#)). In addition, there was some systematic error, as heavy users tended to overestimate their use, while lighter users tended to underestimate theirs. There was also some heterogeneity between countries. A subsequent validation study among subjects from five countries in the Interphone study compared reported mobile-phone use against phone records over an average of two years. This substudy found that the extent of underreporting of number of calls (0.8) and of over-reporting of call duration (1.4) was similar in each group. Differential recall was greater with longer periods of recall, although numbers were small for the group with longest recall period ([Vrijheid et al., 2009b](#)). More recently, a pilot study in Finland for the prospective cohort study of mobile-phone users (COSMOS study) validated reported phone use against phone-company records for 418 subjects who had a single operator ([Heinävaara et al., 2011](#)). The authors found that overestimation of reported mobile-phone use was common and there was moderate agreement ($\text{kappa} = 0.60$) for monthly average duration of calls, although there was more overestimation and less agreement as the call duration increased. A further small validation study in 60 engineers and scientists, who are not representative of the wider community, used mobile-phone records to validate self-reporting and found similar agreement; the conclusion was, that reporting monthly use was more reliable than weekly or daily use ([Shum et al., 2011](#)).

Laterality, i.e. against which ear the mobile phone is mainly held during calls, is another important factor that can influence estimations of exposure within the head. Laterality does not always coincide with the subject's dominant hand and may be related to other activities, such as writing. A validation study of self-reported laterality with hardware-modified phones found that agreement between the information from these phones and self-reported laterality was modest, with a kappa of only 0.3 ([Inyang et al., 2010](#)). [Schüz \(2009\)](#) demonstrated that laterality effects are similar across exposure categories and highlighted the problem of possible reporting bias. The Interphone study has addressed this problem in a sensitivity analysis, whereby different allocations of side-of-head were used; this caused only minor reductions in the odds ratios for the highest quintile of exposure, which suggests that the findings are not sensitive to errors in the recall of laterality of phone use ([Cardis et al., 2011a](#)).

Mobile phones are low-powered RF transmitters, operating at frequencies between 450 and 2700 MHz, with peak powers in the range of 0.1 to 2 W, the power being highest during a call. The handset only transmits RF power when it is turned on, but the newer smartphones regularly give short bursts of power to check e-mails and other Internet services. One study has found that mobile-phone output power is usually higher in rural areas where base stations are further apart, whereas the other factors examined in the study (length of call, moving/stationary, indoor/outdoor) were found to be of less importance as predictors of power output from the phone ([Hillert et al., 2006](#)).

Using a mobile phone in areas of good reception (such as in cities where mobile phone-base stations are close together) also decreases exposure as it allows the phone to transmit at reduced power. Conversely, people using a phone in rural areas where mobile-phone reception is poorer may receive higher RF exposure. This was one

factor examined in a study of 512 subjects in 12 countries who were asked to use GSM software-modified phones; the study, monitored date, time and duration of each call, frequency band and power output for a month ([Vrijheid et al., 2009a](#)). The main predictors of power output were the study location, the network, and the duration of the call, with shorter calls being associated with higher power output. The measured power levels in GSM networks were substantially higher than the average levels theoretically achievable, which has important implications for estimating exposure in epidemiological studies. Rural location was only a major factor in Sweden, where subjects were living in very sparsely populated areas; these results are consistent with those of an earlier paper from [Lönn et al. \(2004\)](#) in Sweden, who reported that the highest power level was used about 50% of the time in the rural areas, but only about 25% of the time in urban areas. This highlights the problem of identifying genuinely sparsely populated rural areas where major differences in power output can be found. Another paper from the Interphone study reported an investigation of the effects of parameters that were thought to influence the level of RF SAR in the brain. Total cumulative specific energy was estimated, based on data collected during the Interphone study, to assess the relative importance of the different factors and these results were used to develop an algorithm, which was tested on study subjects in five countries ([Cardis et al., 2011b](#)). This study found that the type of phone with the highest mean total specific cumulative energy (TSCE) was AMPS800 (5165 J/kg), followed by D-AMPS800 (3946 J/kg), GSM800/900 (2452 J/kg), GSM1800 (4675 J/kg), CDMA1900 (1855 J/kg), and CDMA800 (164 J/kg). The main determinants were communication system, frequency band, and number and duration of mobile-phone calls. The study also identified several uncertainties in relation to SAR estimation, including those related to spatial SAR distribution for each phone

class, error in recall of phone use, and laterality and uncertainties about the most biologically relevant dose metric.

A study in the USA examined the impact of phone type and location by use of software-modified phones driven over several pre-determined routes ([Kelsh et al., 2010](#)). This study found that RF levels were highest for the older analogue phones, intermediate for GSM and TDMA phones, and lowest for CDMA phones. The main predictors of RF level were phone technology and, to a lesser extent, degree of urbanization.

Patterns of personal mobile-phone use have been changing as technology has changed and this can have implications for the strength of the RF field experienced by the user. One important development has been the introduction of the short message service (SMS), which was originally designed for GSM to allow sending non-voice text messages ([Herring, 2004](#)). SMS was first introduced in 1993, but use increased rapidly in the mid-2000s. Text messaging using SMS leads to lower RF exposure than voice calls in two ways: the phone is usually held at least 30 cm from the body during the writing and sending of an SMS and the duration of power output is much shorter (about 11 seconds) than the duration of a voice call.

As with SMS, other mobile-phone communication innovations have been developed that result in lower potential for SAR exposure than voice calls. A person using a mobile phone at least 30 cm away from the body, e.g. when accessing the Internet, with a hands-free device for voice calls or “push-to-talk” with the phone held in front of the head, will therefore have a much lower exposure to RF than someone holding the handset against the head during a voice call.

(b) DECT phones

Another important source of personal RF exposure is the home use of DECT phones, which have been replacing traditional handsets in the home. As the DECT base-station is within

the home and at most some tens of metres from the handset, the average power generated by the DECT phone is less than that of a mobile phone, where the base station may be up to some kilometres away. However, the power output of a DECT base station in close proximity to a person may be comparable to that of a 3G phone, so proximity to a DECT phone base-station should be taken into account when estimating RF exposure in epidemiological studies in which sizeable numbers of subjects have used 3G phones. A recent study of Australian schoolchildren found that 87% had a DECT phone at home, and although there was only a weak correlation ($r = 0.38$) between mobile-phone and DECT-phone use, this suggests that DECT-phone use needs to be considered in the assessment of RF exposure ([Redmayne et al., 2010](#)).

(c) *Other communication technologies and domestic sources*

The incident-field exposures from typical devices used in home and office environments have been assessed ([Kühn et al., 2007a](#)). The maximum E-field exposure values for different device categories are summarized in [Table 1.13](#). The incident-field exposure from cellular base stations may be exceeded by the exposure from these devices due to the generally closer distances involved.

Additionally, an incident exposure of 1 V/m translates to a psSAR value in the brain that is approximately 10 000 times lower than the maximum exposure from a handset. Thus, handsets are by far the most dominant source of RF exposure for the general population.

Within homes there are many other potential sources of RF exposure, including baby monitors, microwave ovens, Wi-Fi, Bluetooth, various types of radios and remote-controlled toys. A study of 226 households in lower Austria measured the peak power of emitted bursts of RF exposure from each of these types of devices in bedrooms, where the residents spend the most

Table 1.13 Worst-case E field at distances of 20 cm and 1 m from typical wireless indoor devices

Device class	Frequency range (MHz)	Worst-case E field (V/m)	
		20 cm	1 m
Baby surveillance	40 – 863	8.5	3.2
DECT	1880 – 1900	11.5	2.9
WLAN	2400 – 2484	3.9	1.1
Bluetooth	2402 – 2480	3.1	1.0
PC peripherals	27 – 40	≤ 1.5	≤ 1.5

DECT, digital enhanced cordless telecommunications; PC, personal computer; WLAN, wireless local area network

Adapted from [Kühn et al. \(2007a\)](#)

time in one position. The highest peak RF values were measured for mobile-phone and DECT base stations in the 2400-MHz band ([Tomitsch et al., 2010](#)).

1.6.2 Occupational exposure

There are many occupations involving potential sources of exposure to RF radiation in the workplace, the more important of which involve work with high-frequency dielectric heaters (PVC welding machines) and induction heaters, broadcast sources, high-power pulsed radars, and medical applications including MRI and diathermy.

(a) *High-frequency dielectric heaters and induction heaters*

High-frequency dielectric heaters (PVC welding machines) functioning at 27 MHz have traditionally involved the highest occupational exposures to RF ([Allen, 1999](#)). This is not a large sector of the industrial workforce, although it is estimated that there are about 1000–2000 PVC dielectric welders in Finland, which has a total population of about five million people. The whole-body average SAR for dielectric heater operators has been estimated to vary from 0.12 to

2 W/kg and it is not uncommon for these workers to report heating effects ([Jokela & Puranen, 1999](#)).

(b) *Broadcasting sources*

The rapid increase in mobile-phone use and other communication technologies worldwide has required increasing numbers of workers to undertake monitoring and maintenance. A study of exposure to RF radiation from two medium-sized antenna towers in Finland was conducted to document worker exposure ([Alanko & Hietanen, 2007](#)). These towers contained transmitting antennae of several different types, mobile-phone networks (GSM900 and GSM1800), radio and digital television substations and other radio systems. Although the measured power density was quite variable, the maximum instantaneous power density at this site was 2.3 W/m², which was recorded during maintenance tasks at the tower with the GSM1800 antennae. For the tower with both GSM900 and GSM1800 antennae, the maximum registered instantaneous power density inside the climbing space was 0.4 W/m². [The Working Group agreed with the authors who concluded that exposures will depend on the different types of antennae located on the towers and that it is usually difficult to predict occupational RF exposures.]

The above approach to assess exposure is based on spot measurements and does not give an estimate of cumulative exposure over working time, which is the approach employed with other types of workplace hazards. Attempts have been made to employ this cumulative dose approach for exposure to RF radiation, but as there are usually many different sources of RF radiation present in a workplace, this is not straightforward. For example, such an approach was used to assess total exposure and estimate an annual dose on fast patrol boats in the Norwegian Navy, which carry high-frequency antennae and radar ([Baste et al., 2010](#)). This study found considerable variation in exposure at different points around the boats, the highest exposures and

annual dose being found in the captain's cabin. These estimates were done for three time periods (1950–79, 1980–94 and 1995+), and relied on recall of transmission characteristics over several decades. The estimated annual doses in the most recent period were about one third of those in the earliest period. The estimated annual doses for the period from 1995 and later ranged between 4.3 and 51 kVh/m.

(c) *Other potential sources of radiofrequency radiation in the workplace*

Portable radios, short-wave and surgical diathermy are other potential sources of RF radiation in the workplace, whereas base stations, microwave links and microwave ovens have been considered unlikely to give rise to substantial exposures ([Allen, 1999](#)). For example, a study of exposure to RF radiation in police officers operating speed guns (measurements made at the seated ocular and testicular positions) found that almost all of the 986 measurements made for 54 radar units were below the detection limit, the highest power-density reading being 0.034 mW/cm² ([Fink et al., 1999](#)).

1.6.3 *Environmental exposure*

The most common sources of RF in the general environment are mobile-phone base stations, which tend to be operated at the lowest power possible for reasons of network efficiency (see Section 1.2; [Allen, 1999](#)). The level of RF exposure is usually poorly correlated with proximity to the antenna, although there is considerable variation in output power from site to site (Section 1.2). A study regarding indoor incident-field exposure from cellular base-station sites was conducted by Austrian Research Centers (ARCS) in the city of Salzburg, Austria ([Coray et al., 2002](#)). [Table 1.14](#) shows two cumulative incident-field exposure values (sum of incident-field exposure from multiple transmitters at one site) measured at different distances from several base-station

Table 1.14 Measurement of indoor incident electric-field (E) strength at base stations in Salzburg, Austria^a

Base station	Measurement 1		Measurement 2	
	Distance to base station (m)	Cumulative incident E field (V/m)	Distance to base station (m)	Cumulative incident E field (V/m)
1	196	0.37	347	0.35
2	88	0.51	108	0.89
3	9	0.034	15	0.037
4	16	0.62	8	1.00
5	85	0.94	152	0.75
6	81	1.8	85	1.71
7	4	3.9	25	1.02
8	93	0.19	208	0.19
9	34	0.40	55	0.63
10	39	1.9	76	2.8
11	174	0.59	220	0.45
12	41	0.70	107	0.67
13	2.5	0.25	5.5	0.15

^a For each base station site, two examples of measurements of cumulative incident field exposure (sum of incident field exposure from multiple transmitters at one site) at different distances are shown.

Compiled by the Working Group from BAKOM Report, [Coray et al. \(2002\)](#)

sites. The values are between 0.1 and 1 V/m for distances of up to several hundreds of metres. Values greater than 1 V/m and up to 3.9 V/m were measured for distances of less than 86 m. These data also underline that the distance to the base station site has a poor correlation for the incident exposure. Similar results were reported in a study that also included outdoor measurement points and addressed the time dependence, i.e. traffic dependence of the exposure from cellular base stations. The results showed a substantial time dependence for base stations with multiple traffic channels. In these cases, clearly lower exposure can be expected at night and at weekends ([Bornkessel et al., 2007](#)).

In an attempt to measure typical exposure to RF radiation over a whole week, volunteers in a Swiss study were asked to wear an RF exposimeter and to complete an activity diary ([Frei et al., 2009b](#)). The main contributions to exposure were found to come from mobile-phone base stations (32.0%), mobile-phone handsets (29.1%) and DECT phones (22.7%).

[Breckenkamp et al.](#) undertook a validation study of exposure to RF radiation in 1132 households in Germany located within 500 m of at least one mobile-phone base station (average number of base stations, 3.4; average number of antennae, 17) ([Breckenkamp et al., 2008](#)). An exposure model was developed, based on 15 parameters related to the base station and the antennae, from the database of the federal network agency and information about the home from the residents and interviewer. Dosimetric measurements were undertaken in the bedroom of the home in 2006. There was considerable variability across cities (range of kappa values, 0.04–0.49), with higher kappa related to low-density housing with buildings comprising more than three floors. There was greater agreement for households located less than 300 m from the base stations and the authors concluded that the model was only useful where high-precision input data were available.

Little is known about geographical variation in exposures in different settings in the general community, but published data related

to exposures within different forms of transport, homes, offices and outdoors in five European countries were reviewed in a recent study ([Joseph et al., 2010](#)). Power density (mW/m^2) was measured in each microenvironment and highest exposures were measured in transportation, followed by outdoor environments, offices and homes. In the Netherlands, the highest exposures were measured in the office environment. In all studies, the lowest exposures were in the home, with exposures of about $0.1 \text{ mW}/\text{m}^2$ recorded in all countries. In transport vehicles, virtually of the exposure was from mobile phones, whereas in offices and homes, the sources were quite variable between countries. [The Working Group suggested that these conclusions should be treated with some caution, as it was not clear how representative the measured microenvironments were.]

In a feasibility study in Germany, the aim of which was to develop reliable exposure metrics for studies of health effects of exposure to RF radiation from mobile-phone base stations, data were collected on distance to base station and spot measurements at the homes of nine controls taking part in a case-control study of cancer. Distance from base station was a poor proxy for the total power density within the home due to the directional characteristics of the base-station beam, scattering, shielding and reflection of the radiated fields and the contribution to power density from other sources ([Schüz & Mann, 2000](#)). [The Working Group noted that use of this metric would be likely to result in considerable exposure misclassification.]

A further study of a random sample of 200 subjects in France used a personal exposure meter to estimate the doses, time patterns and frequencies of RF exposures with measurements of electric-field strength in 12 different bands at regular intervals over 24 hours ([Viel et al., 2009](#)). This allowed differentiation of different sources of RF radiation, including mobile-phone base stations. For each of GSM, DCS and UMTS, more

than 96% of the measurements were below the detection limit and the median of the maximum levels for all three systems ranged between 0.05 and $0.07 \text{ V}/\text{m}$. In addition, exposures were found to vary greatly at similar distances from GSM and DCS base stations, although two peaks were observed (at 280 m mainly in urban areas, and 1000 m mainly in periurban areas), although most distances exceeded the 300 m within which the exposure model developed by [Breckenkamp et al. \(2008\)](#) was found to have the highest agreement with measured levels.

In another study by [Frei et al. \(2009a\)](#), the aim was to develop a model to predict personal exposure to RF radiation. One hundred and sixty-six subjects carried a personal dosimeter for one week and completed a diary. Important predictors of exposure were housing characteristics, ownership of communication devices, time spent in public transport, and other behavioural aspects, with about half of the variance being explained by these factors.

A range of personal exposure meters is now available. These are more robust for the purposes of exposure assessment in epidemiological studies, and a considerable step forward compared with the traditional spot-measurement approach, which is usually chosen for compliance purposes and does not result in a representative estimate of personal exposure ([Mann, 2010](#)). [The Working Group noted that care needs to be taken in interpreting the results of personal exposure measurements, because of the low sensitivity and the failure to account for the fact that they respond to TDMA signals, which may lead to an overemphasis of DECT, Wi-Fi and GSM phone signals in average exposure. Because burst powers may have been measured for these signals, rather than average powers, any exposure proportions attributed to source categories in these studies should be treated with caution when assessing exposure for epidemiological studies.]

1.7 Exposure guidelines and standards

Guidelines and standards for limiting human exposure to RF fields have been developed by several organizations, the most prominent being those of the International Commission on Non-Ionizing Radiation (ICNIRP) and the Institute of Electrical and Electronic Engineers (IEEE). ICNIRP published its present RF guidelines in 1998 ([ICNIRP, 1998](#)) and restated them in 2009 ([ICNIRP, 2009a](#)). IEEE published its present guidelines in 2005 ([IEEE, 2005](#)), but its 1999 guidelines are still used in some countries ([IEEE, 1999](#)).

These guidelines contain restrictions on exposure that are intended to assist those with responsibility for the safety of the general public and workers. The guidelines provide clearly defined exposure levels below which the established acute health effects of exposure are avoided. Exposures can be measured or calculated and compared with these values. If exposures are found to be above the guideline values, measures are put in place to reduce exposure. The guidelines apply to all human exposures to EMFs, irrespective of how such exposures arise, and they do not make specific mention of sources.

The guidelines are not mandatory by themselves, but have been adopted by regulatory authorities and governments in many countries/regions of the world in a variety of different ways. Some regulatory regimes focus on limiting exposures of the public and/or workers, while others focus on limiting product emissions (to control exposures) as part of the certification process before placing products on the market. For example, harmonized technical standards have been implemented in Europe that provide a basis for assessing exposures from equipment such as mobile phones and ensuring that exposures are below values taken from the ICNIRP guidelines. The values in the 1999 IEEE guidelines are used

in a similar way in countries such as the USA and Canada.

1.7.1 Scientific basis

Both ICNIRP and IEEE have reviewed the broad base of the scientific evidence in developing their guidelines and arrived at similar conclusions regarding the evidence for health effects. This consensus is well expressed in the following excerpt taken from the ICNIRP 2009 restatement of its guidelines ([ICNIRP, 2009b](#)):

It is the opinion of ICNIRP that the scientific literature published since the 1998 guidelines has provided no evidence of any adverse effects below the basic restrictions and does not necessitate an immediate revision of its guidance on limiting exposure to high frequency EMFs. The biological basis of such guidance remains the avoidance of adverse effects such as ‘work stoppage’ caused by mild whole body heat stress and/or tissue damage caused by excessive localized heating.

Absorption of RF fields in the body tissues leads to the deposition of energy in these tissues and this energy adds to that produced by metabolism. This energy imposes an additional thermoregulatory burden on the organism and the temperature can increase if the energy absorption rises above a certain level (see Section 1.3). Localized temperature increase can occur in response to localized absorption of energy and the core body temperature can go up in response to generalized absorption of energy throughout the body tissues. The ICNIRP guidelines ([ICNIRP, 1998](#)) conclude from the literature that:

Established biological and health effects in the frequency range from 10 MHz to a few GHz are consistent with responses to a body temperature rise of more than 1 °C. This level of temperature increase results from exposure of individuals under moderate environmental conditions to a wbSAR of approximately 4 W/kg for about 30 minutes.

Table 1.15 Basic restrictions on SAR (W/kg), as taken from the ICNIRP and IEEE exposure guidelines

Body region	Workers/controlled			General public/uncontrolled		
	ICNIRP (1998)	IEEE (1999)	IEEE (2005)^d	ICNIRP (1998)	IEEE (1999)	IEEE (2005)
Whole body ^a	0.4 (6)	0.4 (6)	0.4	0.08 (6)	0.08 (30)	0.08
Head and trunk ^{a,b}	10 (6) [10]	8 (6) [1]	10 (6) [10]	2 (6) [10]	1.6 (30) [1]	2 (30) [10]
Extremities ^{a,b,c}	20 (6) [10]	20 (6) [10]	20 (6) [10]	4 (6) [10]	4 (30) [10]	4 (30) [10]

^a In round brackets after the SAR value is the averaging time in minutes. The averaging times vary with frequency in the IEEE guidelines and the values given are for the 400 MHz to 2 GHz range typically used for mobile communication.

^b In square brackets (where relevant) is the averaging mass in grams: the averaging mass is specified as a contiguous tissue volume by ICNIRP and as in the shape of a cube by IEEE.

^c Extremities are taken as the hands, wrists, feet and ankles in the context of the [IEEE \(1999\)](#) guidelines, distal from the knees and elbows in the [IEEE \(2005\)](#) guidelines, and as the entire limbs in the context of the ICNIRP guidelines.

^d The restrictions apply over the frequency range 100 kHz to 6 GHz in the case of [IEEE \(1999\)](#).

ICNIRP, International Commission on Non-Ionizing Radiation Protection; IEEE, Institute of Electrical and Electronics Engineers; SAR, specific absorption rate.

Compiled by the Working Group

Effects due to whole-body heating are also considered for frequencies below 10 MHz and down to 100 kHz; however, wavelength becomes progressively larger in relation to the body dimensions as frequency decreases to below 10 MHz and coupling to the fields becomes progressively weaker, with the result that less energy is absorbed. Above 10 GHz, absorption of RF fields by the body tissues becomes so strong that the RF fields are considered to be absorbed within a few millimetres of the body surface; hence the guidelines are designed to restrict surface heating.

A further class of thermal effect can be elicited with pulse-modulated RF waveforms, including certain radar signals. This effect is known as the microwave auditory effect and occurs as a result of energy absorption from successive RF pulses, causing pulsed thermal expansion of the head tissues ([ICNIRP, 2009a](#)). [ICNIRP \(1998\)](#) states that repeated or prolonged exposure to microwave auditory effects may be stressful and potentially harmful, and it provides additional guidance for restricting exposures to pulse-modulated fields to avoid this effect.

1.7.2 Basic restrictions

Considering the evidence relating to whole-body heating and localized heating of parts of the body, ICNIRP and IEEE have specified the basic restriction quantities shown in [Table 1.15](#). The information presented here is a summary of the main aspects of the restrictions in the guidelines and serves to provide a simplified comparison for the purposes of this *Monograph*.

From [Table 1.15](#) it is clear that the various sets of guidelines contain similar restriction values and have many common features. Moreover, the 2005 guidelines from IEEE have brought the ICNIRP and IEEE guidelines even closer: the SAR values are now identical and the residual differences now only pertain to averaging times, definition of the extremities, and the shape of the mass used with localized SAR restrictions.

IEEE and ICNIRP both frame their guidelines in terms of two tiers. The first tier includes a wbSAR value that is a factor of 10 lower than the 4 W/kg mentioned above, while the second tier includes restriction values that are five times lower than those in the first tier. In the case of the ICNIRP guidelines, these tiers are presented as restrictions for exposure of workers (tier 1)

Table 1.16 Basic restrictions on induced current density or induced electric field between 30 kHz and 10 MHz, as taken from the ICNIRP and IEEE exposure guidelines

Body region	Workers/controlled				General public/uncontrolled			
	ICNIRP (1998)^a (mA/m ²)	IEEE (1999)^b (mA/m ²)	IEEE (2005)^c (mV/m)	ICNIRP (2010)^d (mV/m)	ICNIRP (1998)^a (mA/m ²)	IEEE (1999)^b (mA/m ²)	IEEE (2005)^c (mV/m)	ICNIRP (2010)^d (mV/m)
Whole body	-	350	-	270	-	157	-	135
CNS	10	-	-	-	2	-	-	-
Brain	-	-	885	-	-	-	294.5	-
Heart	-	-	5647	-	-	-	5647	-
Extremities	-	-	626.9	-	-	-	626.9	-
Other tissues	-	-	626.9	-	-	-	209.3	-

^a Peak rms current density in mA/m², averaged over 1 cm² area perpendicular to the current direction. Applies to the CNS tissues. Applicable frequency range is 1 kHz to 10 MHz.

^b Peak rms current density in mA/m², averaged over any 1 cm² area of tissue in 1 second. Applies anywhere in the body. Applicable frequency range is 3 kHz to 100 kHz.

^c Peak rms internal electric field in mV/m, averaged over a straight-line segment of 5 mm length, oriented in any direction. The averaging time for an rms measurement is 0.2 s. Applicable frequency range is 3.35 kHz to 5 MHz. Values are rounded to four significant digits.

^d Internal electric field in mV/m, averaged over a contiguous tissue volume of 2 × 2 × 2 mm³. The 99th percentile value of the electric field for a specific tissue should be compared with the basic restriction. Applicable frequency range is 3 kHz to 10 MHz.

CNS, central nervous system; rms, root-mean-square value of the electric field strength

Note: All numbers denote the frequency in kHz; all limits in this frequency range increase linearly with frequency. Limits for contact currents also apply (not shown here).

Compiled by the Working Group

and the general public (tier 2). ICNIRP explains that the lower basic restrictions for exposure of the general public take into account the fact that their age and health status may differ from those of workers. The first tier in the IEEE guidelines is described as for controlled environments (subject to a RF safety programme as prescribed by IEEE) and the second tier as for uncontrolled environments, as accessible to the general public.

Electrical effects caused by stimulation of the peripheral and central nervous system are also considered below 10 MHz, although the maximum sensitivity to these effects occurs at considerably lower frequencies, in the tens of hertz to a few kilohertz region ([ICNIRP, 2010](#)). The guidelines should be referred to for further information about these effects; however, the restrictions are summarized in [Table 1.16](#) for frequencies between 30 kHz and 10 MHz.

1.7.3 Reference levels

The guidelines also contain reference levels (called maximum permissible exposures, or MPEs, by IEEE) expressed in terms of electric- and magnetic-field strengths, or plane-wave equivalent power-density incident on the body (see Glossary). Measured or calculated values can be compared with these quantities to verify that the basic restrictions on SAR or induced current/electric fields are not exceeded.

References

- ABS; Australian Bureau of Statistics (2009). *Children's Participation in Culture and Leisure Activities, Australia*. ABS (cat. no. 4901.0). Available at: <http://www.abs.gov.au>
- Adair RK (2002). Vibrational resonances in biological systems at microwave frequencies. *Biophys J*, 82: 1147–1152. doi:10.1016/S0006-3495(02)75473-8 PMID:11867434
- Adair RK (2003). Biophysical limits on athermal effects of RF and microwave radiation. *Bioelectromagnetics*, 24: 39–48. doi:10.1002/bem.10061 PMID:12483664
- Adey WR, Byus CV, Cain CD *et al.* (1999). Spontaneous and nitrosourea-induced primary tumors of the central nervous system in Fischer 344 rats chronically exposed to 836 MHz modulated microwaves. *Radiat Res*, 152: 293–302. doi:10.2307/3580329 PMID:10453090
- AFSSET (2010). *Evaluation des risques sanitaires liés à l'utilisation du scanner corporel à ondes 'millimétriques*. Provision 100. Agence Française de Sécurité Sanitaire de l'Environnement et du Travail. Rapport d'Expertise Collective, février 2010.
- AGNIR (2001). *Possible health effects from terrestrial trunked radio (TETRA)*. Report of an Advisory Group on Non-ionising Radiation. Documents of the NRPB, 12(2). Available at: www.hpa.org.uk.
- AGNIR (2003). *Health effects from radiofrequency electromagnetic fields. Report of an independent Advisory Group on Non-ionising Radiation*. Documents of the NRPB, 14(2). Available at: www.hpa.org.uk.
- Alanko T & Hietanen M (2007). Occupational exposure to radiofrequency fields in antenna towers. *Radiat Prot Dosimetry*, 123: 537–539. doi:10.1093/rpd/ncl505 PMID:17166878
- Allen SG (1999). Rapporteur report: Sources and exposure metrics from RF epidemiology (Part 1). *Radiat Prot Dosimetry*, 83: 143–147.
- Allen SG, Blackwell RP, Chadwick PJ (1994). Review of occupational exposure to optical radiation and electric and magnetic fields with regard to the proposed CEC Physical Agents Directive, Chilton. *NRPB*, R265: 1–68.
- Allis JW & Sinha-Robinson BL (1987). Temperature-specific inhibition of human red cell Na⁺/K⁺ ATPase by 2,450-MHz microwave radiation. *Bioelectromagnetics*, 8: 203–212. doi:10.1002/bem.2250080211 PMID:3040008
- Andersen JB, Nielsen JO, Pedersen GF *et al.* (2007). Room electromagnetics. *Antennas and Propagation Magazine, IEEE*, 49: 27–33. doi:10.1109/MAP.2007.376642
- Anderson V (2003). Comparisons of peak SAR levels in concentric sphere head models of children and adults for irradiation by a dipole at 900 MHz. *Phys Med Biol*, 48: 3263–3275. doi:10.1088/0031-9155/48/20/001 PMID:14620057
- ANFR (2004). Protocol de mesure in situ. Technical Report 2.1, Agence National de Frequence.
- ANSI/IEEE (1991). C95.1, *IEEE Standard for Safety Levels with Respect to Human Exposure to Radio Frequency Electromagnetic Fields, 3kHz to 300 GHz*. New York, NY.
- ANSI/IEEE (2002a). C95.3, *Recommended Practice for Measurements and Computations of Radio Frequency Electromagnetic Fields With Respect to Human Exposure to Such Fields, 100kHz–300GHz*. New York, NY: International Committee on Electromagnetic Safety, The Institute of Electrical and Electronics Engineers Inc.
- ANSI/IEEE (2002b). C95.6, *IEEE Standard for Safety Levels with Respect to Human Exposure to Electromagnetic fields, 0–3 kHz*. New York, NY.
- Aslan E (1970). Electromagnetic radiation survey meter. *IEEE Trans Instrum Meas*, IM-19: 368–372. doi:10.1109/TIM.1970.4313930
- Aydin D, Feychting M, Schüz J *et al.* (2011). Impact of random and systematic recall errors and selection bias in case-control studies on mobile phone use and brain tumors in adolescents (CEFALO study). *Bioelectromagnetics*, 32: 396–407. doi:10.1002/bem.20651 PMID:21294138
- Baba M, Suzuki Y, Taki M *et al.* (2005). Three dimensional visualization of the temperature distribution in a phantom for the assessment of localized exposure to microwaves In *Bioelectromag*, Soc. Annual Meeting, June 2005, Dublin, Ireland: Bioelectromagnetic Society, pp. 250–251.
- Bakker JF, Paulides MM, Christ A *et al.* (2010). Assessment of induced SAR in children exposed to electromagnetic plane waves between 10 MHz and 5.6 GHz. [Epub.] *Phys Med Biol*, 55: 3115–3130.
- Balzano Q (2003). RF nonlinear interactions in living cells–II: detection methods for spectral signatures. *Bioelectromagnetics*, 24: 483–488. doi:10.1002/bem.10125 PMID:12955753
- Balzano Q, Chou CK, Cicchetti R *et al.* (2000). An efficient RF exposure system with precise whole-body average SAR determination for in vivo animal studies at 900 MHz. *IEEE Trans Microw Theory Tech*, 48: 2040–2049. doi:10.1109/22.884193
- Balzano Q & Sheppard A (2003). RF nonlinear interactions in living cells–I: nonequilibrium thermodynamic theory. *Bioelectromagnetics*, 24: 473–482. doi:10.1002/bem.10126 PMID:12955752
- Bangay Z & Zombolas C (2003). Advanced measurement of microwave oven leakage. *Radiat Prot Australas*, 19: 47–51.
- Bassen H, Herman W, Hoss R (1977). EM probe with fiber optic telemetry system. *Microwave J*, 20: 35–47.
- Bassen H, Swicord M, Abita J (1975). A miniature broadband electric field probe. *Annals of the New York*

- Academy of Sciences *Biological Effects of Nonionizing Radiation*, 247: 481–493.
- Bassen HI & Smith GS (1983). Electric field probes - A review. *IEEE Trans Antenn Propag*, 31: 710–718. doi:10.1109/TAP.1983.1143126
- Baste V, Mild KH, Moen BE (2010). Radiofrequency exposure on fast patrol boats in the Royal Norwegian Navy—an approach to a dose assessment. *Bioelectromagnetics*, 31: 350–360. doi:10.1002/bem.20562 PMID:20054844
- Beard B, Kainz W, Onishi T *et al.* (2006). Comparisons of computed mobile phone induced SAR in the SAM phantom to that in anatomically correct models of the human head. *IEEE Trans Electromagn Compat*, 48: 397–407. doi:10.1109/TEMC.2006.873870
- Beiser A (1995). *Concepts of modern physics*, 5th ed. New York: McGraw-Hill
- Belyaev IY (2010). *Dependence of non-thermal biological effects of microwaves on physical and biological variables: implications for reproducibility and safety standards*. In: *Non-thermal effects and mechanisms of interaction between electromagnetic fields and living matter*. ICEMS Monograph, Giuliani L, Soffritti M, editors. Bologna, Italy: National Institute for the Study and Control of Cancer and Environmental Diseases “Bernardino Ramazzini”, pp. 187–217.
- Bernardi P, Cavagnaro M, Pisa S, Piuze E (2003). Specific absorption rate and temperature elevation in a subject exposed in the far-field of radio-frequency sources operating in the 10–900-MHz range. *IEEE Trans Biomed Eng*, 50: 295–304. doi:10.1109/TBME.2003.808809 PMID:12669986
- Binhi VN & Rubin AB (2007). Magnetobiology: the kT paradox and possible solutions. *Electromagn Biol Med*, 26: 45–62. doi:10.1080/15368370701205677 PMID:17454082
- Bit-Babik G, Guy AW, Chou CK *et al.* (2005). Simulation of exposure and SAR estimation for adult and child heads exposed to radiofrequency energy from portable communication devices. *Radiat Res*, 163: 580–590. doi:10.1667/RR3353 PMID:15850420
- Blackman CF, Benane SG, House DE (1991). The influence of temperature during electric- and magnetic-field-induced alteration of calcium-ion release from in vitro brain tissue. *Bioelectromagnetics*, 12: 173–182. doi:10.1002/bem.2250120305 PMID:1854354
- Blackman CF, Kinney LS, House DE, Joines WT (1989). Multiple power-density windows and their possible origin. *Bioelectromagnetics*, 10: 115–128. doi:10.1002/bem.2250100202 PMID:2540755
- Bornkessel C, Schubert M, Wuschek M, Schmidt P (2007). Determination of the general public exposure around GSM and UMTS base stations. *Radiat Prot Dosimetry*, 124: 40–47. doi:10.1093/rpd/ncm373 PMID:17933788
- Boutry CM, Kuehn S, Achermann P *et al.* (2008). Dosimetric evaluation and comparison of different RF exposure apparatuses used in human volunteer studies. *Bioelectromagnetics*, 29: 11–19. doi:10.1002/bem.20356 PMID:17694536
- Breckenkamp J, Neitzke HP, Bornkessel C, Berg-Beckhoff G (2008). Applicability of an exposure model for the determination of emissions from mobile phone base stations. *Radiat Prot Dosimetry*, 131: 474–481. doi:10.1093/rpd/ncn201 PMID:18676976
- Buddhikot MM, Kennedy I, Mullany F, Viswanathan H (2009). Ultra-broadband femtocells via opportunistic reuse of multi-operator and multi-service spectrum. *Bell Labs Technical Journal*, 13: 129–144. doi:10.1002/bltj.20340
- Bürgi A, Theis G, Siegenthaler A, Rösli M (2008). Exposure modeling of high-frequency electromagnetic fields. *J Expo Sci Environ Epidemiol*, 18: 183–191. doi:10.1038/sj.jes.7500575 PMID:17410112
- Burkhardt M, Poković K, Gnos M *et al.* (1996). Numerical and experimental dosimetry of Petri dish exposure setups. *Bioelectromagnetics*, 17: 483–493. doi:10.1002/(SICI)1521-186X(1996)17:6<483::AID-BEM8>3.0.CO;2-# PMID:8986366
- Cardis E, Armstrong BK, Bowman JD *et al.* (2011a). Risk of brain tumours in relation to estimated RF dose from mobile phones: results from five Interphone countries. *Occup Environ Med*, 68: 631–640. doi:10.1136/oemed-2011-100155 PMID:21659469
- Cardis E, Varsier N, Bowman JD *et al.* (2011b). Estimation of RF energy absorbed in the brain from mobile phones in the Interphone Study. *Occup Environ Med*, 68: 686–693. doi:10.1136/oemed-2011-100065 PMID:21659468
- CENELEC (2001). *Basic standard for the measurement of Specific Absorption Rate related to human exposure to electromagnetic fields from mobile phones (300 MHz–3 GHz)*, EN50361.
- CENELEC (2005). *Basic standard to demonstrate the compliance of fixed equipment for radio transmission (110 MHz - 40 GHz) intended for use in wireless telecommunication networks with the basic restrictions or the reference levels related to general public exposure to radio frequency electromagnetic fields, when put into service*, EN50400.
- CENELEC (2008). *Basic standard for the in-situ measurement of electromagnetic field strength related to human exposure in the vicinity of base stations*. CLC/TC 106X, EN50492.
- Challis LJ (2005). Mechanisms for interaction between RF fields and biological tissue. *Bioelectromagnetics*, 26: S7S98–S106. doi:10.1002/bem.20119 PMID:15931683
- Chavannes N, Tay N, Nikoloski N, Kuster N (2003). Suitability of FDTD based TCAD tools for RF design of mobile phones. *IEEE Antennas and Propagation Magazine*, 45: 52–66. doi:10.1109/MAP.2003.1282180
- Chiabrera A, Bianco B, Moggia E, Kaufman JJ (2000). Zeeman-Stark modeling of the RF EMF interaction with ligand binding. *Bioelectromagnetics*, 21: 312–324.

- doi:10.1002/(SICI)1521-186X(200005)21:4<312::AID-BEM7>3.0.CO;2-# PMID:10797459
- Chou CK & Guy AW (1982). Systems for exposing mice to 2,450-MHz electromagnetic fields. *Bioelectromagnetics*, 3: 401–412. doi:10.1002/bem.2250030403 PMID:7181963
- Christ A, Gosselin MC, Christopoulou M *et al.* (2010a). Age-dependent tissue-specific exposure of cell phone users. *Phys Med Biol*, 55: 1767–1783. doi:10.1088/0031-9155/55/7/001 PMID:20208098
- Christ A, Kainz W, Hahn EG *et al.* (2010b). The Virtual Family—development of surface-based anatomical models of two adults and two children for dosimetric simulations. *Phys Med Biol*, 55: N23–N38. doi:10.1088/0031-9155/55/2/N01 PMID:20019402
- Christ A & Kuster N (2005). Differences in RF energy absorption in the heads of adults and children. *Bioelectromagnetics*, 26: Suppl 7S31–S44. doi:10.1002/bem.20136 PMID:16142771
- Christ A, Samaras T, Klingenberg A, Kuster N (2006). Characterization of the electromagnetic near-field absorption in layered biological tissue in the frequency range from 30 MHz to 6,000 MHz. *Phys Med Biol*, 51: 4951–4965. doi:10.1088/0031-9155/51/19/014 PMID:16985280
- Christ A, Samaras T, Neufeld E *et al.* (2007). SAR distribution in human beings when using body-worn RF transmitters. *Radiat Prot Dosimetry*, 124: 6–14. doi:10.1093/rpd/ncm377 PMID:17652110
- Conil E, Hadjem A, Lacroux F *et al.* (2008). Variability analysis of SAR from 20 MHz to 2.4 GHz for different adult and child models using finite-difference time-domain. *Phys Med Biol*, 53: 1511–1525. doi:10.1088/0031-9155/53/6/001 PMID:18367785
- Cooper TG (2002). NRPB-W24 Report “Occupational Exposure to Electric Magnetic Fields in the Context of the ICNIRP Guidelines”. National Radiological Protection Board Report.
- Cooper TG, Allen SG, Blackwell RP *et al.* (2004). Assessment of occupational exposure to radiofrequency fields and radiation. *Radiat Prot Dosimetry*, 111: 191–203. doi:10.1093/rpd/nch334 PMID:15266067
- Cooper TG, Mann SM, Khalid M, Blackwell RP (2006). Public exposure to radio waves near GSM microcell and picocell base stations. *J Radiol Prot*, 26: 199–211. doi:10.1088/0952-4746/26/2/005 PMID:16738416
- Cooray V (2003). *The lightning flash*. Power and Energy Series 34. London, UK: The Institution of Engineering and Technology
- Coray R, Krähenbühl P, Riederer M *et al.* (2002). *Immissionen in Salzburg*. Technical report, BAKOM, Switzerland.
- Crawford ML (1974). Generation of standard EM fields using TEM transmission cells. *IEEE Transact EMC*, 16: 189–195.
- deSalles AA, Bulla G, Rodriguez CE (2006). Electromagnetic absorption in the head of adults and children due to mobile phone operation close to the head. *Electromagn Biol Med*, 25: 349–360. doi:10.1080/15368370601054894 PMID:17178592
- Dimbylow P (2005). Resonance behaviour of whole-body averaged specific energy absorption rate (SAR) in the female voxel model, NAOMI. *Phys Med Biol*, 50: 4053–4063. doi:10.1088/0031-9155/50/17/009 PMID:16177529
- Dimbylow P (2007a). SAR in the mother and foetus for RF plane wave irradiation. *Phys Med Biol*, 52: 3791–3802. doi:10.1088/0031-9155/52/13/009 PMID:17664577
- Dimbylow P & Bolch W (2007b). Whole-body-averaged SAR from 50 MHz to 4 GHz in the University of Florida child voxel phantoms. *Phys Med Biol*, 52: 6639–6649. doi:10.1088/0031-9155/52/22/006 PMID:17975288
- Dimbylow PJ (1997). FDTD calculations of the whole-body averaged SAR in an anatomically realistic voxel model of the human body from 1 MHz to 1 GHz. *Phys Med Biol*, 42: 479–490. doi:10.1088/0031-9155/42/3/003 PMID:9080530
- Dimbylow PJ (2002). Fine resolution calculations of SAR in the human body for frequencies up to 3 GHz. *Phys Med Biol*, 47: 2835–2846. doi:10.1088/0031-9155/47/16/301 PMID:12222849
- Dimbylow PJ, Khalid M, Mann S (2003). Assessment of specific energy absorption rate (SAR) in the head from a TETRA handset. *Phys Med Biol*, 48: 3911–3926. doi:10.1088/0031-9155/48/23/008 PMID:14703166
- Dimbylow PJ, Nagaoka T, Xu XG (2009). A comparison of foetal SAR in three sets of pregnant female models. *Phys Med Biol*, 54: 2755–2767. doi:10.1088/0031-9155/54/9/011 PMID:19369706
- Djafarzadeh R, Crespo-Valero P, Zefferer M *et al.* (2009). *Organ and cns tissue region specific evaluation of the time-averaged far-field exposure in various human body models*. In: *Abstract Collection of BioEM 2009 Davos, the Joint Meeting of the Bioelectromagnetics Society and the European BioElectromagnetics Association*, June 14–19, Davos, Switzerland. Poster presentation P-28 in Poster session 2: Dosimetry (June 16).
- Ebert S (2009). *EMF Risk Assessment: Exposure Systems for Large-Scale Laboratory and Experimental Provocation Studies*. ETH Zurich, Diss. ETH No. 18636, p. 212
- European Commission (2010). *Communication from the Commission to the European Parliament and the Council on the use of security scanners at EU airports*. COM (2010) 311 Final.
- European Telecommunications Standards Institute (2010). *Digital Enhanced Cordless Telecommunications (DECT)*. ETSI-EN300175–2 V2.3.1. Sophia Antipolis Cedex, France: ETSI.
- Fernández C, Bulla G, Pedra A, de Salles A (2005). *Comparison of Electromagnetic Absorption Characteristics in the Head of Adult and a Children for*

- 1800 MHz Mobile Phones, IEEE MTT-S Conference, July 25–28, pp. 523–526.
- Findlay RP & Dimbylow PJ (2005). Effects of posture on FDTD calculations of specific absorption rate in a voxel model of the human body. *Phys Med Biol*, 50: 3825–3835. doi:10.1088/0031-9155/50/16/011 PMID:16077229
- Findlay RP & Dimbylow PJ (2010). SAR in a child voxel phantom from exposure to wireless computer networks (Wi-Fi). *Phys Med Biol*, 55: N405–N411. doi:10.1088/0031-9155/55/15/N01 PMID:20647607
- Findlay RP, Lee AK, Dimbylow PJ (2009). FDTD calculations of SAR for child voxel models in different postures between 10 MHz and 3 GHz. *Radiat Prot Dosimetry*, 135: 226–231. doi:10.1093/rpd/ncp118 PMID:19589878
- Fink JM, Wagner JP, Congleton JJ, Rock JC (1999). Microwave emissions from police radar. *Am Ind Hyg Assoc J*, 60: 770–776. PMID:10671181
- Finkel T (2003). Oxidant signals and oxidative stress. *Curr Opin Cell Biol*, 15: 247–254. doi:10.1016/S0955-0674(03)00002-4 PMID:12648682
- Fixsen D (2009). The temperature of the cosmic microwave background. *Astrophys J*, 707: 916–920. doi:10.1088/0004-637X/707/2/916
- Foster KR (2000). Thermal and nonthermal mechanisms of interaction of radio-frequency energy with biological systems. *IEEE Trans Plasma Sci*, 28: 15–23. doi:10.1109/27.842819
- Foster KR (2007). Radiofrequency exposure from wireless LANs utilizing Wi-Fi technology. *Health Phys*, 92: 280–289. doi:10.1097/01.HP.0000248117.74843.34 PMID:17293700
- Foster KR & Glaser R (2007). Thermal mechanisms of interaction of radiofrequency energy with biological systems with relevance to exposure guidelines. *Health Phys*, 92: 609–620. doi:10.1097/01.HP.0000262572.64418.38 PMID:17495663
- Frei P, Mohler E, Bürgi A *et al.*; QUALIFEX team (2009a). A prediction model for personal radio frequency electromagnetic field exposure. *Sci Total Environ*, 408: 102–108. doi:10.1016/j.scitotenv.2009.09.023 PMID:19819523
- Frei P, Mohler E, Neubauer G *et al.* (2009b). Temporal and spatial variability of personal exposure to radio frequency electromagnetic fields. *Environ Res*, 109: 779–785. doi:10.1016/j.envres.2009.04.015 PMID:19476932
- Fröhlich H (1968). Long range coherence and energy storage in biological systems. *Int J Quantum Chem*, 2: 641–649. doi:10.1002/qua.560020505
- Fujimoto M, Hirata A, Wang J *et al.* (2006). FDTD-Derived Correlation of Maximum Temperature Increase and Peak SAR in Child and Adult Head Models Due to Dipole Antenna *IEEE Trans Electromagn Compat*, 48: 240–247. doi:10.1109/TEMC.2006.870816
- Gabriel C (2005). Dielectric properties of biological tissue: variation with age. *Bioelectromagnetics*, 26: Suppl 7S12–S18. doi:10.1002/bem.20147 PMID:16142779
- Gajsek P, D'Andrea JA, Mason PA *et al.* (2003). *Mathematical modelling using experimental and theoretical methods*. In: *Biological effects of Electromagnetic Fields*. Stavroulakis P, editor. Springer Verlag, pp. 118–170. [to be found in Google Books]
- Gandhi OP, Lazzi G, Tinniswood A, Yu QS (1999). Comparison of numerical and experimental methods for determination of SAR and radiation patterns of handheld wireless telephones. *Bioelectromagnetics*, 4: Suppl 493–101. doi:10.1002/(SICI)1521-186X(1999)20:4+<93::AID-BEM11>3.0.CO;2-8 PMID:10334718
- Gati A, Hadjem A, Wong M-F, Wiart J (2009). Exposure induced by WCDMA mobiles phones in operating networks. *IEEE Trans Wirel Comm*, 8: 5723–5727. doi:10.1109/TWC.2009.12.080758
- Georgiou CD (2010). *Oxidative stress-induced biological damage by low-level EMFs: mechanism of free radical pair electron-spin polarization and biochemical amplification*. In: *Non-thermal effects and mechanisms of interaction between electromagnetic fields and living matter*. ICEMS Monograph, Giuliani L, Soffritti M, editors. Bologna, Italy: National Institute for the Study and Control of Cancer and Environmental Diseases “Bernardino Ramazzini”, pp. 63–113.
- Gosselin MC, Christ A, Kühn S, Kuster N (2009). Dependence of the Occupational Exposure to Mobile Phone Base Stations on the Properties of the Antenna and the Human Body. *IEEE Trans Electromagn Compat*, 51: 227–235. doi:10.1109/TEMC.2009.2013717
- Gosselin MC, Kühn S, Crespo-Valero P *et al.* (2011). Estimation of head tissue-specific exposure from mobile phones based on measurements in the homogeneous SAM head. *Bioelectromagnetics*, n/a doi:10.1002/bem.20662 PMID:21416476
- Guy AW (1971). Analyses of electromagnetic fields induced in biological tissue by thermographic studies on equivalent phantom models. *IEEE Trans Microw Theory Tech*, 34: 671–680. doi:10.1109/TMTT.1986.1133416
- Guy AW, Wallace J, McDougall JA (1979). Circular polarized 2450-MHz waveguide system for chronic exposure of small animals to microwaves. *Radio Sci*, 14: 6S63–74. doi:10.1029/RS014i06Sp00063
- Hadjem A, Lautru D, Dale C *et al.* (2005a). Study of specific absorption rate (sar) induced in the two child head models and adult heads using a mobile phone *IEEE Trans MTT*, 53: 4–11. doi:10.1109/TMTT.2004.839343
- Hadjem A, Lautru D, Gadi N *et al.* (2005b). *Influence of the ear's morphology on Specific Absorption Rate (SAR) Induced in a Child Head using two source models*. IEEE MTT-S Conference, June 12–17.

- Hansen VW, Bitz AK, Streckert JR (1999). RF exposure of biological systems in radial waveguides. *IEEE Transact EMC*, 41: 487–493.
- Heinävaara S, Tokola K, Kurttio P, Auvinen A (2011). Validation of exposure assessment and assessment of recruitment methods for a prospective cohort study of mobile phone users (COSMOS) in Finland: a pilot study. *Environ Health*, 10: 14 doi:10.1186/1476-069X-10-14 PMID:21385407
- Henbest KB, Kukura P, Rodgers CT *et al.* (2004). Radio frequency magnetic field effects on a radical recombination reaction: a diagnostic test for the radical pair mechanism. *J Am Chem Soc*, 126: 8102–8103. doi:10.1021/ja048220q PMID:15225036
- Henderson SI & Bangay MJ (2006). Survey of RF exposure levels from mobile telephone base stations in Australia. *Bioelectromagnetics*, 27: 73–76. doi:10.1002/bem.20174 PMID:16283652
- Herring S (2004). Slouching toward the ordinary: current trends in computer-mediated communication. *New Media Soc*, 6: 26–36. doi:10.1177/1461444804039906
- Hillert L, Ahlbom A, Neasham D *et al.* (2006). Call-related factors influencing output power from mobile phones. *J Expo Sci Environ Epidemiol*, 16: 507–514. doi:10.1038/sj.jes.7500485 PMID:16670713
- Hirata A, Fujimoto M, Asano T *et al.* (2006a). Correlation between maximum temperature increase and peak SAR with different average schemes and masses *IEEE Trans Electromagn Compat*, 48: 569–578. doi:10.1109/TEMC.2006.877784
- Hirata A, Fujiwara O, Shiozawa T (2006b). Correlation between peak spatial-average SAR and temperature increase due to antennas attached to human trunk. *IEEE Trans Biomed Eng*, 53: 1658–1664. doi:10.1109/TBME.2006.877798 PMID:16916100
- Hirata A, Ito N, Fujiwara O (2009). Influence of electromagnetic polarization on the whole-body averaged SAR in children for plane-wave exposures. *Phys Med Biol*, 54: N59–N65. doi:10.1088/0031-9155/54/4/N02 PMID:19141885
- Hirata A, Morita M, Shiozawa T (2003). Temperature increase in the human head due to a dipole antenna at microwave frequencies. *IEEE Trans Electromagn Compat*, 45: 109–116. doi:10.1109/TEMC.2002.808045
- Hirata A, Shirai K, Fujiwara O (2008). On averaging mass of SAR correlating with temperature elevation due to a dipole antenna *Progr. Electrom. Research*, 84: 221–237. doi:10.2528/PIER08072704
- Hombach V, Meier K, Burkhardt M *et al.* (1996). The dependence of EM energy absorption upon human head modeling at 900 MHz. *IEEE Trans Microw Theory Tech*, 44: 1865–1873. doi:10.1109/22.539945
- HPA (2008). Report on MRI
- Hurt WD, Ziriaux JM, Mason PA (2000). Variability in EMF permittivity values: implications for SAR calculations. *IEEE Trans Biomed Eng*, 47: 396–401. doi:10.1109/10.827308 PMID:10743782
- IARC (2002). Non-ionizing radiation, Part 1: static and extremely low-frequency (ELF) electric and magnetic fields. *IARC Monogr Eval Carcinog Risks Hum*, 80: 1–395. PMID:12071196
- ICNIRP; International Commission on Non-Ionizing Radiation Protection (1998). Guidelines for limiting exposure to time-varying electric, magnetic, and electromagnetic fields (up to 300 GHz). *Health Phys*, 74: 494–522. PMID:9525427.
- ICNIRP; International Commission on Non-Ionizing Radiation Protection (2009a). Exposure to high frequency electromagnetic fields, biological effects and health consequences (100 kHz to 300 GHz). la Vecchia P, Matthes R, Ziegelberger G *et al.*, editors. pp. 1–392. Available at: <http://www.icnirp.de/>
- ICNIRP; International Commission on Non-Ionizing Radiation Protection (2009b). Statement on the guidelines for limiting exposure to time varying electric, magnetic, and electromagnetic fields (up to 300 ghz) *Health Phys*, 97: 257–258.
- ICNIRP; International Commission on Non-Ionizing Radiation Protection (2010). Guidelines for limiting exposure to time-varying electric and magnetic fields (1 Hz to 100 kHz). *Health Phys*, 99: 818–836. PMID:21068601
- IEEE (1999). *Standard for Safety Levels with Respect to Human Exposure to Radio Frequency Electromagnetic Fields, 3 KHz to 300 GHz, C95, 1*.
- IEEE (2003). *Recommended Practice for Determining the Spatial-Peak Specific Absorption Rate (SAR) in the Human Body Due to Wireless Communications Devices: Measurement Techniques*, 1528/D1.2. Piscataway, NJ, USA
- IEEE (2005). C95.1, *IEEE Standard for Safety Levels with Respect to Human Exposure to Radio Frequency Electromagnetic Fields, 100 kHz-300 GHz*.
- InfoPlease (2011). Available at: <http://www.infoplease.com/ipa/A0933563.html>
- Inyang I, Benke G, McKenzie R *et al.* (2010). A new method to determine laterality of mobile telephone use in adolescents. *Occup Environ Med*, 67: 507–512. doi:10.1136/oem.2009.049676 PMID:19955574
- Inyang I, Benke G, McKenzie R, Abramson M (2008). Comparison of measuring instruments for radiofrequency radiation from mobile telephones in epidemiological studies: implications for exposure assessment. *J Expo Sci Environ Epidemiol*, 18: 134–141. doi:10.1038/sj.jes.7500555 PMID:17327852
- Inyang I, Benke G, Morrissey J *et al.* (2009). How well do adolescents recall use of mobile telephones? Results of a validation study. *BMC Med Res Methodol*, 9: 36 doi:10.1186/1471-2288-9-36 PMID:19523193
- IPEM (2010). *Guidance on the measurement and use of EMF and EMC*, Report 98. York, UK: Institute of Physics

- and Engineering in Medicine. Available at: <http://www.ipem.ac.uk/publications/ipemreports/Pages/GuidanceontheMeasurementandUseofEMFandEMC.aspx>
- ITU (2008). *Radio Regulations*, Volume 1. International Telecommunication Union. Articles Edition 2008. Available at: <http://www.itu.int/pub/R-REG-RR/en>
- Jaspard F, Nadi M, Rouane A (2003). Dielectric properties of blood: an investigation of haematocrit dependence. *Physiol Meas*, 24: 137–147. doi:10.1088/0967-3334/24/1/310 PMID:12636192
- Jokela K & Puranen L (1999). Occupational RF exposures. *Radiat Prot Dosimetry*, 83: 119–124.
- Jokela K, Puranen L, Gandhi OP (1994). Radio frequency currents induced in the human body for medium-frequency/high-frequency broadcast antennas. *Health Phys*, 66: 237–244. doi:10.1097/00004032-199403000-00001 PMID:8106240
- Joó E, Szász A, Szendrő P (2006). Metal-framed spectacles and implants and specific absorption rate among adults and children using mobile phones at 900/1800/2100 MHz. *Electromagn Biol Med*, 25: 103–112. doi:10.1080/15368370600719042 PMID:16771299
- Joseph W, Frei P, Roösl M *et al.* (2010). Comparison of personal radio frequency electromagnetic field exposure in different urban areas across Europe. *Environ Res*, 110: 658–663. doi:10.1016/j.envres.2010.06.009 PMID:20638656
- Joseph W, Olivier C, Martens L (2002). A robust, fast and accurate deconvolution algorithm for EM-field measurements around GSM and UMTS base stations with a spectrum analyser. *IEEE Trans Instrum Meas*, 51: 1163–1169. doi:10.1109/TIM.2002.808026
- Joseph W, Verloock L, Martens L (2008). Accurate determination of the electromagnetic field due to wimax base station antennas. *Electromagnetic Compatibility IEEE Transactions*, 50: 730–735.
- Jung KB, Kim TH, Kim JL *et al.* (2008). Development and validation of reverberation-chamber type whole-body exposure system for mobile-phone frequency. *Electromagn Biol Med*, 27: 73–82. doi:10.1080/15368370701878895 PMID:18327716
- Kainz W, Christ A, Kellom T *et al.* (2005). Dosimetric comparison of the specific anthropomorphic mannequin (SAM) to 14 anatomical head models using a novel definition for the mobile phone positioning. *Phys Med Biol*, 50: 3423–3445. doi:10.1088/0031-9155/50/14/016 PMID:16177519
- Kainz W, Nikoloski N, Oesch W *et al.* (2006). Development of novel whole-body exposure setups for rats providing high efficiency, National Toxicology Program (NTP) compatibility and well-characterized exposure (No. 20) *Physics in Medicine and Biology*, 51: 5211–5229. PMID:17019034.
- Kanda M (1993). Standard probes for electromagnetic field measurement. *IEEE Trans Antenn Propag*, AP-41: 1349–1364. doi:10.1109/8.247775
- Kännälä S, Puranen L, Sihvonen AP, Jokela K (2008). Measured and computed induced body currents in front of an experimental RF dielectric heater. *Health Phys*, 94: 161–169. doi:10.1097/01.HP.0000286776.79411.1c PMID:18188050
- Kawai H, Nagaoka T, Watanabe S *et al.* (2010). Computational dosimetry in embryos exposed to electromagnetic plane waves over the frequency range of 10 MHz–1.5 GHz *Phys Med Biol*, 55: 1–11. doi:10.1088/0031-9155/55/1/N01 PMID:19949261
- Kelsh MA, Shum M, Sheppard AR *et al.* (2010). Measured radiofrequency exposure during various mobile-phone use scenarios. *J Expo Sci Environ Epidemiol*, doi:10.1038/jes.2010.12 PMID:20551994
- Keshvari J & Lang S (2005). Comparison of radio frequency energy absorption in ear and eye region of children and adults at 900, 1800 and 2450 MHz. *Phys Med Biol*, 50: 4355–4369. doi:10.1088/0031-9155/50/18/008 PMID:16148398
- Khalid M, Mee T, Peyman A *et al.* (2011). *Exposure to electromagnetic fields from wireless computer networks: duty factor of Wi-Fi devices operating in schools: Non-Ionizing Radiation & Children's Health*. International Joint Workshop, 18–20 May, 2011. Ljubljana, Slovenia.
- Kim BC & Park S-O (2010). Evaluation of RF electromagnetic field exposure levels from cellular base stations in Korea. *Bioelectromagnetics*, 31: 495–498. PMID:20564176
- Kowalczyk C, Yarwood G, Blackwell R *et al.* (2010). Absence of nonlinear responses in cells and tissues exposed to RF energy at mobile phone frequencies using a doubly resonant cavity. *Bioelectromagnetics*, 31: 556–565. doi:10.1002/bem.20597 PMID:20607742
- Kramer A, Müller P, Lott U *et al.* (2006). Electro-optic fiber sensor for amplitude and phase detection of radio frequency electromagnetic fields. *Opt Lett*, 31: 2402–2404. doi:10.1364/OL.31.002402 PMID:16880836
- Kühn S (2009). *EMF Risk Assessment: Exposure Assessment and Compliance Testing in Complex Environments*. Swiss Federal Institute of Technology, Zurich, Switzerland: Hartung-Gorre Verlag Konstanz. PhD thesis, Diss. ETH Nr. 18637, Defense: 29 September 2009, doi:10.3929/ethz-a-006037728.10.3929/ethz-a-006037728
- Kühn S, Cabot E, Christ A *et al.* (2009a). Assessment of the radio-frequency electromagnetic fields induced in the human body from mobile phones used with hands-free kits. *Phys Med Biol*, 54: 5493–5508. doi:10.1088/0031-9155/54/18/010 PMID:19706964
- Kühn S, Gosselin M, Crespo-Valero P, *et al.* (2010). *Cumulative Exposure in Time and Frequency Domains of the Central Nervous System*. Final Report SNF 405740-113591 SNF NRP57 Source for Table 1.6

- Kühn S, Jennings W, Christ A, Kuster N (2009b). Assessment of induced radio-frequency electromagnetic fields in various anatomical human body models. *Phys Med Biol*, 54: 875–890. doi:10.1088/0031-9155/54/4/004 PMID:19141880
- Kühn S, Kuster N (2007). *Experimental EMF exposure assessment*. In: *Handbook of Biological Effects of Electromagnetic Fields*, 3rd ed. Barnes FS, Greenebaum B, editors. Boca Raton: CRC Press.
- Kühn S, Schmid T, Kuster N (2007b). *System specific probe calibration*. Presentation at the IEEE TC-34 / FCC SAR round table meeting, College Park, MD, USA, October 18, 2007.
- Kühn S, Urs Lott S, Kramer A *et al.* (2007a). Assessment methods for demonstrating compliance with safety limits of wireless devices used in home and office environments. *IEEE Trans Electromagn Compat*, 49: 519–525. doi:10.1109/TEMC.2007.903042
- Kuster N & Balzano Q (1992). Energy absorption mechanism by biological bodies in the near field of dipole antennas above 300 MHz. *IEEE Trans Vehicular Technol*, 41: 17–23. doi:10.1109/25.120141
- Kuster N & Schönborn F (2000). Recommended minimal requirements and development guidelines for exposure setups of bio-experiments addressing the health risk concern of wireless communications. *Bioelectromagnetics*, 21: 508–514. doi:10.1002/1521-186X(200010)21:7<508::AID-BEM4>3.0.CO;2-F PMID:11015115
- Kuster N, Schuderer J, Christ A *et al.* (2004). Guidance for exposure design of human studies addressing health risk evaluations of mobile phones. *Bioelectromagnetics*, 25: 524–529. doi:10.1002/bem.20034 PMID:15376239
- Kuster N, Torres VB, Nikoloski N *et al.* (2006). Methodology of detailed dosimetry and treatment of uncertainty and variations for in vivo studies. *Bioelectromagnetics*, 27: 378–391. doi:10.1002/bem.20219 PMID:16615059
- Lee A-K, Byun J-K, Park J-S *et al.* (2009). Development of 7-year-old Korean child model for computational dosimetry *ETRI J*, 31: 237–239. doi:10.4218/etrij.09.0208.0342
- Lee A-K, Choi H-D, Choi J-I (2007). Study on SARs in Head Models With Different Shapes by Age Using SAM Model for Mobile Phone Exposure at 835 MHz. *IEEE Trans Electromagn Compat*, 49: 302–312. doi:10.1109/TEMC.2007.897124
- Lee AK & Yun J (2011). A Comparison of Specific Absorption Rates in SAM Phantom and Child Head Models at 835 and 1900 MHz. *IEEE Trans Electromagn Compat*, 99: 1–9.
- Lee C, Lee C, Park SH, Lee JK (2006). Development of the two Korean adult tomographic computational phantoms for organ dosimetry. *Med Phys*, 33: 380–390. doi:10.1118/1.2161405 PMID:16532944
- Lévêque P, Dale C, Veyret B, Wiart J (2004). Dosimetric analysis of a 900-MHz rat head exposure system. *IEEE Trans Microw Theory Tech*, 52: 2076–2083. doi:10.1109/TMTT.2004.831984
- Liburdy RP & Penn A (1984). Microwave bioeffects in the erythrocyte are temperature and pO₂ dependent: cation permeability and protein shedding occur at the membrane phase transition. *Bioelectromagnetics*, 5: 283–291. doi:10.1002/bem.2250050215 PMID:6732882
- Lin JC (2007). Dosimetric comparison between different quantities for limiting exposure in the RF band: rationale and implications for guidelines. *Health Phys*, 92: 547–553. doi:10.1097/01.HP.0000236788.33488.65 PMID:17495655
- Lönn S, Forssén U, Vecchia P *et al.* (2004). Output power levels from mobile phones in different geographical areas; implications for exposure assessment. *Occup Environ Med*, 61: 769–772. doi:10.1136/oem.2003.012567 PMID:15317918
- Lu Y, Yu J, Ren Y (1994). Dielectric properties of human red blood cells in suspension at radio frequencies. *Bioelectromagnetics*, 15: 589–591. doi:10.1002/bem.2250150612 PMID:7880172
- Mann S (2010). Assessing personal exposures to environmental radiofrequency electromagnetic fields. *C R Phys*, 11: 541–555. doi:10.1016/j.crhy.2010.11.005
- Mantiply ED, Pohl KR, Poppell SW, Murphy JA (1997). Summary of measured radiofrequency electric and magnetic fields (10 kHz to 30 GHz) in the general and work environment. *Bioelectromagnetics*, 18: 563–577. doi:10.1002/(SICI)1521-186X(1997)18:8<563::AID-BEM5>3.0.CO;2-0 PMID:9383245
- Martens L (2005). Electromagnetic safety of children using wireless phones: a literature review. *Bioelectromagnetics*, 26: Suppl 7S133–S137. doi:10.1002/bem.20150 PMID:16059915
- Martínez-Búrdalo M, Martín A, Anguiano M, Villar R (2004). Comparison of FDTD-calculated specific absorption rate in adults and children when using a mobile phone at 900 and 1800 MHz. *Phys Med Biol*, 49: 345–354. doi:10.1088/0031-9155/49/2/011 PMID:15083675
- McIntosh RL & Anderson V (2010). SAR versus S(inc): What is the appropriate RF exposure metric in the range 1–10 GHz? Part II: Using complex human body models. *Bioelectromagnetics*, 31: 467–478. PMID:20354998
- Meyer FJ, Davidson DB, Jakobus U, Stuchly MA (2003). Human exposure assessment in the near field of GSM base-station antennas using a hybrid finite element/method of moments technique. *IEEE Trans Biomed Eng*, 50: 224–233.
- Mezei G, Benyi M, Muller A (2007). Mobile phone ownership and use among school children in three Hungarian cities. *Bioelectromagnetics*, 28: 309–315. doi:10.1002/bem.20270 PMID:17216610
- Moros EG, Straube WL, Pickard WF (1999). The radial transmission line as a broad-band shielded exposure system for microwave irradiation of large numbers

- of culture flasks. *Bioelectromagnetics*, 20: 65–80. doi:10.1002/(SICI)1521-186X(1999)20:2<65::AID-BEM1>3.0.CO;2-W PMID:10029133
- Nagaoka T, Kunieda E, Watanabe S (2008). Proportion-corrected scaled voxel models for Japanese children and their application to the numerical dosimetry of specific absorption rate for frequencies from 30 MHz to 3 GHz. *Phys Med Biol*, 53: 6695–6711. doi:10.1088/0031-9155/53/23/004 PMID:18997264
- Nagaoka T, Togashi T, Saito K *et al.* (2007). An anatomically realistic whole-body pregnant-woman model and specific absorption rates for pregnant-woman exposure to electromagnetic plane waves from 10 MHz to 2 GHz. *Phys Med Biol*, 52: 6731–6745. doi:10.1088/0031-9155/52/22/012 PMID:17975294
- Nagaoka T, Watanabe S (2009). *Estimation of variability of specific absorption rate with physical description of children exposed to electromagnetic field in the VHF band.* International conference of the IEEE EMBS.
- Narda STS (2005). *Electric Field Probe For EMR-200 and EMR-300.* (December 16, 2005). Available at: <http://www.narda-sts.com>.
- NASA (2011). *Sun FactSheet.* National Aeronautics and Space Administration. Available at: <http://nssdc.gsfc.nasa.gov/planetary/factsheet/sunfact.html>
- NCRP; National Council on Radiation Protection and Measurements (1986). *Biological Effects and Exposure Criteria for Radiofrequency Electromagnetic Fields.* NCRP Report 86, Recommendations of the National Council on Radiation Protection and Measurements.
- Neubauer G, Preiner P, Cecil S *et al.* (2009). The relation between the specific absorption rate and electromagnetic field intensity for heterogeneous exposure conditions at mobile communications frequencies. *Bioelectromagnetics*, 30: 651–662. PMID:19551765
- Nielsen (2010). *Media industry fact sheet.* Available at: <http://blog.nielsen.com/nielsenwire/press/nielsen-fact-sheet-2010.pdf>
- Nikoloski N, Fröhlich J, Samaras T *et al.* (2005). Reevaluation and improved design of the TEM cell in vitro exposure unit for replication studies. *Bioelectromagnetics*, 26: 215–224. doi:10.1002/bem.20067 PMID:15768424
- NOAA (2011). *Science on a Sphere: Annual lightning flash rate.* Available at: <http://www.srh.noaa.gov/>
- Olivier C & Martens L (2005). Optimal settings for narrow-band signal measurements used for exposure assessment around GSM base stations. *IEEE Trans Instrum Meas*, 54: 311–317. doi:10.1109/TIM.2004.838114
- Olivier C & Martens L (2006). Theoretical derivation of the stochastic behavior of a WCDMA signal measured with a spectrum analyzer. *IEEE Trans Instrum Meas*, 55: 603–614. doi:10.1109/TIM.2006.870330
- Petersen RC & Testagrossa PA (1992). Radio-frequency electromagnetic fields associated with cellular-radio cell-site antennas. *Bioelectromagnetics*, 13: 527–542. doi:10.1002/bem.2250130608 PMID:1482416
- Peyman A, Gabriel C (2002). *Variation of the dielectric properties of biological tissue as a function of age.* Final Technical Report, Department of Health, UK.
- Peyman A & Gabriel C (2007). Development and characterization of tissue equivalent materials for frequency range 30 – 300 MHz *Electron Lett*, 43: 19–20 doi:10.1049/el:20073455
- Peyman A, Gabriel C, Grant EH *et al.* (2009). Variation of the dielectric properties of tissues with age: the effect on the values of SAR in children when exposed to walkie-talkie devices. *Phys Med Biol*, 54: 227–241. doi:10.1088/0031-9155/54/2/004 PMID:19088390
- Peyman A, Holden SJ, Watts S *et al.* (2007). Dielectric properties of porcine cerebrospinal tissues at microwave frequencies: in vivo, in vitro and systematic variation with age. *Phys Med Biol*, 52: 2229–2245. doi:10.1088/0031-9155/52/8/013 PMID:17404466
- Peyman A, Khalid M, Calderon C *et al.* (2011). Assessment of exposure to electromagnetic fields from wireless computer networks (Wi-Fi) in schools; results of laboratory measurements. *Health Phys*, 100: 594–612. doi:10.1097/HP.0b013e318200e203
- Peyman A, Rezazadeh AA, Gabriel C (2001). Changes in the dielectric properties of rat tissue as a function of age at microwave frequencies. *Phys Med Biol*, 46: 1617–1629. doi:10.1088/0031-9155/46/6/303 PMID:11419623
- Poković K (1999). *Advanced Electromagnetic Probes for Near-Field Evaluations.* PhD thesis, Diss. ETH Nr. 13334, Zurich.
- Poković K, Schmid T, Fröhlich J, Kuster N (2000b). Novel probes and evaluation procedures to assess field magnitude and polarization. *IEEE Trans Electromagn Compat*, 42: 240–245. doi:10.1109/15.852419
- Poković K, Schmid T, Kuster N (2000a). Millimeter-resolution E-field probe for isotropic measurement in lossy media between 100 MHz and 20 GHz. *IEEE Trans Instrum Meas*, 49: 873–878. doi:10.1109/19.863941
- Porter SJ, Capstick MH, Faraci F, Flintoft ID (2005). *AR testing of hands-free mobile telephones.* *Mobile Telecommunications and Health Research Programme.* Available at: [http://www.mthr.org.uk/research_projects/dti_funded_projects/porter\(sar\).htm](http://www.mthr.org.uk/research_projects/dti_funded_projects/porter(sar).htm)
- SProhofsky EW (2004). RF absorption involving biological macromolecules. *Bioelectromagnetics*, 25: 441–451. doi:10.1002/bem.20013 PMID:15300730
- Redmayne M, Inyang I, Dimitriadis C *et al.* (2010). Cordless telephone use: implications for mobile phone research. *J Environ Monit*, 12: 809–812. doi:10.1039/b920489j PMID:20383359
- Repacholi MH (2001). Health risks from the use of mobile phones. *Toxicol Lett*, 120: 323–331. doi:10.1016/S0378-4274(01)00285-5 PMID:11323191
- Ritz T, Wiltschko R, Hore PJ *et al.* (2009). Magnetic compass of birds is based on a molecule with optimal directional sensitivity. *Biophys J*, 96: 3451–3457. doi:10.1016/j.bpj.2008.11.072 PMID:19383488

- Rudge AW (1970). An electromagnetic radiation probe for near-field measurements at microwave frequencies. *J Microw Power*, 5: 155–174.
- Samaras T, Kalampaliki E, Sahalos JN (2007). Influence of Thermophysiological Parameters on the Calculation of Temperature Rise in the Head of Mobile Phone Users *IEEE Trans Electromagn Compat*, 49: 936–939. doi:10.1109/TEMC.2007.908257
- Schmid G, Lager D, Preiner P *et al.* (2007b). Exposure caused by wireless technologies used for short-range indoor communication in homes and offices. *Radiat Prot Dosimetry*, 124: 58–62. doi:10.1093/rpd/ncm245 PMID:17566000
- Schmid G, Neubauer G, Illievich UM, Alesch F (2003). Dielectric properties of porcine brain tissue in the transition from life to death at frequencies from 800 to 1900 MHz. *Bioelectromagnetics*, 24: 413–422. doi:10.1002/bem.10122 PMID:12929160
- Schmid G, Preiner P, Lager D *et al.* (2007a). Exposure of the general public due to wireless LAN applications in public places. *Radiat Prot Dosimetry*, 124: 48–52. doi:10.1093/rpd/ncm320 PMID:17562659
- Schmid G & Überbacher R (2005). Age dependence of dielectric properties of bovine brain and ocular tissues in the frequency range of 400 MHz to 18 GHz. *Phys Med Biol*, 50: 4711–4720. doi:10.1088/0031-9155/50/19/019 PMID:16177499
- Schönborn F, Burkhardt M, Kuster N (1998). Differences in energy absorption between heads of adults and children in the near field of sources. *Health Phys*, 74: 160–168. doi:10.1097/00004032-199802000-00002 PMID:9450585
- Schubert M, Bornkessel C, Wuschek M, Schmidt P (2007). Exposure of the general public to digital broadcast transmitters compared to analogue ones. *Radiat Prot Dosimetry*, 124: 53–57. doi:10.1093/rpd/ncm337 PMID:17617635
- Schuderer J, Schmid T, Urban G *et al.* (2004a). Novel high-resolution temperature probe for radiofrequency dosimetry. *Phys Med Biol*, 49: N83–N92. doi:10.1088/0031-9155/49/6/N04 PMID:15104331
- Schuderer J, Spät D, Samaras T *et al.* (2004b). In Vitro Exposure Systems for RF Exposures at 900 MHz. *IEEE Trans Microw Theory Tech*, 52: 2067–2075. doi:10.1109/TMTT.2004.832010
- Schüz J (2009). Lost in laterality: interpreting “preferred side of the head during mobile phone use and risk of brain tumour” associations. *Scand J Public Health*, 37: 664–667. doi:10.1177/1403494809341096 PMID:19581357
- Schüz J & Mann S (2000). A discussion of potential exposure metrics for use in epidemiological studies on human exposure to radiowaves from mobile phone base stations. *J Expo Anal Environ Epidemiol*, 10: 600–605. doi:10.1038/sj.jea.7500115 PMID:11140443
- Seibersdorf Research (2011). *Precision Conical Dipole PCD 8250*. Available at: <http://www.seibersdorf-laboratories.at>
- Sektion NIS (2002). *BUWAL und Sektion Hochfrequenz, EMV und Verkehr*. Mobilfunk-Basisstationen (GSM). Messempfehlung. February 2002.
- Sheppard AR, Swicord ML, Balzano Q (2008). Quantitative evaluations of mechanisms of radiofrequency interactions with biological molecules and processes. *Health Phys*, 95: 365–396. doi:10.1097/01.HP.0000319903.20660.37 PMID:18784511
- Shum M, Kelsh MA, Sheppard AR, Zhao K (2011). An evaluation of self-reported mobile phone use compared to billing records among a group of engineers and scientists. *Bioelectromagnetics*, 32: 37–48. doi:10.1002/bem.20613 PMID:20857456
- Singal T (2010). *Wireless communications*. New Delhi: Tata McGraw Hill Education Private Limited.
- Smith GS (1981). Analysis of miniature electric field probes with resistive transmission lines. *IEEE Trans Microw Theory Tech*, MTT-29: 1213–1224. doi:10.1109/TMTT.1981.1130534
- Stuchly MA (1979). Interaction of radiofrequency and microwave radiation with living systems. A review of mechanisms. *Radiat Environ Biophys*, 16: 1–14. doi:10.1007/BF01326892 PMID:382232
- Taurisano MD & Vander Vorst A (2000). Experimental thermographic analysis of thermal effects induced on a human head exposed to 900 MHz fields of mobile-phones. *IEEE Trans Microw Theory Tech*, 48: 2022–2032. doi:10.1109/22.884191
- Thurai M, Goodridge VD, Sheppard RJ, Grant EH (1984). Variation with age of the dielectric properties of mouse brain cerebrum. *Phys Med Biol*, 29: 1133–1136. doi:10.1088/0031-9155/29/9/009 PMID:6483977
- Thurai M, Steel MC, Sheppard RJ, Grant EH (1985). Dielectric properties of developing rabbit brain at 37 degrees C. *Bioelectromagnetics*, 6: 235–242. doi:10.1002/bem.2250060304 PMID:3836667
- Timmel CR, Till U, Brocklehurst B *et al.* (1998). Effects of weak magnetic fields on free radical recombination reactions. *Mol Phys*, 95: 71–89. doi:10.1080/00268979809483134
- Tinniswood AD, Furse CM, Gandhi OP (1998). Power deposition in the head and neck of an anatomically based human body model for plane wave exposures. *Phys Med Biol*, 43: 2361–2378. doi:10.1088/0031-9155/43/8/026 PMID:9725610
- Togashi T, Nagaoka T, Kikuchi S *et al.* (2008). TDTD calculations of specific absorption rate in fetus caused by electromagnetic waves from mobile radio terminal using pregnant woman model. *IEEE Trans Microw Theory Tech*, 56: 554–559. doi:10.1109/TMTT.2007.914625
- Togo H, Shimizu N, Nagatsuma T (2007). Near-field mapping system using fiber-based electro-optic probe

- for specific absorption rate measurements *IEICE Trans Electron*, 90: C436–442. doi:10.1093/ietele/e90-c.2.436
- Tomitsch J, Dechant E, Frank W (2010). Survey of electromagnetic field exposure in bedrooms of residences in lower Austria. *Bioelectromagnetics*, 31: 200–208. PMID:19780092
- Uusitupa T, Laakso I, Ilvonen S, Nikoskinen K (2010). SAR variation study from 300 to 5000 MHz for 15 voxel models including different postures. *Phys Med Biol*, 55: 1157–1176. doi:10.1088/0031-9155/55/4/017 PMID:20107250
- Valberg PA (1995). Designing EMF experiments: what is required to characterize “exposure”? *Bioelectromagnetics*, 16: 396–401, discussion 402–406. doi:10.1002/bem.2250160608 PMID:8789071
- Van Leeuwen GM, Lagendijk JJ, Van Leersum BJ *et al.* (1999). Calculation of change in brain temperatures due to exposure to a mobile phone. *Phys Med Biol*, 44: 2367–2379. doi:10.1088/0031-9155/44/10/301 PMID:10533916
- Vermeeren G, Gosselin MC, Kühn S *et al.* (2010). The influence of the reflective environment on the absorption of a human male exposed to representative base station antennas from 300 MHz to 5 GHz. *Phys Med Biol*, 55: 5541–5555. doi:10.1088/0031-9155/55/18/018 PMID:20808028
- Vermeeren G, Joseph W, Olivier C, Martens L (2008). Statistical multipath exposure of a human in a realistic electromagnetic environment. *Health Phys*, 94: 345–354. doi:10.1097/01.HP.0000298816.66888.05 PMID:18332726
- Viel JF, Clerc S, Barrera C *et al.* (2009). Residential exposure to radiofrequency fields from mobile phone base stations, and broadcast transmitters: a population-based survey with personal meter. *Occup Environ Med*, 66: 550–556. doi:10.1136/oem.2008.044180 PMID:19336431
- Vrijheid M, Armstrong BK, Bédard D *et al.* (2009b). Recall bias in the assessment of exposure to mobile phones. *J Expo Sci Environ Epidemiol*, 19: 369–381. doi:10.1038/jes.2008.27 PMID:18493271
- Vrijheid M, Cardis E, Armstrong BK *et al.* Interphone Study Group (2006). Validation of short term recall of mobile phone use for the Interphone study. *Occup Environ Med*, 63: 237–243. doi:10.1136/oem.2004.019281 PMID:16556742
- Vrijheid M, Mann S, Vecchia P *et al.* (2009a). Determinants of mobile phone output power in a multinational study: implications for exposure assessment. *Occup Environ Med*, 66: 664–671. doi:10.1136/oem.2008.043380 PMID:19465409
- Wainwright P (2000). Thermal effects of radiation from cellular telephones. *Phys Med Biol*, 45: 2363–2372. doi:10.1088/0031-9155/45/8/321 PMID:10958200
- Wang J & Fujiwara O (2003). Comparison and evaluation of electromagnetic absorption characteristics in realistic human head models of adult and children for 900-MHz mobile telephones. *IEEE Trans Microw Theory Tech*, 51: 966–971. doi:10.1109/TMTT.2003.808681
- Wang J, Fujiwara O, Kodera S, Watanabe S (2006). FDTD calculation of whole-body average SAR in adult and child models for frequencies from 30 MHz to 3 GHz. *Phys Med Biol*, 51: 4119–4127. doi:10.1088/0031-9155/51/17/001 PMID:16912372
- Whiteside H & King RWP (1964). The loop antenna as a probe. *IEEE Trans Antenn Propag*, AP-12: 291–297. doi:10.1109/TAP.1964.1138213
- WHO (2010a). *Radio frequency (RF) fields - new 2010 research agenda*. Available at: http://whqlibdoc.who.int/publications/2010/9789241599948_eng.pdf.
- WHO (2010b). Fact Sheet N°193
- Wiat J, Dale C, Bosisio AD, Le Cornec A (2000). Analysis of the Influence of the Power Control and Discontinuous Transmission on RF Exposure with GSM Mobile Phones. *IEEE Trans Electromagn Compat*, 42: 376–385. doi:10.1109/15.902307
- Wiat J, Hadjem A, Gadi N *et al.* (2005). Modeling of RF head exposure in children. *Bioelectromagnetics*, 26: Suppl 7S19–S30. doi:10.1002/bem.20155 PMID:16142772
- Wiat J, Hadjem A, Gadi N *et al.* (2007). *RF Exposure assessment in children head: Present questions and future challenges*. International Conference on Electromagnetics in Advanced Applications (ICEAA), Sept. 17–21, Torino, pp. 1034–1035.
- Wiat J, Hadjem A, Wong MF, Bloch I (2008). Analysis of RF exposure in the head tissues of children and adults. *Phys Med Biol*, 53: 3681–3695. doi:10.1088/0031-9155/53/13/019 PMID:18562780
- Wickersheim K-A & Sun M-H (1987). Fiberoptic thermometry and its applications. *J Microw Power*, 22: 85–94.
- Willett JC, Bailey JC, Leteinturier C, Krider EP (1990). Lightning electromagnetic radiation field spectra in the interval from 0.2 to 20 MHz. *J Geophys Res*, 95: D1220367–20387. doi:10.1029/JD095iD12p20367
- World Bank; International Monetary Fund (2009). *Global Monitoring Report 2009: A Development Emergency*. Washington DC, USA. Available at: <https://openknowledge.worldbank.org/handle/10986/2625>
- Wu T, Tan L, Shao Q *et al.* (2011). Chinese adult anatomical models and the application in evaluation of RF exposures. *Phys Med Biol*, 56: 2075–2089. doi:10.1088/0031-9155/56/7/011 PMID:21386138

